# Automatic Disturbance Rejection Using Quasilinear Control


Session: 2011-2013

**Submitted by:**

Ghulam Shabbir 2011-MS-CE-01

**Supervised by:**

Dr. Yasir Saleem

Department of Computer Science and Engineering

**University of Engineering and Technology**

**Lahore Pakistan**

# Automatic Disturbance Rejection Using Quasilinear Control

Submitted to the faculty of the Computer Science and Engineering Department of the University of Engineering and Technology Lahore in partial fulfillment of the requirements for the Degree of

Master of Science

in

**Computer Engineering**.

| | |
|---|---|
| **Internal Examiner** | **External Examiner** |
| Signature: | Signature: |
| Name: | Name: |
| Designation: | Designation: |
| **Chairman** | **Dean** |
| Signature: | Signature: |
| Prof. Muhammad Shahbaz | Name: |


Department of Computer Science and Engineering

**University of Engineering and Technology**

**Lahore Pakistan**

# Declaration

I declare that the work contained in this thesis is my own, except where explicitly stated otherwise. In addition this work has not been submitted to obtain another degree or professional qualification.

Signed: _____

Date: _____

# Acknowledgments

Without support of God Almighty enlightenment nothing can be perceived and nothing can be achieved. I acknowledge Allah enlightening support, when I have been in the darkness and emptiness. May Allah empower me to be grateful to Him always.

May Allah sanctify my close relative and family members with well aspirations, good fitness and flourishing long lives and be source of prayers for me. As they have been a constant and soothing support for me.

I specifically acknowledge the support of my Advisor/Supervisor, who has been supporting and pushing to completion of this work. His knowledge and guidance support will always stay in memories of mine forever.

...

*To my teachers and specifically to Dr. Yasir Saleem*

*To my father Muhammad Waryam, the true mentor for me*

*To my family; my daughter, my son and my wife...*

# Contents

# List of Figures

# List of Tables

# Abbreviations

| | |
|---|---|
| **QLC** | Quaslinear Control |
| **ADRC** | Active Disturbance Rejection Control |
| **PID** | Proportional Integral Derivative |
| **MLS** | Magnetic Levitation System |
| **TD** | Tracking Differentiator |
| **ESO** | Extended State Observer |
| **TE** | Tracking Error |

# Abstract

In control theory, when controllers are designed it is assumed that there exists a value of controller effort than can stabilize the system and additionally, the reference can be tracked. If on the other hand, the plant model of the system is unstable, or if it has modeling errors, the controller effort needs to be unbounded. Physically speaking every controller needs to be realized using analog hardware or using digital hardware. The output terminals of the controller cannot drive a signal having boundless magnitude. For instance, if the controllers are implemented using operational amplifier, the output of the amplifier is always bounded by the DC supply voltages. If the supply voltage is $V_s$ volts, then the maximum signal that can be driven by the amplifier without getting into saturation would be in the range $L_- \sim L_+$.

The solution of the issue is presented by quasilinear controller theory. To demonstrate the issue, three controllers for magnetic levitation system (MLS) are designed in this work. First controller is designed using loop-shaping methods. As the MLS is highly non-linear, so its linearized model can frequently and abruptly actuate saturation non-linearity. It is shown, the systems transient performance, steady state performance and the disturbance rejection is exactly what is required. But the controller effort signal reaches a value of 50 plus units in tracking the unit step reference. Second controller has been designed using active disturbance rejection control (ADRC) theory. The ADRC controller performs better than loop-shaping controller, in terms of transient specifications, steady state specifications and disturbance rejection. Also, this controller does not need accurate plant model, so it does counteract modeling errors more effectively than loop-shaping control. But this controller has exhibited huge controller effort to do the perfect job. Third controller (which is the proposed solution) is designed using quasilinear control theory (QLC). It is shown that this controller not only satisfies the performance specifications, but the magnitude of controller efforts remains within the bounds. And it never actuates the saturation non-linearity. ...

# Chapter 1

# Introduction

The theory of control systems has evolved to revolutionize the human comfort. Quasilinear control theory is the recent addition in this field. In this theory the availability of linear plant is assumed and non-linear instrumentation is designed for the smooth operation of closed loop system. This chapter presents the introduction of proposed research work. As this work is based on Quasilinear Control (QLC) theory, literature review follows the introduction and is followed by motivational remarks. The chapter will end with the problem statement and the objectives of this work.

## 1.1 Overview

Control systems is the study of designing controller so that the complete control system serves according as the defined objectives. The controllers can be classified according to the domain they work in, according as the way they perform their jobs. The controller could be discrete or continuous. Primarily all controllers are designed in continuous domain. With the advent of innovative and sophisticated digital technologies, controllers are tried to be implemented digitally. But, unfortunately, every controller cannot be digitized. Conversely, every controller cannot be implemented using analog technologies.

Controllers can be categorized as classical controllers, non-classical controllers and hybrid controllers. PID controllers, loop-shaping controllers and lead-lag controllers are the examples of Classical controllers. Classical controllers are designed and are based on intricate mathematical tools. The design of these controllers is claimed to be of deterministic nature. But, when these controllers are designed, the conflict between number of unknown parameters and the number of equations occur. To overcome these conflicts experienced designers do assume the values of

some parameters and if the satisfactory performance is not attained, the design process is repeated again and again. To facilitate the design process, some help from modern mathematical tools is obtained such as state-space analysis, optimal control and H-infinity loop shaping etc. feedback controllers and observer-based feedback controllers are also classified as classical by some authors.

Adaptive control is the control strategy taken by a controller which must adapt to a controlled system with parameters which vary, or are initially uncertain. For example, as an aircraft flies, its mass will slowly decrease as a result of fuel consumption; a control law is needed that adapts itself to such changing conditions. Adaptive control is different from robust control in that it does not need a priori information about the bounds on these uncertain or time-varying parameters. Robust control guarantees that if the changes are within given bounds the control law needs not be changed, while adaptive control is concerned with control law changing themselves. Adaptive control has emerged from classical control theories and the availability of high-end computational tools, it looks that it has become independent from those theories[4]. PID control, although it is said to classical control, do have the capability to adapt with varying control system requirements. Neural networks and fuzzy logic are easing the process of creating adaptive controllers. Artificial intelligence and machines are the recent actors in this area.

Hybrid controllers are the controllers which combine both classical and non-classical theories to ease control system design and help embed adaptiveness. If artificial neural networks, fuzzy logic, ANFIS (Adaptive Network-based Fuzzy Inference System) which the combination of neural network and fuzzy logic; and others are used as controllers in their intrinsic sense, this would be modern and non-classical control. PID controller due to its inherent structure is the best controller amongst its contemporary controller and still it is the dominating controller in industrial applications. But, PID gains once designed cannot be changed online. The use of fuzzy logic and neural network has made it possible that its parameters could be varied while it is there in the process loop. As this is the combination of classical and non-classical control, this would be called hybrid control. A number of such example can be found in literature. Some examples of this conjunction will be presented in literature review.

While designing the controller, it is assumed that controller can apply infinitely huge effort to reduce control error. Such an effort is dictated by uncertain changes in reference input, disturbances and measurement noise. As these inputs cannot be avoided in any circumstances, so to track the reference successfully, controller might need to apply large effort. The amount of effort is constrained by the

practical implementations. For instance, analog controllers are implemented using operational amplifiers. The peak output values are determined and are restricted by the supply voltages. For smooth operation of the system, it is required that maximum output must stay below the supply voltage, otherwise the controller will be saturated. Similar situation might occur in pneumatic systems, where controllers are implemented using pneumatic components. The movement of the valve is actuated by the controller. If the controller applies sudden and huge effort, the actuator might get stuck. This type of situation is called actuator saturation. This phenomenon of saturation is called non-linearity. For the smooth operation of control systems, these kinds of non-linearities and others like, backlash, relaying etc. must be avoided. Back-stepping control is one of the methods which can be used to avoid saturation particularly. But there is a need of some method which could universally be used in such situations as pointed above.

The methods used to non-linear systems are Jacobin linearization, compensation of static nonlinearity, linearization by local feedback, input-to-state linearization, input-to-output linearization, Lyapunov redesign, backstepping, sliding mode control, gain scheduling, relay control etc. [25]. Each method is based on the assumption that the plant model is nonlinear. But none of them considers the actuator linearities explicitly. Backstepping control is considered to be interacting on such kind of nonlinearities indirectly by backstepping estimated ?virtual control input?. Because it has superior characteristics to its contemporary methods, its numerous applications can be found in literature. For example in non-holonomic robots references might actuator non-linearity while tracking the referenced tracking, solution has been proposed using backstepping [10]. In [9] it has been applied on lateral behavior control of a vehicle, [44] applies to a cluster of vehicles for coordinated flow in a defined field and [30] considers and use of backstepping for the flight behavior control.

But it poses certain difficulties. Firstly, the backstepping design is based on Lyapunov function for the estimation of virtual control inputs, so it will not easier and or it could even be impossible to find a suitable Lyapunov function. Secondly, it need that all states of the system must be measurable, if this is not possible, they must be observable from the measurement of output. The estimation of states from the output often need a nonlinear observer, which is again a challenging task. Lastly, the design is sensitive to parameter perturbations [25]. The solution lies in Linearized (or linear) Plant and Non-Linear Instrumentation (LPNI). This can be differentiated from the above mentioned in the sense that Linear Instrumentations (controllers in the wider) are designed for the Non-linear Plants, so this could be

called as Non-linear Plant Linear Instrumentation (NPLI) just to give a broader comparison with the work presented in this report.

## 1.2 Literature Review

Initially, the QLC theory has been presented for the linear and stable plants under the assumptions that some inputs might ignite non-linearities like saturation. In this work, it has been demonstrated that QLC controller can control the unstable plants as well without exciting non-linearities, even better that loop-shaping control and ADRC (Active Disturbance Rejection Control). So in this some section glimpses from past work in loop shaping, ADRC and in QLC will be presented.

### 1.2.1 Loop-Shaping Control

There are three ways of representing the frequency response analysis: 1) polar plots; also known as Nyquist plot; is the plot of complex numbers (in polar form) in complex plane when frequency is varied, 2) Bode Plot, is the plot of log-magnitude versus frequency and phase (in degree) versus frequency onto two separate diagrams and 3) Log-magnitude versus phase plot, is the plot of log-magnitude (on y-axis) versus phase on (x-axis) when the frequency is varied. The characteristics of all frequencies analysis methods are similar and depend upon the loop transfer function $L(s) = G_P(s)G_C(s)$. So the loop shaping control is the art of manipulating $L(s)$ so that desired frequency response characteristics are obtained [6], [38].

The controller $G_C(s)$ could be a lead compensator, a lag compensator or lead-lag compensator. Looping shaping is concerned with choosing the right set of controller parameters, so that the specified goal is achieved. Since this is the oldest control methods, so almost all modern mathematical techniques have been employed to optimize the design [36]. A classic, compact and in-depth account of loop-shaping control can be found in [23], beginning from simple concepts to H-Infinity control and modern optimization methods.

The basic theme of loop shaping has found un-numerable applications. Transcutaneous Energy Transfer is the way of wireless energy transfer, and is best controlled by shaping various loops [24]. As mentioned earlier many intricate mathematical methods have been used to design loops for given conditions including AI [45]. Another stunning extension of loop-shaping is the incorporation of the concept of signal-to-noise ratio (SNR). This extension has resulted the definition of reference-to-disturbance ratio (RDR), directs the loop-shaping to attain

high RDR [2]. Iterative learning control is another extension of loop-shaping control [61]. Buck regulators are the power converters which step down the input DC power to desired level. The models of these converters are inherently non-linear, but their linearized versions are used to design controllers. One useful form of the buck converter is the dual output converter. It has two loops to be shaped, and convex optimization has done the job [14]. As the power converters are inherently non-linear, so their linearized models are used for controller design. Another redesigned loop-shaping control with FOPID (Fractional-Order-PID) using H2/H-Infinity optimization has obtained. This core of this design is based upon frequency response shaping, so this is an excellent example of spells of loop shaping [13]. The crossed loops in a networked control systems are sometimes referred to as butterfly loops. Design of these loops towards specified requirements is also called loop-shaping [39]. Loop-shaping design also provides robust designs, such an example is the wind-turbine power conversion system. Here robustness is the key design parameter due to stochastic nature of input power [26].

In summary, it can be said that loop shaping is a control system design methods based upon shaping the loop transfer function. More precisely, a loop transfer function consists of plant, actuator and sensor controller transfer functions. It is assumed that all transfer functions are known except the controller transfer function. So the task of loop shaping is to determine the controller parameters, such the bode plot or Nyquist plot get the desired shape. This can be accomplished using any linear or non-linear optimization.

### 1.2.2 Active Disturbance Control

Although exact time of birth of PID control cannot be traced, yet it is believed that it development and extensive deployment commenced in the era of 1920s to 1940s. This age can be said to age of peak renascence and was mostly forced by World War I and WORLD War II. It played vital role in the industrialization of many countries in the post war era specifically. Since then it is ruler of industry and has attracted overwhelming response from the control designers. Its amazingly simple and its simple actions do amazing control actions. But, at the same time the tuning of its parameters demands the highest level of skills. So its simplicity seems to loose attention. But, it?s not the case now-a-days with the development of amazing computational resources. Despite its beauty of simplicity, the popularity of analog controllers is becoming in the era of digital controllers, because they cannot take full advantage of digital revolution [29]. To retain the existence of such a hugely successful controller until now, it is aided with modern methods of soft computing like fuzzy logic, neural networks. Conversely, modern control

techniques are strengthened with PID mechanisms. But there is a need of some paradigm shift that does not alter its basic structure, but enhances its control capability. If such an effort is not put-forth, this can disappear in the modern digital world due to their hugely beneficial methods of digital control. Now the question arise, what kind of control can replace PID, the answer is ADRC (Active Disturbance Rejection Control). The justification to this choice will be clarified in the upcoming lines.

The new replacement to PID, has actually strengthened the use of PID. It has been brought-forth from some of the shortcomings of PID control. There FOUR basic drawbacks in the PID control lead to the development of ADRC. This new paradigm shift is based on the developing (1) an almost smoother transient response with the help of a simple differential equation (2) the design of noise-tolerant differentiator and (3) the powerful nonlinear feedback. This revolutionary was proposed firstly in Chinese language and in Chinese technical literature. Whose English version was also drafted by the original author. It is perhaps the first official and formal document in which the framework of ADRC has been proposed for the English readers. A survey of literature also reveals that so far Chinese researchers are dominating this particular control scheme [29].

Complete and comprehensive ADRC framework consists of four individual components: de-effector to set-point jumps, tracking differentiator, non-linear feedback and total disturbance estimator [29]. The development of extended state observer (ESO) has attracted the most attention of researchers. Particularly, linear version of this work is being used extensively. In linear version set-point jumps are remedied with linear ESO and PID serves the purpose of controller [31]. There was no explicit mention of the stability conditions for ADRC control. As ADRC is a kind of non-linear control, so its stability conditions have been developed using Lyapunov describing function, which uses circle criteria on the Lauri system (the plant transformed to Laurie system) [42]. In another work output feedback stability is described with the details on design non-linear ESO [42]. Some significant works has been undertaken to make ADRC adaptive, so that the overall system could be made adaptive. This notion has been employed in the design process of adaptive ESO to overcome nonlinearities and stochastic disturbances [59], [33] and [50]. Frequency methods have been applied on ADRC in [57] using describing function.

A number ADRC applications have been reported in literature. In [8] ADRC is applied for the efficient energy storage of flywheel technology. [60] gives the application of ADRC to control the position of magnetic and rodless pneumatic

cylinder. In [58] a novelty has been brought forth in the design of ESO. The study concerning the problem of aperiodic-disturbance estimation and rejection in a modified repetitive-control system (MRCS) with an equivalent-input-disturbance (EID) estimator is presented in [62]. A MIMO application of ADRC has been explored in [51]. In [32] new dimension of ADRC have been explored toward its discrete implementation considering bump-less transfer and rate limitations. The aspects of robustness of ADRC have been pointed out in [55]. In this article [41], robust ADRC has been applied for speed control capability of induction motors drives. The article [7] combines the robustness and adaptiveness features of ADRC. The research work in [34] presents the application of ADRC for the control PWM rectifiers. The rectifiers in turn are being used to control the speed of sensor-less motor. [56] give the application of ADRC for trajectory control in aircrafts.

### 1.2.3 Quasilinear Control Theory

If the relationship between input variable(s) and output variable(s) of a system is linear without any bounds or restrictions on the variables, this is known a linear system. But if the linearity between the variables is bounded by the system within defined limits, the system is called Quasilinear [49]. The term quasilinear has been used extensively for the characterization of PDE (Partial Differential Equation) systems. The systems described by PDEs are classified as linear, quasilinear and non-linear. QLC theory deals with the systems described by quasilinear ODEs. As the systems variables are bounded by quasi-linearity, violations of these bounds might result in non-linear phenomena such as shocks, steepening, and breaking of responses within the system [28].

The concept of quasi-linearity has many dimensions. This notion with a broader perspective has been utilized to describe the phenomena in quantum mechanics and quantum control under Hilbert space [54]. Quasi-linearity has also been identified and formulated in quadratic and hyperbolic PDE systems. The obtainment of flatness in the solution of such systems is the consequence of quasi-linearity [35]. As quasi-linearity is a way of characterizing of PDE system, backstepping control has been implemented on a two-by-two hyperbolic quasilinear system. It should be noted that here QLC is not a controller design method [53]. Quasilinear PDE are also used for description of distributed parameters systems (commonly known as distributed systems). In one research direct parametric control has been on such systems. In another work the method of varying delays has employed on such system [18], [17]. C.K. Li et. el have used quasilinear modeling for power converters, while they have used conventional and contemporary methods for the

control of power flow [40]. Optimal can also be implemented on quasilinear systems [43] In one of his research, Guang-Ren Duan applies output feedback control to a system modeled using quasilinear system [19]. Relay control applied to industrial motors modeled by QPDE is another example quasilinear modeling. Here parametric control has been utilized to simulate smooth relay control [16].

All references cited in the above paragraph employ quasi-linearity as a system modeling tool. But, now it has evolved into a control method which deals with kinds of non-linearities explicitly. It is pointed out that in all the above stated examples non-linearities has not been dealt with exclusively, although some control methods, such as backstepping control, provide implicit counteraction.

The quasilinear control theory of the day provides a smart combination of classical control and quasi-linearity. This QLC is based on the assumptions

- that the input signals (reference, disturbance or noise) are of probabilistic nature. These exogenous signals can activate non-linearities
- that the plant is linear (or its linearized model is available), but due probabilistic inputs system instrumentations can be trapped into non-linear phenomenon. [this assumption is called Linear Plant Non-Linear Instrumentation (LPNI) in literature]
- that the non-linear phenomenon could be inherent in the instrument beyond certain bounds

For the above said assumption, QLC (Quasilinear control) theory presents the methods of controller and reference design, so that non-linearities are never activated [11], [47]. Following two shortcomings can be identified in this theory so far [11]:

- This theory assumes that plant, controller in their individual sense and the closed-loop system must be stable
- It enforces an upper bound on the magnitude of reference to be tracked for any closed-loop system.

Although, the aforementioned things limit the use this theory. But there are two big advantages in this use of this theory [11]:

- The control designer can know the exact value of upper bound on the reference to be tracked. Thus it gives deeper insights into the plant shortcomings.

- It helps the design of such controller that will never cause the plant get into non-linearity. This is the biggest achievement of this theory towards implementation perspectives.

Non-linearities can be divided into two big classes: symmetric non-linearities and asymmetric non-linearities. QLC theory has been developed to counteract both kinds of non-linearities [47].

Considerable amount of applications has been designed using this theory. Perhaps the first major application of this theory is in the controllers that would regulate the power output from a wind turbine [47] [27]. Design of controllers using state-space analysis is becoming more and more popular. There are certain reasons to this rapid growth: state-space analysis gives deeper look into the system?s behavior; it gives direct control to accessible states of the system. These notions have been extended in QLC theory for the development of Eigen-structure assignment for the non-linear systems [20].

This work will comparison of three control methods loop-shaping control (the classical control), ADRC (Active Disturbance Rejection Control) and Quasilinear control. Loop shaping theory will be presented in second chapter and third chapter will elaborate of use of ADRC. Last and fourth chapter will present quasilinear for the problem at hand. So rest of the material will be referenced in their respective places accordingly.

## 1.3 Motivation

Jacobian linearization of Taylor series linearization has not work well for highly non-linear systems. Although linearization brings easiness in the design process, but attainment of particular objectives often remains unsuccessful. The process of designing linear controller for linearized plant might be called Linear-Plant-Linear-Instrumentation strategy. To over this difficulty, some other methods like [25] input-state linearization, input-output linearization, feedback linearization were proposed. These methods do not counteract the non-linearities in a direct action sense firstly, and secondly, they do poses one more shortcomings like the accessibility of system states and unsuitability of physical implementations. These difficulties have effectively been overcome by quasilinear control.

Consider the system shown in FIGURE 1.1. $\mathbf{r(t)}$ is the reference input to tracked by the system, $y(t)$ is the output from the system, $\mathbf{d(t)}$ is the disturbance input, $G_C(s)$ and $G_P(s)$ are the linear controller and linear plant respectively. The function $f(.)$ is the actuator function and g(.) is the sensor function.

$$u_a(t) = f(u(t)) \tag{1.1a}$$

$$b(t) = g(y(t)) \tag{1.1b}$$

The saturation nonlinearity is ubiquitously exhibited by actuators and the sensors are often trapped by other nonlinearities like dead zone, hysteresis and friction etc. The function f is actuator is characterizing the actuator nonlinear phenomenon, while the function g is presenting the nonlinear phenomenon of sensors. Given such situation, [12] theory of quasilinear control can aid the control designer with the followings

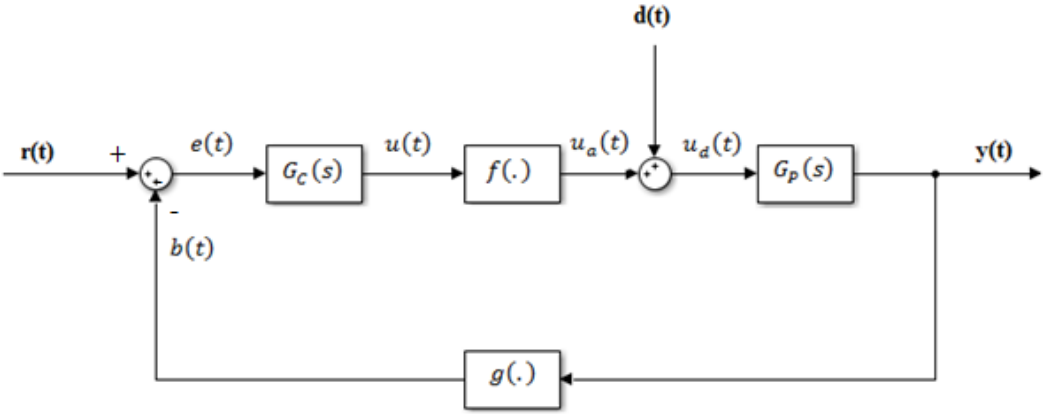


FIGURE 1.1: Quasilinear Control System

**L1-Calculating Performance Parameters:** Given system specifications $G_C(s)$, $G_P(s)$, $f(u(t))$, $g(y(t))$, Quasilinear Control (QLC) can be used to find performance parameters of the system. The performance parameters of QLC theory are not different than classical control theory. Like classical theory the performance parameters of QLC are percentage overshoot, rise times, settling time, gain margin, phase margin, disturbance rejection and reference tracking.

**L2-Controller Design in Narrow Sense:** Given the system particulars $G_P(s)$, $f(u(t))$ and $g(y(t))$, QLC theory aids the design of controller $G_C(s)$ so that overall specified system performance (time domain performance or frequency domain performance or both) is achieved.

**L3-Controller Design in Wide Sense:** This implies that given the $G_P(s)$, its controller $G_C(s)$ and its instrumentations $f(u)$, $g(y)$ can also be designed in a way that the overall LPNI meets the performance specifications.

**L4-Partial Recovery of Performance:** Assuming that actuator and sensor are linear and a controller $G_{pr}(s)$ is designed which satisfies the linear system

performance. QLC allows that a suitable actuator and/or sensor are chosen, so that given specifications are adequately met. Such situations can arise for large scale systems.

**L5-Complete Recovery of Performance:** If possible QLC also allows the redesign of $G_{pr}(s)$ so the closed loop LPNI meets the performance specifications completely. Usually, in this approach, only one parameter of the controllers is redesigned. The process could be repeated for some other parameter so that performance specifications are satisfied.

The QLC approach is based on stochastic linearization. Two distinct features of stochastic linearization. Firstly, the non-linear actuator and sensor functions can be replaced by constant gain which are proportional to the statistical expectation of u(t) and secondly, as the gains are calculated using past statistics of $u(t)$, so the unusual behavior of the system can be predicted and timely action from the controllers are induced with saturating the controller or actuator itself.

Magnetic levitation system is a highly nonlinear system. If the linear model of this plant is perturbed slightly out of the specified bounds, drastic and undesired behavior is observed if with the best linear controller. The design QLC is motivated by the excellent features of QLC theory for highly nonlinear system such as magnetic levitation system.

## 1.4 Problem Statement

Magnetic levitation systems (MLS) are being employed for the development of swift trains. This is the reason that it has attracted the attention of many researchers. Magnetic levitation system (MLS) is a highly nonlinear plant, so its control needs careful and robust controller design.The reference [21] presents the design IMC based PID controller, while [46] gives performance comparison of Jacobian linearization, feedback linearization and sliding mode control for MLS control. A model of MLS is shown in FIGURE 1.2. The dynamics this MLS model can be given by [21]

$$m\frac{d^2h(t)}{dt} = mg + f_{em}(h, i, t) \tag{1.2}$$

All terms in (1.2) are self-explanatory. But for formal completeness, all terms in the equations are explained. In (1.2) $m$ is the mass of the ball $r$ is the reference position of the ball and $y$ is the actual position of the ball read by the sensor. The variable $u$ is the output from controller which is converted to current by current driver, because the electromagnet is controlled by the changing current. From (1.2) it can be noted it is a relationship between the relative position of the ball

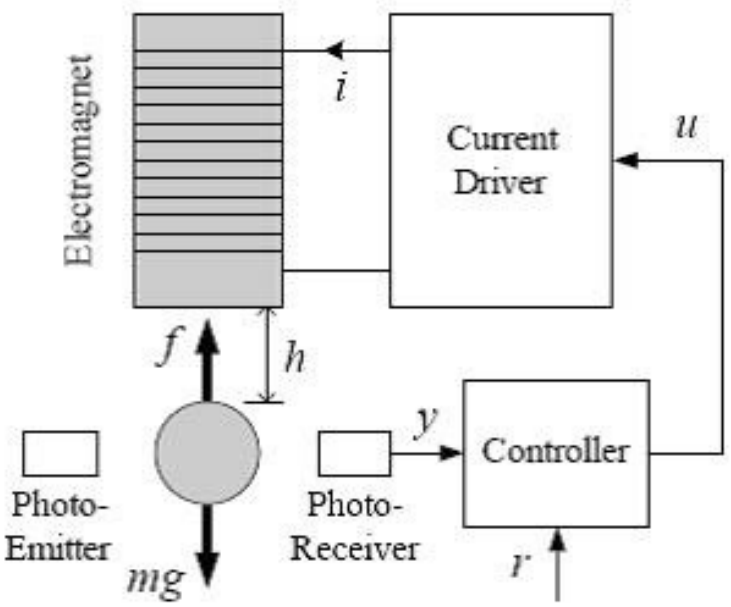


FIGURE 1.2: Magnetic Levitation System

and the current flowing into the electromagnet. Also the relationship is highly nonlinear because the electromagnetic force $f_{em}(h, i, t)$ is given by [21]

$$f_{em}(h, i, t) = -C\left(\frac{i(t)}{h(t)}\right)^2 \tag{1.3}$$

From (1.2) and (1.3)

$$m\frac{d^2h(t)}{dt} = mg - C\left(\frac{i(t)}{h(t)}\right)^2 \tag{1.4}$$

The constant $C$ is considered to be constant, but it is not, because its dependent upon the levitation point. In this work quasilinear control of MLS will be presented and will be compared with some of the existing methods.

So, the problem statement of this work becomes: Given the relationship (1.4)

- Linearize (1.4) at suitable levitation point
- Find a suitable current driver, so the voltage from the controller shown in FIGURE 1.2 could be converted to current to drive the electromagnet.
- Design Loop-Shaping based PID controller for the linearized plant
- Design the ADRC (Active Disturbance Rejection Controller) for the linearized and nonlinear plant
- Apply the QLC problem **L3** on the system to obtain the quasilinear controller

- Finally, compare the performances of all control techniques mentioned above.

## 1.5 Research Objectives

Based on the problem statement, followings are the objectives.

☐ PID design for Magnetic Levitation Systems using Loop-Shaping Control

☐ Design of Active Disturbance Rejection Control (ADRC) for MLS plant

☐ Design of Quasilinear Controller (QLC) for MLS Plant

## 1.6 Outline of the Thesis

This thesis report will consist of FIVE chapters. First chapter has presented the in depth introduction to the work at hand. Second chapter will elaborate the design process of Loop-Shaping PID controller following the linearization of plant in (1.4). Third chapter will present the in depth design process of ADRC. In fourth chapter QLC theory will be presented. The final and fifth chapter will present the design process in QLC theory. The final section of this chapter will end the report with conclusive remarks on the results obtained.

# Chapter 2

# Loop Shaping Control

This chapter is all about loop shaping. Loop shaping is based upon frequency response methods. Initially, the performance specification of this method will be described in a comprehensive manner. The design methods and their fundamental limitations will follow specifications description. It will be presented that how these loop shaping can be applied for the design of PID controller. The collective study will be applied on our plant given by (1.4) to produce the results.

## 2.1 Loop Shaping Problem Formulation

The characteristic equation of the closed-loop system is given by $[1+G_C(s)G_P(s)]$. This equation establishes the core requirement of any design problem. Specifically, the product $L(s) = G_C(s)G_P(s)$ is the heart of many control problems. This transfer function is the heart of loop shaping design as well. The plat transfer function $G_P(s)$ is generally known, so loop-shaping is the art of determining the parameters of $G_C(s)$ such that frequency response of $L(s)$ behaves as specified. In this section a formal structure of this control problem will be presented.

### 2.1.1 Introductory Concepts

FIGURE: 1.1 is repeated in FIGURE: 2.1 with some additional signals and a filtration block $G_F$. Using FIGURE 2.1, following transfer functions can be obtained

$$G_{yr} = \frac{G_F G_C G_P}{1 + G_C G_P} \tag{2.1a}$$

$$G_{ur} = \frac{G_F G_C}{1 + G_C G_P} \tag{2.1b}$$

$$G_{er} = \frac{G_F}{1 + G_C G_P} \tag{2.1c}$$

$$G_{yd} = \frac{G_P}{1 + G_C G_P} \tag{2.1d}$$

$$G_{ud} = -\frac{G_C G_P}{1 + G_C G_P} \tag{2.1e}$$

$$G_{ed} = -\frac{G_P}{1 + G_C G_P} \tag{2.1f}$$

$$G_{yn} = \frac{1}{1 + G_C G_P} \tag{2.1g}$$

$$G_{un} = -\frac{G_C}{1 + G_C G_P} \tag{2.1h}$$

$$G_{en} = -\frac{1}{1 + G_C G_P} \tag{2.1i}$$

They can be written be in matrix form as

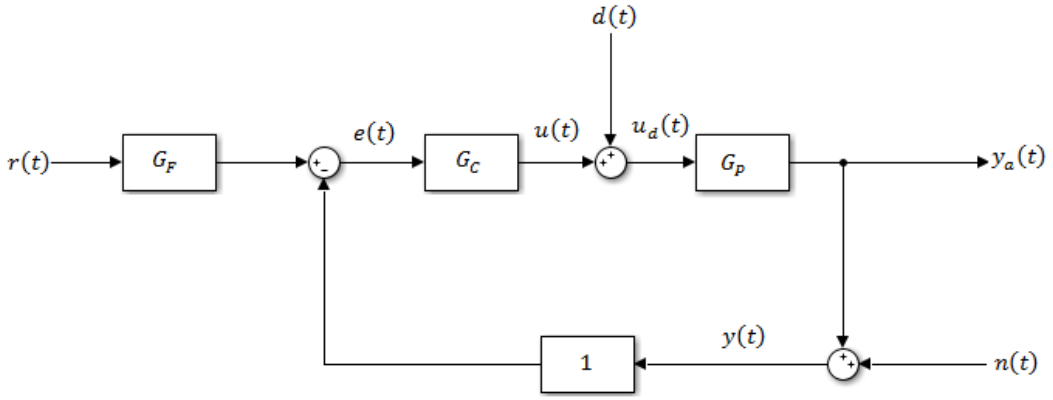


FIGURE 2.1: Loop Shaping Problem Formulation

$$\begin{bmatrix} y \\ u \\ y_a \end{bmatrix} = \begin{bmatrix} \frac{G_F G_C G_P}{1+G_C G_P} & \frac{G_P}{1+G_C G_P} & \frac{1}{1+G_C G_P} \\ \frac{G_F G_C}{1+G_C G_P} & -\frac{G_C G_P}{1+G_C G_P} & -\frac{G_C}{1+G_C G_P} \\ \frac{G_F G_C G_P}{1+G_C G_P} & \frac{G_P}{1+G_C G_P} & -\frac{G_C G_P}{1+G_C G_P} \end{bmatrix} \begin{bmatrix} r \\ d \\ n \end{bmatrix} \tag{2.2}$$

From above equation (2.2) following six common transfer functions can be identified.

$$\begin{matrix} \frac{G_F G_C G_P}{1+G_C G_P} & \frac{G_F G_C}{1+G_C G_P} & \frac{G_C G_P}{1+G_C G_P} \\ \frac{G_C}{1+G_C G_P} & \frac{G_P}{1+G_C G_P} & \frac{1}{1+G_C G_P} \end{matrix}$$

Now letting $G_F = 1$, which usually the case, only four transfer functions are left. These four transfer function are enough to describe the system behavior. How the system will react to disturbances is given by $\frac{G_P}{1+G_C G_P}$, how the system will respond to measurement noise

is characterized by $\frac{1}{1+G_C G_P}$, how the reference will be tracked by the closed-loop system is described by $\frac{G_C G_P}{1+G_C G_P}$ and how the controller will react to measurement noise is given by $\frac{-G_C}{1+G_C G_P}$. These transfer functions are given special names as follows

$$\textbf{Complementary Sensitivity Function } T = \frac{G_C G_P}{1 + G_C G_P} \tag{2.3}$$

$$\textbf{Sensitivity Function } G_S = \frac{1}{1 + G_C G_P} \tag{2.4}$$

$$\textbf{Load Sensitivity Function } G_D = \frac{G_P}{1 + G_C G_P} \tag{2.5}$$

$$\textbf{Noise Sensitivity Function } G_N = -\frac{G_C}{1 + G_C G_P} \tag{2.6}$$

The complementary transfer function is the relationship between reference input and the measured output, sensitivity function is the relationship between measured output and the measurement noise, load sensitivity is the relationship between load disturbance and the output and finally noise sensitivity is the reaction of the controller to measurement noise. The equations (2.3) through (2.6) are the steady state characterization of the system and give one set of constraints to loop shaping design. In view of the above discussion the control procedure must ensure the followings

- ☐ Design the controller $G_C(s)$ such that $G_S$, $G_D$ and $G_N$ are minimized and $T$ approached to unity.
- ☐ Choose suitable the filter transfer function $G_F(s)$, if required, so that reference is tracked successfully.

### 2.1.2 Design Specifications

As the loop shaping is based on frequency response methods, the performance parameters are defined in terms of frequency response

analysis. Performance parameters are defined using the complementary sensitivity function. Replacing s with j in complementary sensitivity function

$$T(j\omega) = \frac{G_C(j\omega)G_P(j\omega)}{1 + G_C(j\omega)G_P(j\omega)} \tag{2.7}$$

Magnitude response of a typical closed-loop transfer function (here it is the name of complementary sensitivity function) is shown in FIGURE 2.2. The terms shown in this Figure are the performance parameters of loop-shaping control. The term $M_r$ is the resonant peak,

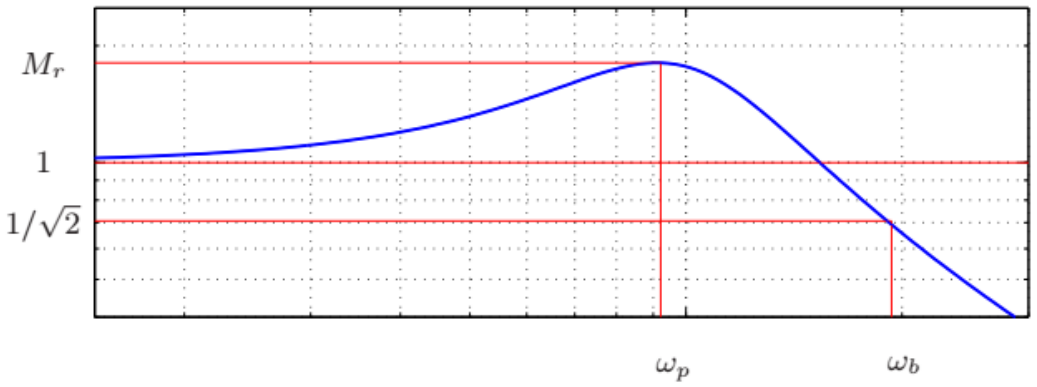


FIGURE 2.2: Loop-Shaping Parameters [6]

the highest value of $|T(j\omega)|$. The parameter $\omega_p$ is the frequency at which the resonant peak occurs. The term $\omega_b$ is the bandwidth of the systems. This represents the range of frequencies from zero frequency to the frequency at which the magnitude drops to 1/2 times its DC gain. These three parameters form one set of parameters.

Another set of parameters is based on frequency response margins. Also these parameters describe the relative stability of closed loop system, although these parameters are defined on loop transfer function $L(s) = G_P(s)G_C(s)$. These parameters are gain margin and phase margin. Gain margin can be defined as [38]

$$\textbf{Gain Margin } (GM) = 20\log\left|\frac{1}{L(j\omega_{pc})}\right| \tag{2.8}$$

Whereas $\omega_{pc}$ is the phase cross-over frequency. Phase crossover $\omega_{pc}$ is the frequency at which $\arg(L(j\omega_{pc})) = 180\,\text{deg}$. Positive gain margin indicates that the system is stable and negative gain margin indicates that the closed loop system is unstable, while zero gain margin implies marginally stable system. This is also the measure of robustness. Whereas robustness refers to invulnerability of the system output to the changes in system parameters up to certain limits.

Only the knowledge of gain margin can produce misleading results. The knowledge of another parameter called phase margin will complete stability information. Phase margin is defined as [38]

$$\textbf{Phase Margin } (PM) = \arg(j\omega_{gc}) - 180^{\circ} \tag{2.9}$$

While $\omega_{gc}$ is the gain crossover frequency. Gain crossover is the frequency at which $20\log\|L(j\omega_{gc})\| = 0dB$. Phase margin is said to be better indicator of robustness. A phase margin of about 30 degrees to 60 degrees shows adequate robustness.

The parameters resonant peak, resonant frequency and bandwidth are defined on the basis of closed loop transfer function and the parameters gain margin, phase margin are defined using loop transfer function. Some useful design and/or performance can be defined on the basis of gang of four sensitivity functions. There are also a number of useful specifications on the sensitivity function and the complementary sensitivity function:

**Peak Sensitivity and Peak Sensitivity Frequency:** Maximum value of magnitude response of sensitivity function is called the peak sensitivity denoted as $M_S$ and the corresponding frequency at this phenomenon occurs is called peak sensitivity frequency.

**Sensitivity Crossover Frequency:** The minimum value of frequency at which the sensitivity function becomes greater than unity for the first time. This parameter indicates the disturbance immunity of closed loop system. The disturbances of frequencies lower than this value are successfully attenuated.

**Peak Complementary Sensitivity and Peak Complementary Sensitivity Frequency:** As their names imply the maximum value of magnitude response of complementary sensitivity function is called the peak complementary sensitivity and the corresponding value of frequency at which this maximum occurs is called peak complementary sensitivity frequency.

From (2.3) to (2.6), and noting that $L = G_C G_P$

$$T = \frac{L}{1+L} \tag{2.10a}$$

$$G_S = \frac{1}{1+L} \tag{2.10b}$$

$$T + G_S = 1 \tag{2.10c}$$

The equations (2.10) present tradeoffs amongst various design parameters.

### 2.1.3 Relationship Between Time-Domain and Frequency-Domain Design Parameters

The most dominant time domain parameters are rise time $t_r$, settling time $t_s$ and percentage overshoot. Roughly narrating, the time taken by the response to reach the final value for the first time is called rise time. The time taken by the systems output to settle within 4 to 2% of final values is called settling time. Percentage overshoot is defined as

$$\%Overshoot = \left( \frac{y_{max} - y_{final}}{y_{final}} \right) 100$$

The [6] product of bandwidth and rise time is approximately given by $\omega_b t_r \approx 2$. From here it can be seen that higher the bandwidth lower will be rise and settling time. Likewise, percentage overshoot and resonant peak are also proportional. The bandwidth of the closed loop system is approximately equal to the gain crossover frequency. This implies that higher the gain crossover, so higher would be the bandwidth. This may also give suitable phase margin, thus showing good robustness of the system. There is another point to be noted that the proportionality between percentage overshoot of time domain and the resonant in frequency is not strict. Resonant peak of about 1.1 to 1.2 will imply reasonable overshoot.

## 2.2 Loop Shaping a Multi-Objective Optimization Problem

The concepts introduced in the preceding chapter present essentially the constraints of loop shaping design. This section is devoted to present loop shaping design as a multi-objective optimization problem. Before it is formally narrated, some historic notes will be presented first.

### 2.2.1 Loop Shaping Literature Review

Inspired from communication theory [3] the control of any control system can be divided into reference channel control (RCC) and disturbance channel control (DCC). These two control can merely be represented as two transfer function, the reference to output transfer function and disturbance to output transfer function. Assuming that the frequency contents and reference and disturbance inputs is same, like SNR, reference to disturbance ratio (RDR) is defined as

$$RDR = \frac{|T_R(j\omega)|}{|T_D(j\omega)|} \tag{2.11}$$

With this the task of control system design becomes maximization of this ratio. In [16] the controller design for automatic voltage regulator (AVR) is presented as loop-shaping multi-objective optimization problem. The solution is obtained using $H_2/H_\infty$ norms. In [15] the notion of loop-shaping is proposed inspired from MIMO controller design approach which is based on a family of nonparametric MIMO models. The fundamental notion of the approach is to shape a family of open-loop transfer function matrices of a MIMO system by minimizing the summation of the squared second norms. [26] proposes the direct application of loop-shaping, but in advanced manner. The design of PID using loop-shaping is described quite intuitively in this [5] online document. A comprehensive treatment of loop-shaping control is outlined in [23].

### 2.2.2 Statement of Loop-Shaping Control under Multi-Objective Optimization

In view of the above discussion the design statement of loop-shaping can be written as:
Let the controllers $G_C(s)$ is defined by the set of $k$ parameters $\{p_1,\ p_2,\ p_3, \cdots\ p_k\}$, then choose the values of parameters such that for the closed loop system following objectives are met.

$$\text{minimize} \begin{cases} G_S & \text{Sensitivity} & (2.4) \\ G_D & \text{Load Sensitivity} & (2.5) \\ G_N & \text{Noise Sensitivity} & (2.6) \end{cases} \tag{2.12}$$

$$30^\circ < \text{Phase Margin} < 60^\circ \tag{2.13a}$$

$$\text{Gain Margin} > 0 \text{ dB} \tag{2.13b}$$

To aid with better design another objective on RDR [3] can be added

$$\text{minimize } |G_C(j\omega)|^2 \tag{2.14}$$

Some authors [36] do include the time domain objectives as well. They form another set of objective. The most important parameters of time domain design are rise time, settling time, and overshoot. This implies that

$$0 \leq \text{Percentage Overshoot } POS \leq POS_{desired} \tag{2.15a}$$

$$\text{Rise Time } t_r \leq t_{r(desired)} \tag{2.15b}$$

$$\text{Settling Time } t_s \leq t_{s(desired)} \tag{2.15c}$$

Subject to

$$\{\epsilon_1,\ \epsilon_2,\ \epsilon_3,\ \cdots\ ,\epsilon_k\} \leq \{p_1,\ p_2,\ p_3,\ \cdots\ ,p_k\} \leq \{\eta_1,\ \eta_2,\ \eta_3,\ \cdot,\ \eta_k\} \tag{2.16}$$

Whereas $\epsilon'$s and $\eta'$s are forming the bounds on corresponding parameters $p'$s. For LTI systems these bounds can be formulated using Routh-Hurwitz criteria.

From the preceding formulation, four sets of objectives can be identified. The formulation of an optimization program to satisfy all these objectives will be too complex. So, most of the authors do choose a subset from objectives. For instance, if the objective of required phase margin is achieved, all other objectives are essentially satisfied. So inspired from this fact, a subset of objectives will be selected to design the controller in this chapter.

### 2.2.3 Loop Shaping Design Procedure

The loop-shaping control design procedure can be divided into FOUR major stages. The stages are plant and instrumentation analysis, selection of a suitable control algorithm form, selection of a suitable

of subset of design objective and determination of controller parameters.

**System Analysis Stage:** Before the actual design process starts, it is necessary to know the plant. If the plant is nonlinear it must be linearized at specified/desired set-point (because loop-shaping design is applicable to linear systems only). As loop-shaping is mainly a frequency domain design method (although it is not limited to frequency domain design in recent times), so frequency response analysis will be necessary. Particular knowing the bandwidth, phase margin and gain margin will provide good insights into the design process. Additionally, knowing the time domain parameters like rise time, settling time and overshoot will help drive the design towards specified goals.

**Selection of Suitable Controller:** The selection of controller is often dictated by the experience and understanding the designer have. The selection should closely correspond to results obtained in system analysis. The controller must overcome the shortcomings identified in the system analysis. The foremost requirement is to bring the stability in the system if the system was identified to unstable. And if the system was stable initially, it should improve the relative stability of the system and the closed-loop system should be tracking the system successfully. The form of the controller could be a transfer function $G_C(s) = \frac{N_C(s)}{D_C(s)}$ representing the lead compensator, lag compensator or lead-lag compensator. The selection of lead compensator or lag compensator of the lead-lag compensator is dictated by the need to improve transient characteristics, steady-state characteristics or both respectively. PID controller could also be the choice because it can effectively improve on the shortcomings identified as compared with its counterparts.

**The Selection of Control-Design Objectives:** Relationships described in (2.12) through (2.12) describe various objectives of loop-shaping design. The selection of particular objective is the results of system analysis and the specifications to be met by the control system. If the number of objective is increased, the optimization program becomes complex and need high computational resources. This would be a tighter design process. But the careful (and lesser number of objectives) selection of objectives can lead to simpler optimization programs and the solution will be obtained quickly. The iteration of simpler design process would be easier as compared with complex design process.

**Obtaining the Controller Parameters:** In this stage of design process the optimization problem will be formulated based on system analysis results, controller selected and control objectives. The formulation will be solved analytically or computationally depending upon the requirements and complexity of the control design process. The whole process can be iterated if the design specifications have not been satisfied.

## 2.3 Controller Design for Magnetic Levitation System (MLS)

In this section the process of loop-shaping design will be applied on magnetic levitation system. The section will begin with development of mathematical model of magnetic levitation system followed by PID controller design. The section will end with the simulation and results.

### 2.3.1 Modeling MLS

From FIGURE 2.1 [21]

$$m\frac{d^2h(t)}{dt} = mg + f_{em}(h, i, t) \tag{2.17}$$

In this equation $m$ is the mass of the magnetic ball, $h$ is the distance from electromagnet and $f_{em}$ is the electromagnetic force, the function of $h$, the current passing through the coil of electromagnet and time $t$. The electromagnetic can be given by [22]

$$f_{em}(h,i,t) = 1/2i^2(t)\frac{dL_m(h)}{dh} \tag{2.18}$$

The quantity $L_m(h)$ gives the variable inductance due to presence of metallic ball. This inductance is inversely proportional to the position of the ball relative to the electromagnet and is given by

$$L_m(h) = L + \frac{L_0 h_0}{h} \tag{2.19}$$

The parameter $L$ gives the inductance of the coil itself and $L_0$ is the inductance at the point of levitation $h_0$. Using (2.18) in (2.19)

$$f_{em}(h,i,t) = -L_0 h_0 \left(\frac{i(t)}{h(t)}\right)^2 = -k_L \left(\frac{i(t)}{h(t)}\right)^2 \tag{2.20}$$

Whereas $k_L$ is supposed to be constant as demonstrated by (2.20), but its value depends on the point of levitation. As the controller applied will be of linear nature, so linearization of (2.20) is required. (2.20) can be expressed using Taylor series as

$$f_{em}(h,i,t) = -k_L \left(\frac{I_o}{h_o}\right)^2 - \left(\frac{2k_L I_o}{h_o^2}\right)(i-I_o) + \left(\frac{2k_L I_o^2}{h_o^3}\right)(h-h_o) + \cdots \tag{2.21}$$

Under steady state condition, the velocity and acceleration of ball will be zero, i.e. $\frac{dh(t)}{dt} = \frac{d^2h(t)}{dt^2} = 0$. This will only happen when the ball has been levitated at $h_o$ with the steady state current of $I_o$. Under these conclusions, (2.17) implies that

$$m\frac{d^2h(t)}{dt} = mg + f_{em}(h,i,t) = 0 \;\; \text{OR} mg - k_L \left(\frac{I_o}{h_o}\right)^2 = 0$$

From equation (2.20)

$$mg - \frac{L_0 I_0^2}{h_0} = 0 \tag{2.22}$$

Equation (2.22) can be used to obtain the values of steady-state parameters. Retaining only the linear terms in (2.19), and using the resulting relation in (2.17)

$$m\frac{d^2h(t)}{dt^2} = mg - k_L\left(\frac{I_o}{h_o}\right)^2 - \left(\frac{2k_L I_o}{h_o^2}\right)(i - I_o) + \left(\frac{2k_L I_o^2}{h_o^3}\right)(h - h_o)$$

Using the relationship of (2.22) and let $\hat{i} = i - I_o$, $\hat{h} = h - h_o$, the linearized mechanical model of MLS will be

$$\frac{d^2h(t)}{dt} = -\left(\frac{2k_L I_o}{mh_o^2}\right)\hat{i} + \left(\frac{2k_L I_o^2}{mh_o^3}\right)\hat{h}$$

Using the value of $k_L$ from (2.20), the constants from above relation can be defined as

$$k_1 = \left(\frac{2k_L I_o}{mh_o^2}\right) = \frac{2h_0 L_0 I_0}{mh_0^2} = \frac{2L_0 I_0}{mh_0^2} \tag{2.23a}$$

$$k_2 = \left(\frac{2k_L I_o^2}{mh_o^3}\right) = \frac{2L_0 h_0 I_0^2}{mh_0^3} = \frac{2L_0 I_0^2}{mh_0^2} \tag{2.23b}$$

Thus the linearized version of MLS model becomes

$$\frac{d^2\hat{h}(t)}{dt^2} = -k_1\hat{i}(t) + k_2\hat{h}(t) \tag{2.24}$$

Using Laplace transform, the transfer function of the system will be

$$\frac{\hat{(}H)(s)}{\hat{I}(s)} = \frac{k_1}{s^2 - k_2} \tag{2.25}$$

In real scenarios [52], [37], [1] each coil does have some resistance, let it be $R_c$, and let the $L$ is the inductance of the coil, then the current passing through the coil and voltage signal from the controller can

be related as

$$L\frac{d\hat{i}(t)}{dt} + R_c\hat{i}(t) = u(t)$$

Using Laplace transform, it can be given by

$$\frac{\hat{I}(s)}{U(s)} = \frac{1}{Ls + R_c} = \frac{(1/L)}{s + (R_c/L)} = \frac{k_3}{s + k_4} \tag{2.26}$$

Using the fact that dynamics of coil and metallic ball levitation are in cascade, the transfer function of the MLS plant will become

$$\frac{\hat{H}(s)}{\hat{I}(s)}\frac{\hat{I}(s)}{U(s)} = -\frac{k_1}{s^2 - k_2}\frac{k_3}{s + k_4} \tag{2.27}$$

Using the parameters values from Table ?? , the transfer function

| Parameter | Definition | Value |
|---|---|---|
| $m$ | Mass of Magnetic Ball | 0.00564 Kg |
| $R_c$ | Resistance of Coil | 60 Ω |
| $L$ | Inductance of Coil | 282.2mH |
| $h_o$ | Point of Levitation | 0.02 m |
| $I_o$ | Current through coil Corresponding to $h_o$ | 0.02 A |
| $L_o$ | (2.22) | 2.7636 H |
| $k_1$ | (3.23a) | 980 |
| $k_2$ | (3.23b) | 980 |
| $k_3$ | (2.26) | 3.544 |
| $k_4$ | (2.26) | 212.615 |

TABLE 2.1: MLS Plant Parameters

of the plant will be

$$\frac{\hat{H}(s)}{I(s)} = -\left(\frac{980}{s^2 - 980}\right)\left(\frac{3.544}{s + 212.615}\right)$$

$$\frac{\hat{H}(s)}{I(s)} = -\frac{3473}{s^3 + 213s^2 - 980s - 208363} \tag{2.28}$$

### 2.3.2 Plant Analysis

From (2.28) it can clearly be seen that the plant is unstable. FIGURE 2.3 shows the pole-zero plot of plant. From where it can be seen that one of poles lie in right half of s-plane. So the task of the controller will be two-fold, make the system stable in the firstly and cause the control system to follow the reference successfully.

FIGURE 2.4 shows the bode diagram of the system. It indicates infinity gain margin and phase margin which is a good thing, but the system is unstable. As the system is unstable, so there is no reason that the system will be satisfying sensitivity constraints. So in terms of frequency response analysis, the task of the controller will be make the stable and meet the objectives laid down by loop-shaping design. Following the outlines stated so far, next subsection presents the design of PID controller.

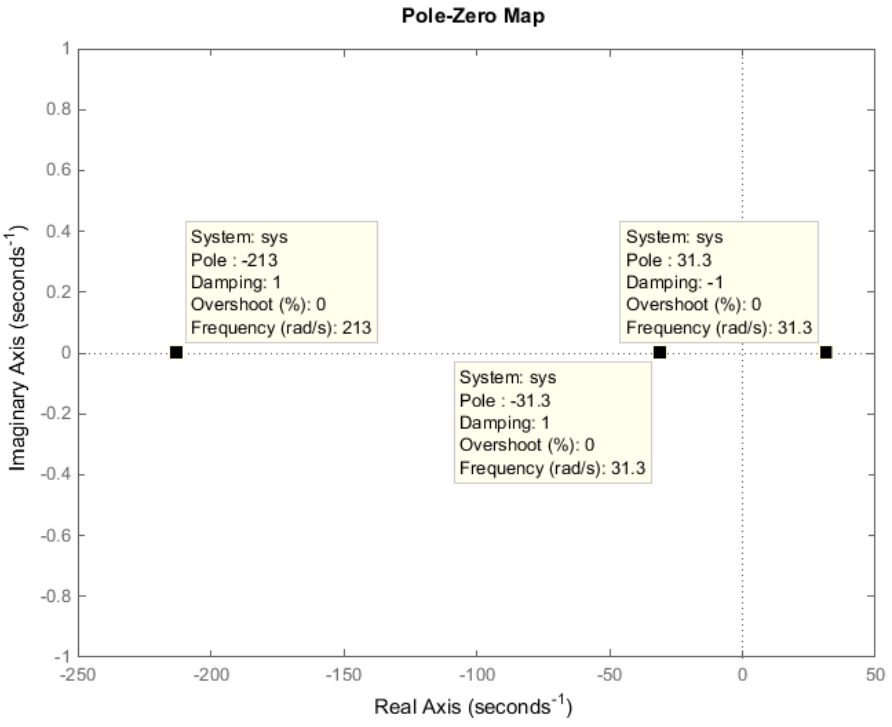


FIGURE 2.3: Pole-Zero Plot of MLS Plant

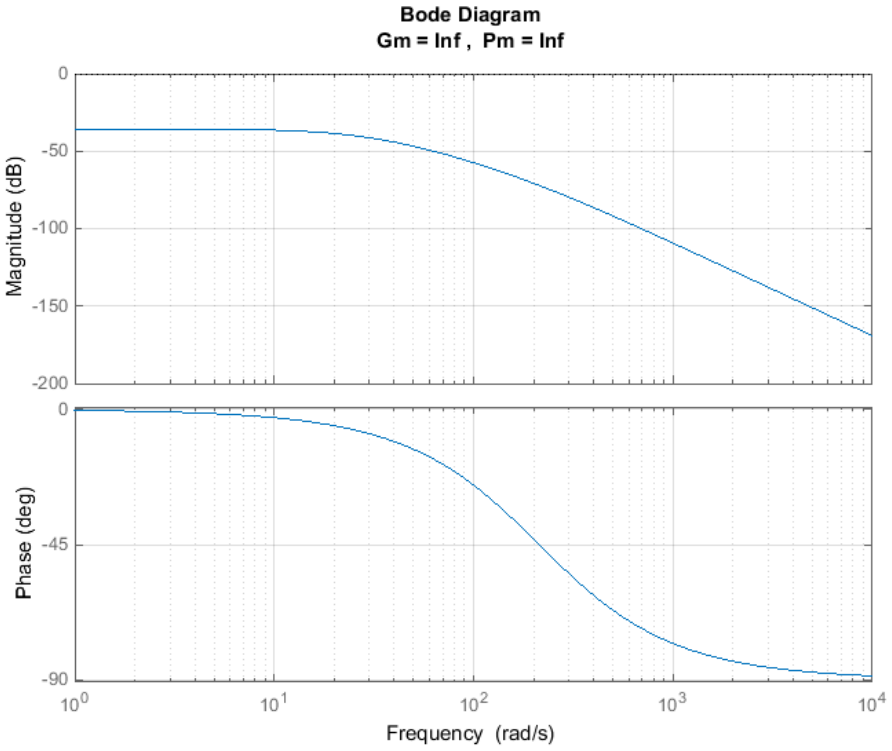


FIGURE 2.4: Frequency Response Analysis

### 2.3.3 Control Design Using Loop-Shaping

The transfer function of a typical PD controller is given by

$$G_C(s) = k_p + \frac{k_i}{s} + \frac{k_d s}{s + p_f} \tag{2.29}$$

Which can be modified to

$$G_C(s) = \frac{K(1 + T_1 s)(1 + T_2)}{s(1 + s)} \tag{2.30}$$

Thus the loop transfer function becomes

$$L(s) = \frac{-3473K(1 + T_1 s)(1 + T_2 s)}{s(1 + {}_1 s)(s^2 + 213s^2 - 980s - 20363)} \tag{2.31}$$

With this the design objectives of loop-shaping become (along with roots of $1 + L(s) = 0$, all lie in the left half of s-plane)

- ☐ Rise Time: $t_r \leq 0.2\,sec$

☐ Settling Time: $t_s \leq 0.4\,sec$

☐ Percentage Overshoot: $0 \leq \text{POS} \leq 10$

☐ Bandwidth: $\omega_b \geq 10\,rad/sec$

☐ Phase Margin: $30^\circ < \Phi_m \leq 60^\circ$

The controller is designed using MATLAB, and this comes out to be

$$G_C(s) = \frac{(-1.086 \times 10^5)(s + 1.705)(s + 5.15)}{s(s + 7821)} \tag{2.32}$$

From (2.32), PID controller gains can easily be calculated. FIGURE

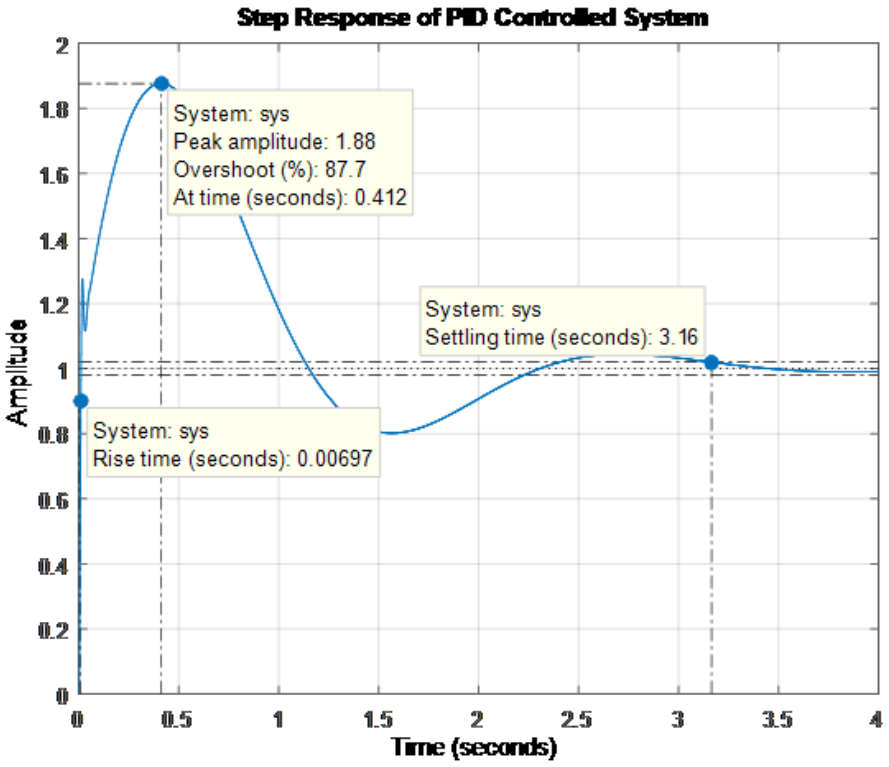


FIGURE 2.5: Step Response of PID Controller

2.5 shows the time domain response of the PID controlled system, while FIGURE 2.6 shows the frequency response with margins.

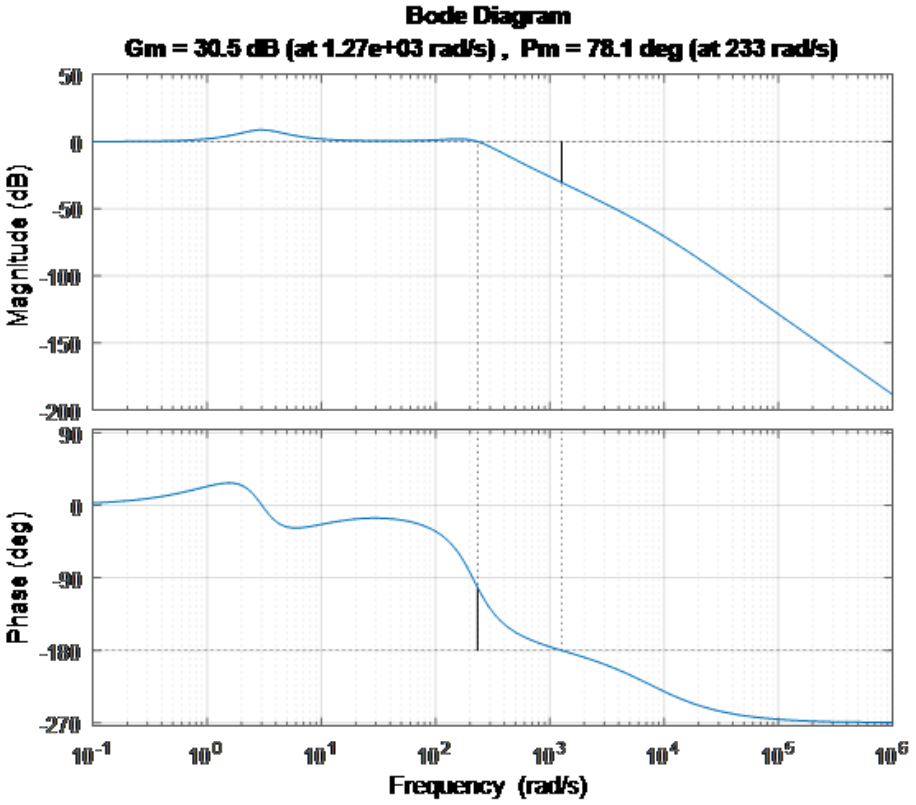


FIGURE 2.6: Stability Margins of PID Controlled System

From FIGURE 2.5 it can be seen that PID controller could not meet all time domain specifications. Specifically, percentage overshoot is completely inacceptable. FIGURE 2.6 shows the frequency response stability margins. It is usually the case that if the magnitude response grows up for lower frequencies than gain cross-over frequencies, and decays down from gain cross-over the closed-loop systems inherits robustness and disturbance/noise rejection properties. From its magnitude response it can be seen that, it will reject disturbances/noises, but will not robust to system parameters changes. From the value of phase margin, the above argument can be validated. A phase closer to 60 degree favors robustness. The controller has brought stability in the closed-loop system but desired response has not been met. It is the lacking of robustness that, overshoot has risen to unacceptable values and the settling is not what is desired. FIGURE 2.7 shows the disturbance response

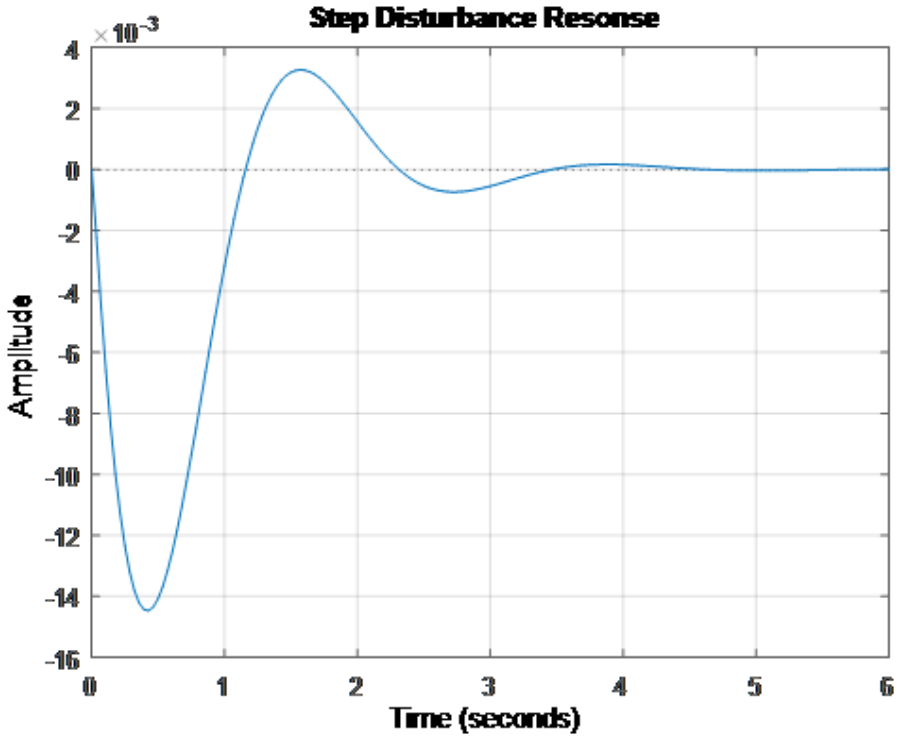


FIGURE 2.7: Disturbance Response

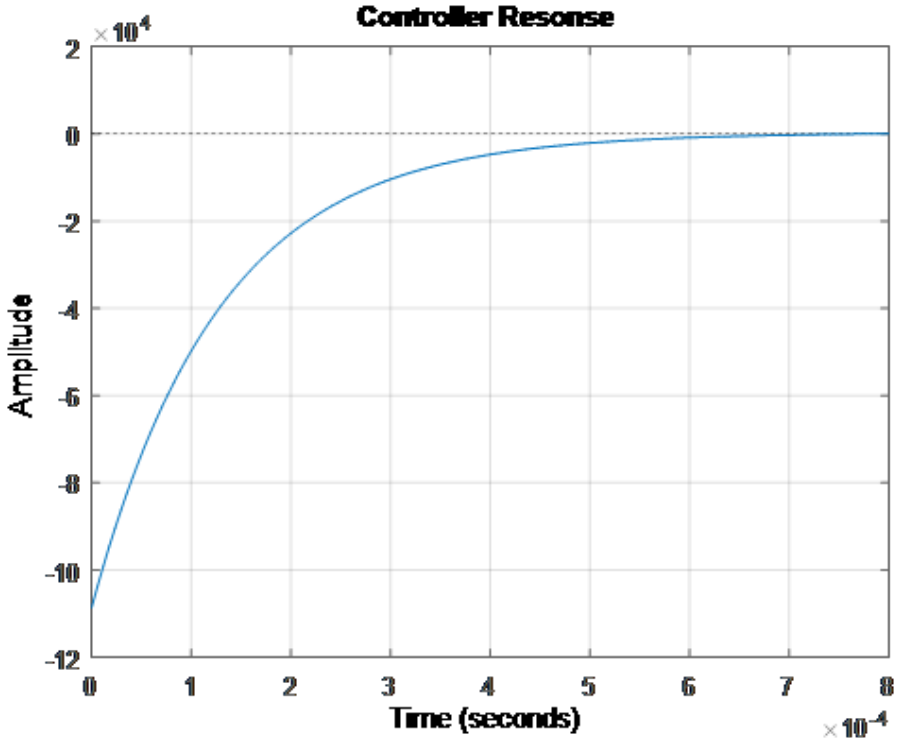


FIGURE 2.8: Controller's Response

of the system, while FIGURE 2.8 shows the controllers response to reference input. From it can be seen that the system offers almost perfect rejection to disturbances, but with the expense of huge controllers effort. Obtainment of such a huge efforts is often physically non-realizable.

## 2.4 Conclusive Remarks

Loop-shaping control is a frequency domain design method. The term loop-shaping has been coined because of the fact that the parameters of the controller in the loop transfer function are designed is such a way that loop response inhibits desired characteristics. Since it is based upon optimization of response of the loop transfer functions, many methods have been proposed to solve for the controller parameters. But as the controller order and form is not fixed, the design might require several iterations. And if the controller order is fixed, the designed controller is not ensured to meet the required specifications. This is perhaps due to the fact that this design method does not incorporate the design required directly in the optimization problem. But if by somehow, the constraints are developed incorporating the design requirements, the optimization problem becomes undesirable complex and non-linear and can cost huge computational time.

In this chapter PID controller has successfully been design and it has rejected the disturbance successfully. But as expected, the controller effort is boundless. This controller has not met the theoretical expectations of meeting the design requirements. Better solutions for the control magnetic levitation system will be presented in the upcoming chapters.

# Chapter 3

# Active Disturbance Rejection Control

Minimization or even elimination of effects of disturbance and measurement noise has always been a challenge for the control engineers. The effects caused by latter inputs might always incur due to sudden changes in reference input. All such kind of issues have systematically been addressed in ADRC (Active Disturbance Rejection Control). The issues are set-point jump, tracking differentiator, estimating the effect of disturbance from the systems output and linear feedback control. Such changes in set-point are controlled with reference profile generator. The reference profile generator ensures that sudden changes in set-point do not causes abruptness in the system. Classical controllers usually have derivative control as part of their control algorithm. Derivative control has tendency of picking and amplifying noise. ADRC provides the solution to such a situation. Linear feedback estimates all the states of the systems and the controller exerts its efforts according the amount of feedback, without estimating the effects of disturbances or noises explicitly. But ADRC dedicates an extra state (in some cases more than one state) for estimation of undesired effects, thus the controller counteracts them

more effectively. Such a state observer is called extended state observer (ESO). Although, the implementation of non-linear controller might pose some challenges, but non-linear controller performs the required control action. Such implementations might help avoidance of actuator misbehavior. In this chapter a comprehensive account of this theory is presented.

## 3.1 ADRC Framework

As pointed earlier, active disturbance rejection control consists essentially of FOUR components. These four components have been derived from some of shortcomings of PID controller. FIGURE-3.1 shows the block diagram of error-based PID control system. In this diagram $v$ is the set point, $y$ is the output from controller and $u$ is the controller actuation. The error signal $e$ is defined as $e = v - y$. This actuation signal $u$ from the controller can be defined as

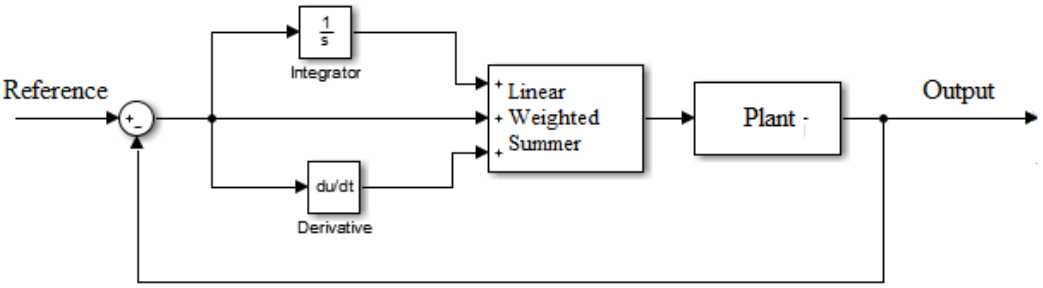


FIGURE 3.1: Classical PID Control

$$u = k_o \int e(t)dt + k_1 e + k_2 \frac{de(t)}{dt} \tag{3.1}$$

This is primitive control mechanism offered by PID. It is such a powerful controller, that in some cases it does not need the plant model for its design. This point is elaborated now. A second order

plant can be represented as

$$\begin{cases} \dot{x}_1 = x_2 \\ \dot{x}_2 = a_1 x_1 + a_2 x_2 + bu \\ y = x_1 \end{cases} \tag{3.2}$$

Using the definition of error $e_1 = v - y = v - x_1$, this implies that

$$\dot{e}_1 = -\dot{x}_1 = e_2 \Rightarrow e_2 = -x_2$$

$$\dot{e}_2 = -\dot{x}_2$$

Using these relations and equation (3.1)

$$\begin{cases} \dot{e}_1 = e_2 \\ \dot{e}_2 = -[a_1(v - e_1) + a_2(-a_2) + bu \end{cases}$$

this leads to

$$\begin{cases} \dot{e}_1 = e_2 \\ \dot{e}_2 = a_1 e_1 + a_2 e_2 - a_1 v - bu \end{cases}$$

From (3.1) let $e_0 = \int e(t)dt$, this implies that $\dot{e}_0 = e_1 = e$, thus (3.1) can be written as

$$u = k_o e_0 + k_1 e_1 + k_2 e_2 \tag{3.3}$$

Using this relationship in above equation

$$\begin{cases} \dot{e}_0 = e_1 \\ \dot{e}_1 = e_2 \\ \dot{e}_2 = a_1 e_1 + a_2 e_2 - a_1 v - b(k_o e_0 + k_1 e_1 + k_2 e_2) \end{cases}$$

$$\begin{cases} \dot{e}_0 = e_1 \\ \dot{e}_1 = e_2 \\ \dot{e}_2 = -bk_o e_0 + (a_1 - bk_1)e_1 + (a_2 - bk_2)e_2 - a_1 v \end{cases} \tag{3.4}$$

From this preceding relationship, it can clearly be seen that if the controller parameters be chosen such that, $bk_0 > 0$, $a_1 - bk_1 < 0$ and

$a_2 - bk_2 < 0$, the error dynamics will die out and the system will be tracking the reference input. From the above analysis it can be found that PID controller can easily be tuned for any kind of plant as given by (3.2) and (3.4) gives the design equation. Some basic shortcomings have been identified in literature in the applications of PID. Firstly, the controller can actuate sudden actions if the set-point is jump, often is the case that set-point is often in the form of a step input. This sudden application of set-point can trigger unusual in some complex systems. PID control has no remedy for this issue. Secondly, the D-part of PID controller is sensitive to noise. To avoid this issue, a minor type of first order filter is cascaded with D-part. But this solution can undermine the overall performance of PID. Thirdly, the summation of three error dynamics can cause unusual behavior. And finally, the integral term in PID cannot be avoided, since it ensures the steady state performance of the system. D-term is often avoided if it is not needed critically. As the I-term introduces a pole on the origin, so it can cause saturation of the actuators and sometimes can lead to instability. The solutions to all these problems are offered by ADRC framework as detailed below.

### 3.1.1 Setpoint Profile Design

To avoid the bad effects of set-point, smoother profile can be designed as follows. For the design of such a profile, it is assumed that the plant is nth order integrator. A nth order plant can be modeled as

$$\begin{cases} \dot{x}_1 = x_2 \\ \dot{x}_2 = x_3 \\ \quad \vdots \\ \dot{x}_n = u \end{cases} \tag{3.5}$$

Letting $|u| \leq r$, $u$ can be given by

$$u = -r \operatorname{sign}\left(x_1 - v\frac{x_n|x_n|}{2r}\right) \tag{3.6}$$

Using the principle outlined by (E3.6), the transient can be obtained from the solution (E3.7)

$$\begin{cases} \dot{v}_1 = v_2 \\ \dot{v}_2 = v_3 \\ \vdots \\ \dot{v}_n = -r \operatorname{sign}\left(x_1 - v\frac{x_n|x_n|}{2r}\right) \end{cases} \tag{3.7}$$

The parameter $v$ is the set point and the value of parameter $r$ determines the speed of transient profile. That is $r$ is the design parameter. Discrete time implementation of (E3.7) is also possible within a digital processor. But the relationships are very complex to be implemented. Often such an implementation is avoided. But if the transient profile design inevitable, first of second order filters are used to smooth out troubling spike in set-point jumps.

### 3.1.2 Tracking Differentiator

Tracking differentiator is the second fundamental component in the design and application of ADRC. In PID framework, it often implemented as

$$U_d(s) = \frac{k_d s}{T_f s + 1} = \frac{k_d}{T_f}\left(1 - \frac{1/T_f}{s + 1/T_f}\right) E(s) \tag{3.8}$$

Whereas $k_d$ is the derivative constant, $T_f$ is the filters time constant $u_d$ is the D-part of actuation signal and e is the error signal. A time-domain description of (3.8) can be written as

$$u_d(t) = \frac{k_d}{T_f}\left(e(t) - e(t - T_f)\right) \tag{3.9}$$

From (3.9) it can be seen even if the amount of noise is very small, it will be amplified by the gain $\frac{k_d}{T_f}$ . One possible solution to this issue is to minimize $k_d$ and/or to increase $T_f$. But such a choice can lead to almost no contribution from derivative control term. A better remedy is given in the framework of ADRC.

The error derivative can be given by another way

$$\dot{e} \equiv \frac{e(t-\tau_1) - e(t-\tau_2)}{\tau_2 - \tau_1} \tag{3.10}$$

The transfer function of this approximation can be given by

$$W_1(s) = \frac{1}{\tau_2 - \tau_1}\left(\frac{1}{\tau_1 s + 1} - \frac{1}{\tau_2 s + 1}\right) \tag{3.11}$$

This provides enough attenuation to the noise, depending upon the proper choice of parameters $\tau_1$ and $\tau_2$. A second order approximation to derivative has also been suggested. Which can be given by

$$W_2(s) = \frac{s}{(\tau s + 1)^2}$$

Whose time domain description will be

$$\ddot{e} = -r\left(e - v(t)\right) - 2r\dot{e}) \tag{3.12}$$

The implementation of equation (3.12) can be inspired by (3.7).

### 3.1.3 Non-Linear Feedback Controller

Third fundamental component of ADRC is the non-linear feedback controller. This type of controller can be defined as

$$u = \text{fal}(e, \alpha, \delta) = \begin{cases} \frac{e}{\delta^{-\alpha}} & x \leq \delta \\ |e|^{\alpha}\text{sign}(e) & x > \delta \end{cases} \tag{3.13}$$

Whereas the discrete time realization of (3.13) is given by

$$\text{fhan}(x_1,\ x_2,\ \cdots,\ x_n,\ r,\ h_0)$$

similar to (3.7). From (3.13), it can be seen that this kind of control could be very useful. Not only it can ensure stability, but the non-linear saturation might also be avoided.

### 3.1.4 The Extended State Observer

The most important component of ADRC is the extended state observer. It is well known that a nth order system can have n states and if the states are not directly measureable, nth order state observer/estimator is designed to obtain the states from the measurement of output. The term extended state observer has been formed due to the fact more than n states are estimated. The extra states give the information about the presence of disturbance and unusual behavior within the system. Thus extended state observer plays an important role in the rejection disturbance. Let a plant is described as

$$\begin{cases} \dot{x}_1 = x_2 \\ \dot{x}_2 = x_3 \\ \vdots \\ \dot{x}_n = x_{n-1} + f(x_1,\ x_2,\ \cdots,\ x_n,\ w(t),\ t) + bu \\ \dot{x}_{n+1} = g(t) \end{cases}$$

Here $f$ represents the total disturbance and this is to be estimated by $x_{n+1}$. In most cases, one extra state is considered adequate for the estimation of disturbances. But if required mode more than one states can also be estimated. Putting everything together, following configuration of ADRC, shown in FIGURE 3.2, is obtained as suggested fundamentally. In the upcoming section some design methods of ADRC are presented.

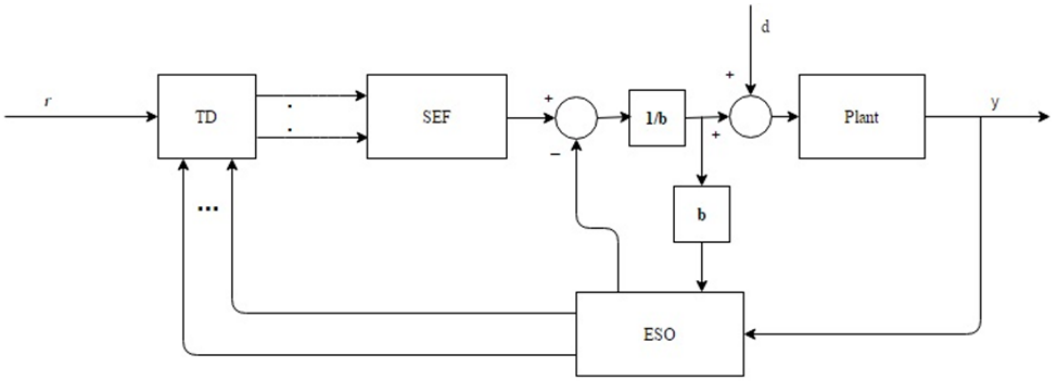


FIGURE 3.2: ADRC Framework

## 3.2 Linear ADRC

From the above discussion it can be seen than all three major components of ADRC: tracking differentiator, extended state observer and state error feedback are non-linear in nature. Each component contains one or more parameters, the design of is not straightforward. Additionally, it might require a number of iterations due to fact that no stability criterion exist on which the design could be processed. In [42] extended circle criterion to ensure closed-loop stability has been presented, but using this criterion as a design might need a number of criterion.

Fortunately, linear versions of ADRC has also been developed, which inherits stability methods and design methods from classical control theory. The best thing is that theme features of ADRC like smooth reference tracking, active disturbance rejection has been retained by the linear version of ADRC.

This subsection is concerned with the design methods of ADRC. The section will begin with the process of designing linear ESOs for first order and second order system. Methods of designing generalized ADRC will follow. Since linear ADRC is retaining the good features of fundamental ADRC, so the discussion of non-linear ADRC will be avoided in this work.

### 3.2.1 Design of ADRC for First Order Systems

Consider the first order plant

$$\frac{Y(s)}{U(s)} = G_p(s) = \frac{k}{s+a} \tag{3.14}$$

Then

$$\dot{y} + ay(t) = ku(t)$$

Let there is a disturbance input d(t) and let $k = k_0 + \Delta k$, then the output-input relationship can be written as

$$\dot{y} + ay(t) + d(t) = (k_0 + \Delta k)u(t)$$

$$\dot{y} + \underbrace{ay(t) + d(t) + \Delta k u(t)} = k_0 u(t)$$

$$\dot{y} + f(t) = k_0 u(t) \tag{3.15}$$

The function $f(t)$ represents clutter, disturbances, noises, modeling errors and parametric variations etc. Now the job of ESO becomes to estimate everything which can perturb the smooth functioning of the systems and to remove it. As the observer design process has been inspired by Kalman filtering concepts, so state-space modeling of the system in (3.15) is required.

$$\begin{bmatrix} \dot{x}_1 \\ \dot{x}_2 \end{bmatrix} = \begin{bmatrix} 0 & 1 \\ 0 & 0 \end{bmatrix} \begin{bmatrix} x_1 \\ x_2 \end{bmatrix} + \begin{bmatrix} 0 \\ k_0 \end{bmatrix} u(t) + \begin{bmatrix} 0 \\ 1 \end{bmatrix} f(t)$$

As the system input and output are accessible, so the states of the system can be estimated along with the function $f(t)$. One way doing this is to use Luenberger observer. According to this proposed method

$$\begin{bmatrix} \dot{\hat{x}}_1 \\ \dot{\hat{x}}_2 \end{bmatrix} = \begin{bmatrix} 0 & 1 \\ 0 & 0 \end{bmatrix} \begin{bmatrix} \hat{x}_1 \\ \hat{x}_2 \end{bmatrix} + \begin{bmatrix} 0 \\ k_0 \end{bmatrix} u(t) - \begin{bmatrix} l_1 \\ l_2 \end{bmatrix} (\hat{x}_1 - y(t))$$

$$\begin{bmatrix} \dot{\hat{x}}_1 \\ \dot{\hat{x}}_2 \end{bmatrix} = \begin{bmatrix} -l_1 & 1 \\ -l_2 & 0 \end{bmatrix} \begin{bmatrix} \hat{x}_1 \\ \hat{x}_2 \end{bmatrix} + \begin{bmatrix} 0 \\ k_0 \end{bmatrix} u(t) + \begin{bmatrix} l_1 \\ l_2 \end{bmatrix} y(t) \tag{3.16}$$

Using the control law $u(t) = \frac{u_0(t)-f(t)}{k_0}$ , with $u_0(t) = k_p(r(t) - y(t))$, the equation (3.15) becomes

$$\dot{y} + k_p y(t) = k_p r(t) \tag{3.17}$$

Equation (3.16) shows the observer implementation equation and (3.17) gives the controller equation. From (3.16) and (3.17) it can be seen that it is entirely independent of what the actual system is. This is the notion which makes it different from model predictive control. From (3.16), the system matrix of the ESO will be

$$A - LC = \begin{bmatrix} -l_1 & 1 \\ -l_2 & 0 \end{bmatrix}$$

Therefore, the characteristic equation of the observer becomes

$$|sI - A + LC| = s^2 + l_1 s + l_2 = 0 \tag{3.18}$$

As the system is first-order, the unknown the controller parameter $k_p$ can be determined based on required settling time. For the first order system, settling time can approximately be given by

$$t_s \cong \frac{4}{\tau}$$

For the system in (3.17), $= \frac{1}{k_p}$ , therefore

$$k_p = \frac{4}{t_s}$$

Once the controller gain has been calculated, the observer parameters can be determined as follows. As the observer is to estimate the states, so it must faster than controller. One crude of doing so is to

set observe poles at

$$P_{1,2}^{ESO} = (5 \sim 10) \times P^{CL} = \frac{4(5 \sim 10)}{t_s}$$

With the desired characteristic equation of the extended observer becomes

$$(s - P_1^{ESO})(s - P_2^{ESO}) = s^2 - (P_1^{ESO} + P_2^{ESO})s + (P_1^{ESO} P_2^{ESO}) \quad (3.19)$$

Thus comparing (3.18) and (3.19)

$l_1 = -(P_1^{ESO} + P_2^{ESO})$ and $l_2 = (P_1^{ESO} P_2^{ESO})$

This completes the design of ADRC for the first order systems.

### 3.2.2 ADRC Design for Second Order System

Next considering a second order plant

$$\frac{Y(s)}{U(s)} = G_P(s) = \frac{k}{s^2 + a_1 s + a_0}$$

The time domain description of this system will be

$$\ddot{y} + a_1 \dot{y} + a_0 y = ku$$

Similar to second order case, this can be rewritten as

$$\ddot{y} + \underbrace{a_1 \dot{y} + a_0 y + d(t) - \Delta k u(t)} = k_0 u(t)$$

Its state-variables representation will be

$$\begin{bmatrix} \dot{x}_1 \\ \dot{x}_2 \\ \dot{x}_3 \end{bmatrix} = \begin{bmatrix} 0 & 1 & 0 \\ 0 & 0 & 1 \\ 0 & 0 & 0 \end{bmatrix} \begin{bmatrix} x_1 \\ x_2 \\ x_3 \end{bmatrix} + \begin{bmatrix} 0 \\ k_0 \\ 0 \end{bmatrix} u(t) + \begin{bmatrix} 0 \\ 0 \\ 1 \end{bmatrix} \dot{f}(t)$$

Where as usual, $x_3 = f(t)$ is representing the disturbance and modeling errors in the system. Assuming that an estimator that will

produce faithful estimation of the state of the system, an implementation of the observer system can be given by

$$\begin{bmatrix}\dot{\hat{x}}_1\\ \dot{\hat{x}}_2\\ \dot{\hat{x}}_3\end{bmatrix} = \begin{bmatrix}0 & 1 & 0\\ 0 & 0 & 1\\ 0 & 0 & 0\end{bmatrix}\begin{bmatrix}\hat{x}_1\\ \hat{x}_2\\ \hat{x}_3\end{bmatrix} + \begin{bmatrix}0\\ k_0\\ 0\end{bmatrix} u(t) - \begin{bmatrix}l_1\\ l_2\\ l_3\end{bmatrix}[\hat{x}_1 - y(t)]$$

$$\begin{bmatrix}\dot{\hat{x}}_1\\ \dot{\hat{x}}_2\\ \dot{\hat{x}}_3\end{bmatrix} = \begin{bmatrix}-l_1 & 1 & 0\\ -l_2 & 0 & 1\\ -l_3 & 0 & 0\end{bmatrix}\begin{bmatrix}\hat{x}_1\\ \hat{x}_2\\ \hat{x}_3\end{bmatrix} + \begin{bmatrix}0\\ k_0\\ 0\end{bmatrix} u(t) + \begin{bmatrix}l_1\\ l_2\\ l_3\end{bmatrix} y(t) \tag{3.20}$$

From equation (3.20) the system matrix of the observer will be

$$A - LC = \begin{bmatrix}-l_1 & 1 & 0\\ -l_2 & 0 & 1\\ -l_3 & 0 & 0\end{bmatrix}$$

And hence the characteristic equation will be

$$|sI - A + LC| = s^3 + l_1 s^2 + l_2 s + l_3 \tag{3.21}$$

With the availability of states, control law can be defined as

$$u(t) = \frac{1}{k_0}(u_0(t) - \hat{f}(t))$$

Whereas $u_0(t)$ is defined as

$$u_0(t) = k_p\,(r(t) - \hat{y}(t)) - k_d\dot{y}$$

The desired equation of the system becomes

$$\ddot{y} + k_d\dot{y} + k_p y = k_p u \tag{3.22}$$

The most common ways of designing second-order system are based on settling time and percentage overshoot specifications. Given desired percentage overshoot, the value of damping ratio $\zeta$ can be determined from

$$\% \text{ OS} = 100 \exp(-\frac{\zeta\pi}{\sqrt{1-\zeta^2}})$$

Once the value of $\zeta$ is known, the value of un-damped natural frequency $\omega_n$ is given by 2 % settling time criterion

$$t_s = \frac{4}{\zeta\omega_n}$$

Then closed loop roots of the system are given by

$$s_{1,2}^{CL} = -\zeta\omega_n \pm j\sqrt{1-\zeta^2}$$

Similar to first order system, the observer poles can be obtained from

$$P_{1,2}^{ESO} = (5 \sim 10) \times P_{1,2}^{CL}$$

Third pole can be placed even farther from $\text{Re}(P_{1,2}^{ESO})$ on real axis in the left half of s-plane.

### 3.2.3 Design of Generalized ADRC

From the conclusions above, any Nth order system can be represented by

$$y^{(n)} + f(t) = k_0 u(t)$$

Generalizing (3.16) and (3.20), it can be shown that ESO implementation equation for an nth-orde system will be

$$\begin{bmatrix} \dot{\hat{x}}_1 \\ \dot{\hat{x}}_1 \\ \vdots \\ \dot{\hat{x}}_n \end{bmatrix} = \begin{bmatrix} 0 & 1 & 0 & \cdots & 0 \\ 0 & 0 & 1 & \cdots & 0 \\ \vdots & \vdots & \vdots & \vdots & \vdots \\ 0 & 0 & 0 & \cdots & 1 \\ 0 & 0 & 0 & \cdots & 0 \end{bmatrix} \begin{bmatrix} \hat{x}_1 \\ \hat{x}_2 \\ \vdots \\ \hat{x}_n \end{bmatrix} + \begin{bmatrix} 0 \\ 0 \\ \vdots \\ 0 \\ k_0 \\ 0 \end{bmatrix} u(t) - \begin{bmatrix} l_1 \\ l_2 \\ \vdots \\ l_{n-1} \\ l_n \end{bmatrix} (\hat{x}_1 - y(t))$$

And desired characteristic equation of the observer will become

$$|sI - A + LC| = s^n + l_1 s^(n-1) + l_2 s^(n-2) + \ + l_(n-1)s + l_n = 0$$

Defining a control law

$$u(t) = \frac{u_0(t) - f(t)}{k_0}$$

whereas

$$u_0(t) = k_1(r(t) - \hat{x}_1(t)) - k_2\hat{x}_2(t) - k_3\hat{x}_3(t) - \cdots - k_n\hat{x}_n(t)$$

A number of procedures can be found in literature. One way of doing so is to compare the desired and defined characteristic equations. Ackermans can also be used for this purpose. And Finally LQR methods can also be used to find the best pole locations both for feedback controller and ESO (Extended-State-Observer).

## 3.3 ADRC Control Design for MLS Plant

This section presents the implementation of ADRC on the MLS plant.

### 3.3.1 The Plant Model

From equation (2.28)

$$\frac{Y(s)}{U(s)} = -\frac{3473}{s^3 + 213s^2 - 980s - 208363}$$

In differential equation form

$$\dddot{y} + 213\ddot{y} - 980\dot{y} - 208363y = -3473u(t)$$

$$\dddot{y} + underbrace213\ddot{y} - 980\dot{y} - 208363y + d(t) + 3473u(t) = u(t)$$

$$\dddot{y} + f(t) = u(t)$$

Thus the state-space representation of the system will be

$$\begin{bmatrix} \dot{x}_1 \\ \dot{x}_2 \\ \dot{x}_3 \\ \dot{x}_4 \end{bmatrix} = \begin{bmatrix} 0 & 1 & 0 & 0 \\ 0 & 0 & 1 & 0 \\ 0 & 0 & 0 & 1 \\ 0 & 0 & 0 & 0 \end{bmatrix} \begin{bmatrix} x_1 \\ x_2 \\ x_3 \\ x_4 \end{bmatrix} + \begin{bmatrix} 0 \\ 0 \\ 1 \\ 0 \end{bmatrix} u(t) + \begin{bmatrix} 0 \\ 0 \\ 0 \\ 1 \end{bmatrix} \dot{f}(t) \tag{3.23}$$

### 3.3.2 ADRC Controller Design

Assuming that the observer to be designed will faithfully estimate the states, then Luenberger form of the observer will be

$$\begin{bmatrix} \dot{\hat{x}}_1 \\ \dot{\hat{x}}_2 \\ \dot{\hat{x}}_3 \\ \dot{\hat{x}}_4 \end{bmatrix} = \begin{bmatrix} 0 & 1 & 0 & 0 \\ 0 & 0 & 1 & 0 \\ 0 & 0 & 0 & 1 \\ 0 & 0 & 0 & 0 \end{bmatrix} \begin{bmatrix} \hat{x}_1 \\ \hat{x}_2 \\ \hat{x}_3 \\ \hat{x}_4 \end{bmatrix} + \begin{bmatrix} 0 \\ 0 \\ 1 \\ 0 \end{bmatrix} u(t) - \begin{bmatrix} l_1 \\ l_2 \\ l_3 \\ l_4 \end{bmatrix} \{\hat{x}_1(t) - y(t)\}$$

$$\begin{bmatrix} \dot{\hat{x}}_1 \\ \dot{\hat{x}}_2 \\ \dot{\hat{x}}_3 \\ \dot{\hat{x}}_4 \end{bmatrix} = \begin{bmatrix} -l_1 & 1 & 0 & 0 \\ -l_2 & 0 & 1 & 0 \\ -l_3 & 0 & 0 & 1 \\ -l_4 & 0 & 0 & 0 \end{bmatrix} \begin{bmatrix} \hat{x}_1 \\ \hat{x}_2 \\ \hat{x}_3 \\ \hat{x}_4 \end{bmatrix} + \begin{bmatrix} 0 \\ 0 \\ 1 \\ 0 \end{bmatrix} u(t) + \begin{bmatrix} l_1 \\ l_2 \\ l_3 \\ l_4 \end{bmatrix} y(t) \tag{3.24}$$

Using a control law $u(t) = \{u_0(t) + f(t)\}$, whereas

$$u_0(t) = k_1[r(t) - \hat{y}(t)] - k_2\dot{\hat{y}}(t) - k_3\ddot{\hat{y}}(t)$$

The design equation for out controller becomes

$$\dddot{y} + k_3\ddot{y} + k_2\dot{y} + k_1 y = k_1 u$$

From here the characteristic equation of the system will be

$$s^3 + k_3 s^2 + k_2 s + k_1 = 0 \tag{3.25}$$

Using the control specifications of Chapter 2, the required damping ratio is $\zeta = 0.7$ and undamped natural frequency for $t_s = 0.4\,sec$ is $\omega_n = \frac{100}{7}$. Thus the dominant closed-loop poles of the system should be at

$$s_{1,2} = -10 \pm j10.2$$

To minimize the effect third pole, this should be placed about 5 to 10 times farther into the LH of s-plane. So let $s_3 = -80$. Thus the desired characteristic equation becomes

$$(s + 80)(s^2 + 20s + 204.04) = s^3 + 100s^2 + 1804.04s + 16323.2 = 0 \tag{3.26}$$

Values of all controller parameters can easily be obtained by comparing equations (3.25) and (3.26). For faster estimation of states, let the dominant poles be multiplied by 15, then the characteristic equation of the ESO becomes

$$(s^2 + 300s + 45909)^2 = 0$$

Thus the parameters of ESO can be calculated from

$$s^4 + 600s^3 + 181818s^2 + 27545400s + (2.1076 \times 10^9) = 0 \tag{3.27}$$

From equation (3.27) observer parameters can easily be obtained. This completes the ADRC control design. The characteristic equation of the ESO will be

$$s^4 + l_1 s^3 + l_2 s^2 + l_3 s + l_4 = 0$$

Comparing equation (3.27) with (3.24), following observer implementation equations are obtained.

$$\dot{\hat{x}}_1 = -600\hat{x}_1 + \hat{x}_2 + 600y(t)$$

$$\dot{\hat{x}}_2 = -181818\hat{x}_1 + \hat{x}_3 + 181818y(t)$$

$$\dot{\hat{x}}_3 = -27545400\hat{x}_1 + \hat{x}_4 + 27545400y(t) + u(t)$$

$$\dot{\hat{x}}_4 = -(2.1076 \times 10^9)\hat{x}_1 + (2.1076 \times 10^9)y(t)$$

### 3.3.3 System Simulations

FIGURE-3.3 shows the implementation of ADRC control for MLS plant. In this design and implementation two component of ADRC scheme has been used (It consists originally of transient profiler, extended-state-observer (ESO) and feedback controller).

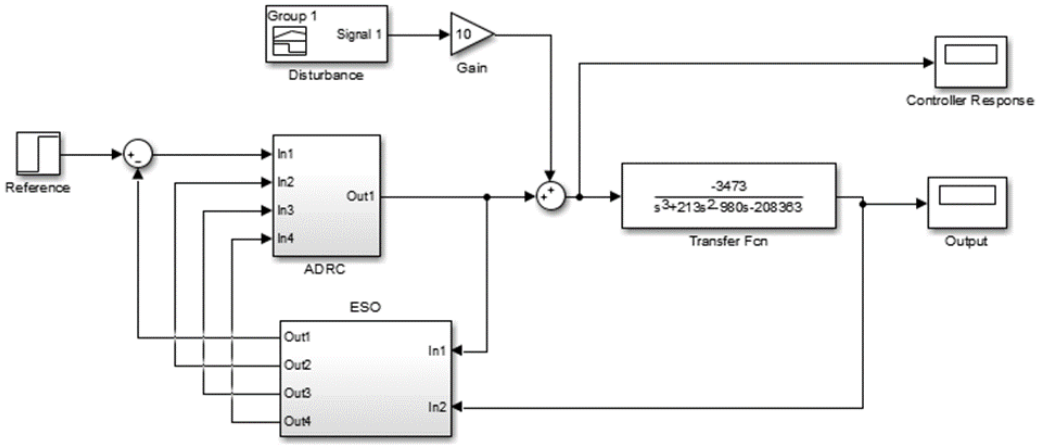


FIGURE 3.3: ADRC Control System

### 3.3.4 Results

FIGURE 3.5 shows the step and disturbance responses of the system based on ADRC control. From here it can be seen that although the original system is unstable, the ADRC controller not only stabilizes the system, but ensures satisfaction of design requirements. A small steady state error can be seen which could be of less concern in many cases in comparison to advantages the method has brought. These good things are, that the system has no overshoot, settling time is lower than for what value the controller was designed, it has provided good rise.

FIGURE 3.4 shows both reference and disturbance inputs. The disturbance input has been generated using Gaussian process. This disturbance input was applied to the system along with reference, and from the systems response it can be seen that it has not affected the system performance.

Along with step and disturbance responses, FIGURE 3.5 also shows the controller effort. From here it can be seen that the controller does not show any response to disturbance input. So it can be said that the controller has given perfect rejection of disturbance inputs and faithful tracking of reference signals. But the controller poses some serious issues in regards to its practical implementations. These issues have been pointed out in the next section.

## 3.4 Conclusive Remarks

As stated above, that FIGURE 3.5 shows perfect tracking of reference input. But from the same figure it can be seen that initially when the step input is applied, the controller effort is approaching a value of about 60 units which is enormous. Such a large signal can quickly and easily saturate the controller. If the controller is

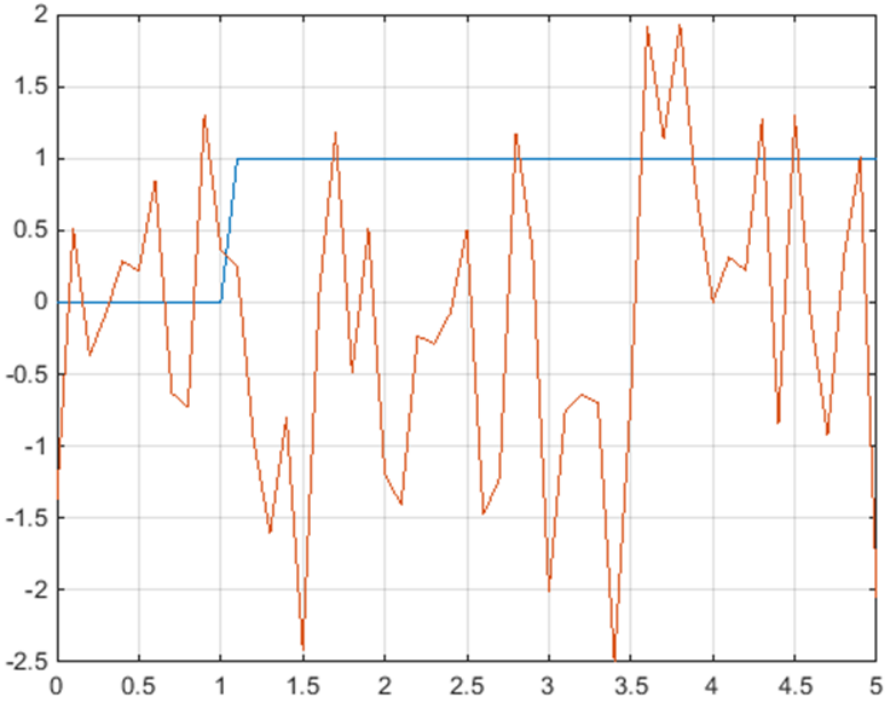


FIGURE 3.4: Step and Disturbance Inputs to ADRC Controlled System

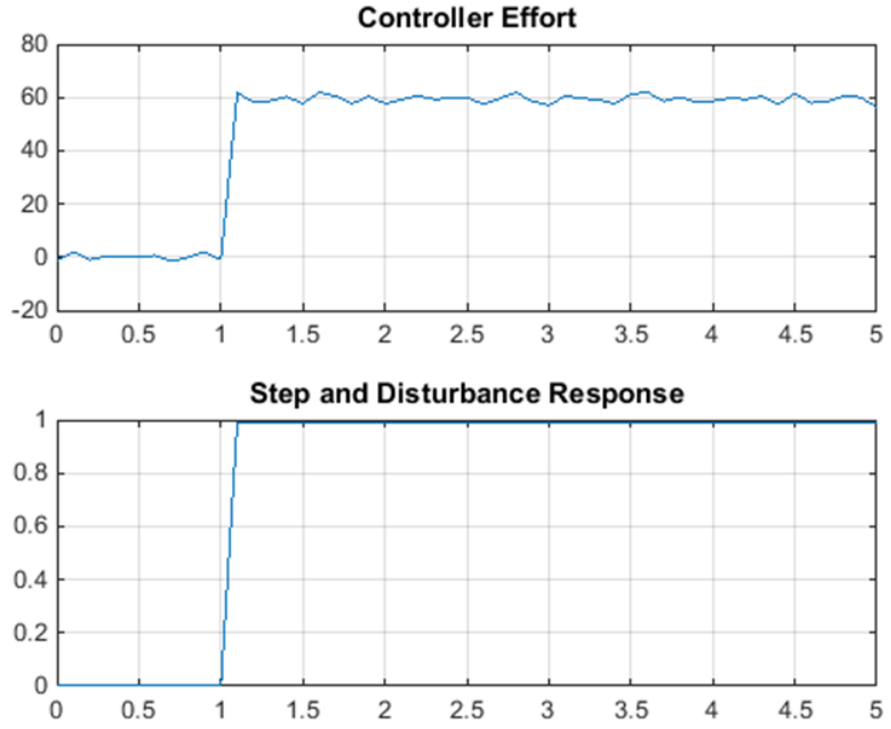


FIGURE 3.5: Step and Disturbance Responses along with Controller Effort

restricted to certain limits (keeping in view that it will be implemented physically with some kind of hardware), the output response completely deteriorates and the controller is unable to enforce corrections. This can be seen in FIGURE 3.6 and FIGURE 3.7. FIGURE 3.6 shows the output after saturation limits are applied and FIGURE 3.7 shows the controller effort. Controller gives the feel of eagerness to impose corrections according as the reference inputs. But as its effort is limited by the saturation, so it is unable to. From these results it can be concluded that due to limited output from the controller, the output may not track the input. So while designing controllers, this limitation must be considered. The solution to this problem has adequately been addressed in quasilinear control theory, which will be presented in upcoming chapters.

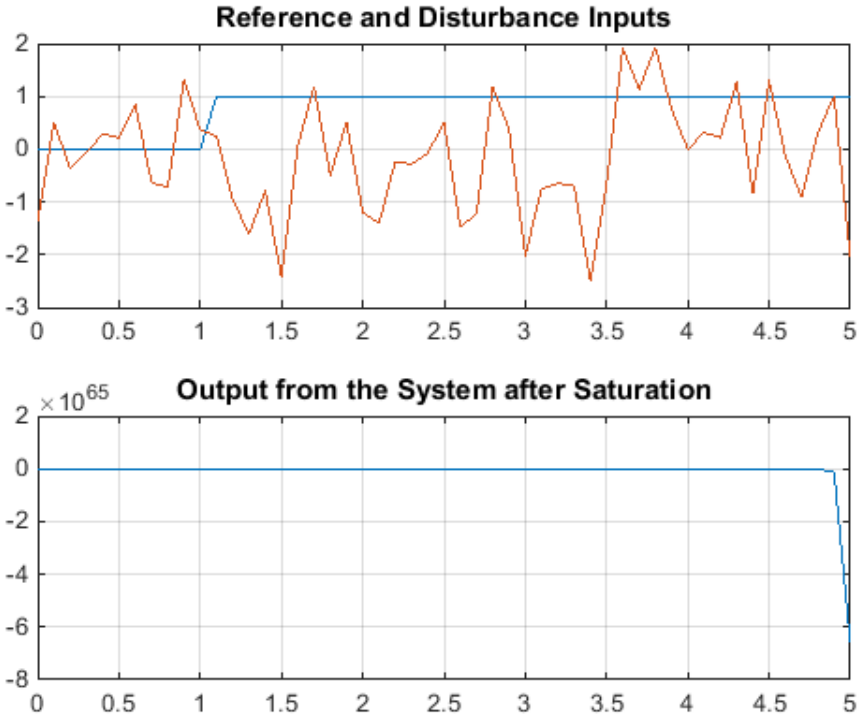


FIGURE 3.6: Input/Output Waves after Saturation Imposition

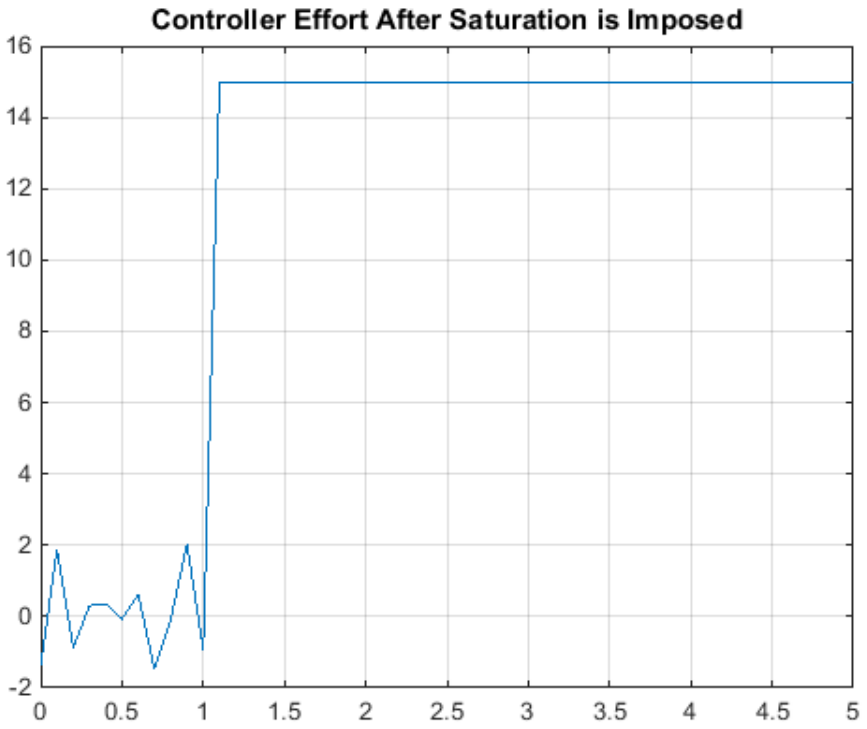


FIGURE 3.7: Saturated Controller Effort

# Chapter 4

# Quasilinear Control

This chapter presents a brief introduction to stochastic linearization the main mathematical gizmo of this work. The term quasilinear was introduced in about 1886 in the context of the solutions of partial differential equations for the systems exhibiting complex non-linearities. The term quasilinear refers to the fact, that if the input and out of the system are linear within acceptable limits, the system is said to be quasilinear. If some system is not lying under the criterion of quasilinear, and the process of transforming such system to become quasilinear, is called quasilinearization. In control theory, the non-linear instruments are linearized assuming that the non-linearity will never be actuated under defined variances and means. But, such an expectation is always impractical. This chapter will start with an introduction of quasilinearization in control theory and the developed notions will be applied to the linearization of saturation non-linearity. Then the concepts and developed principles will be applied to the closed loop systems and required solution requirements will be established.

## 4.1 Introductory Concepts

This section describes the subject of quasilinear control theory (QLC). The tactic of QLC is based on a quasilinearization practice stated

to as stochastic linearization. This technique was established about half century ago and is being utilized in the design of various control systems. But noteworthy work has been proposed in just the last decade. Stochastic linearization assumes that the signals under consideration will be random. In classical control theory, the control systems are designed against faithful tracking of steps, ramps and parabolic inputs. But in practice, the references and disturbances could pose random variations to the system. For instance, in the hard disk drive control problem, the read/write head in both track-seeking and track-following operations is affected by reference signals that are well modeled by Gaussian colored processes. Many other examples can be narrated in which references can be modeled as random processes. Thus, along with disturbances, QLC assumes that the reference signals are random processes and, using stochastic linearization, provides methods for designing controllers for both reference tracking and disturbance rejection problems. The controllers designed based on deterministic inputs, might miss-behave to random changes and the controller effort might actuate non-linearities. QLC provides solution to this issue as well.

### 4.1.1 The Concept of Stochastic Linearization

FIGURE 4.2 explains the basic theme of QLC theory. Let $u(t)$ is the actuation signal from the controller having the characteristics of wide-sense-stationary (WSS) normal process with standard deviation of $\sigma_u$ and $\mu_u$. If the signal is written as $u(t) = u_0(t) + \mu_u$, then $u_0$ (t) is zero mean Gaussian process. The function $f(u)$ is a piece-wise differentiable function, which is a transformation of input signal into non-linear actuator signal. If the function $v(t) = f(u(t))$ is represented by $\hat{v}(t) = Nu_0(t) + M$, whereas the constants must

minimize the error function

$$\varepsilon(N, M) = E[v(t) - \hat{v}(t)]^2 \tag{4.1}$$

This is known as quasilinearization and the constants $N$ and $M$ are

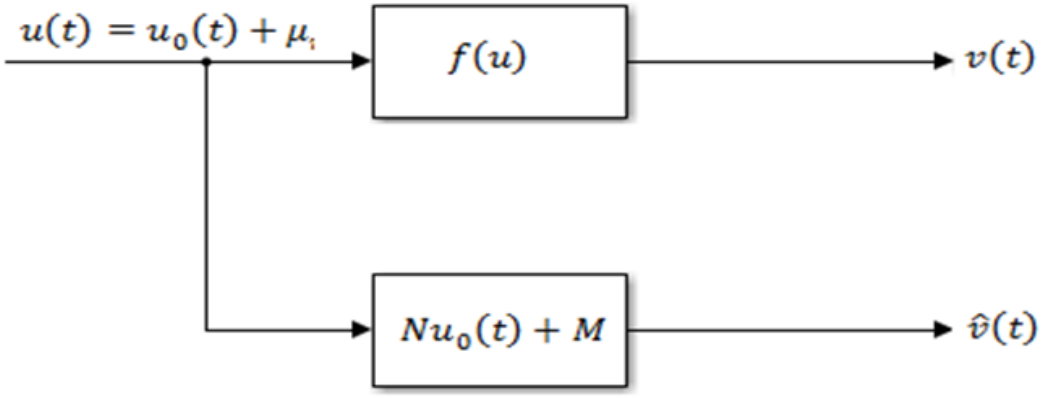


FIGURE 4.1: Saturated Controller Effort

the quasilinear gains and $E$ is the expectation operator. The error function is minimized if

$$N = E\left[\left.\frac{df(u)}{du}\right|_{u=u(t)}\right] \tag{4.2a}$$

$$M = E\left[f(u)|_{u=u(t)}\right] \tag{4.2b}$$

Equation (4.2 can be proved as follows. Differentiating (4.1) wrt $N$, and equating to zero

$$\frac{\partial E}{\partial N} = E\left[-2u_0(t)f(u) - Nu_0(t) - M\right] = 0$$

$$E\left[u_0(t)f(u)\right] - NE\left[u_0^2(t)\right] - ME\left[u_0(t)\right] = 0$$

As the $u_0(t)$ is a zero mean Gaussian process, therefore

$$N = \frac{E[u_0(t)f(u)]}{E[u_0^2(t)]} = \frac{E[u_0^2(t)]E[f'(u)]}{E[u_0^2(t)]} = E[f'(u)]$$

This proves (4.2a). (4.2b) can be proved by differentiating (4.1) wrt $M$ and equating to zero

$$\frac{\partial E}{\partial M} = E[-2f(u) - Nu_0(t) - M] = 0$$

$$M = E[f(u)]$$

Thus QLC can be defined as converting the unbounded signals to bounded using stochastic linearization under the assumptions, that the input signals are random processes. This big concept can be used to avoid saturation and other nonlinear effects within the system. A

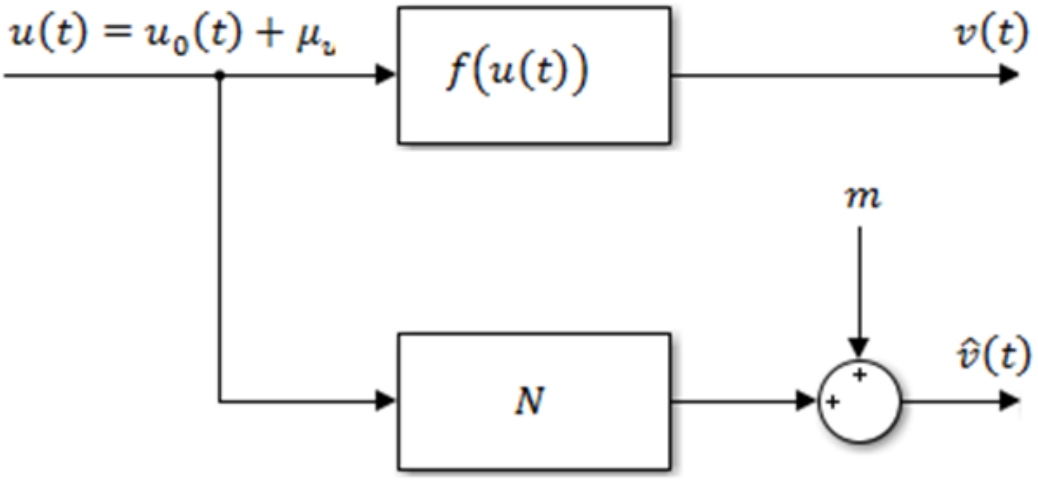


FIGURE 4.2: Feasible Quantization

more feasible and practical situation of quasilinear linearization is depicted in FIGURE 4.2.

According to this model, the quasilinear gain N multiplies with $u(t)$ itself, not with $u_0(t)$. This kind of quasilinearization model suits better in closed-loop configuration as compared with that of FIGURE 4.1. From FIGURE 4.2

$$m = M - N\mu_u \tag{4.3}$$

As in this work the effects of saturation are to be overcome, it will

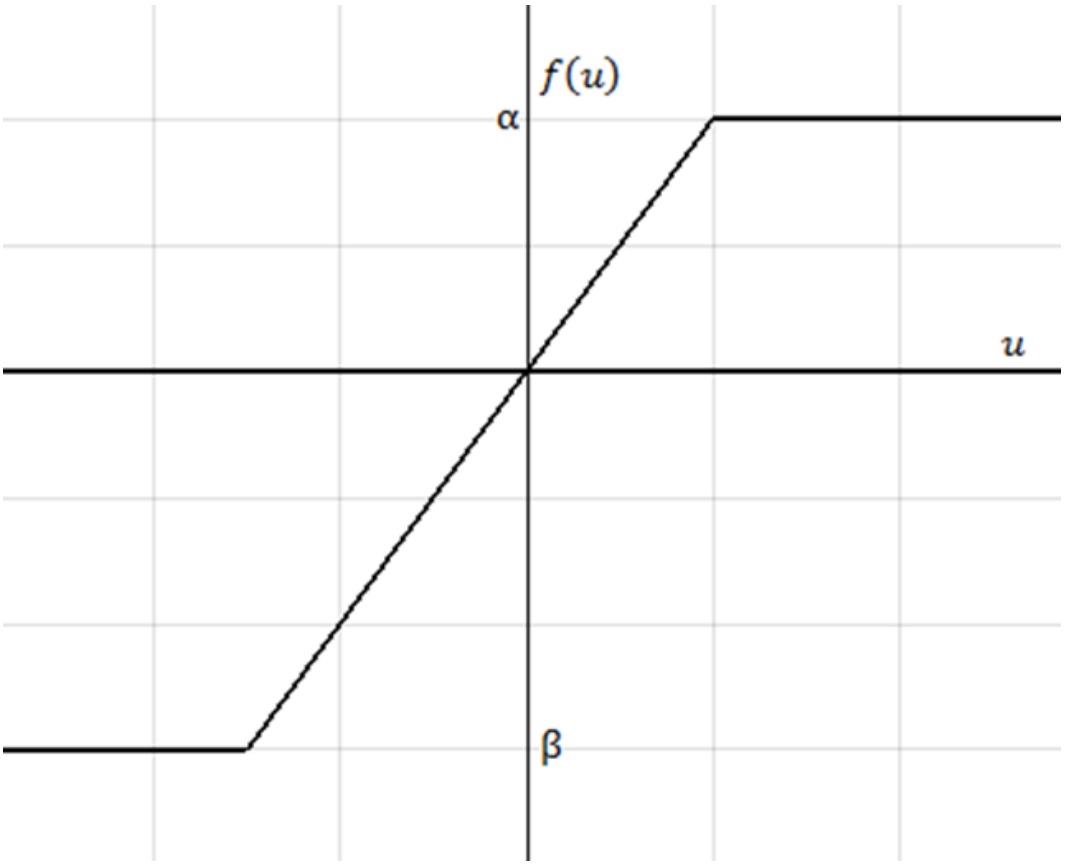


FIGURE 4.3: Saturation Non-Linearity

be worthwhile to quasilinear this non-linearity. FIGURE 4.3 shows the saturation non-linearity.

Mathematically it can be defined as

$$f(u) = \begin{cases} \alpha & ; \quad u \geq \alpha \\ u & ; \quad \beta < u < \alpha \\ \beta & ; \quad u \leq \beta \end{cases} \tag{4.4}$$

Taking derivative with respect to $u$

$$\frac{df(u)}{du} = \begin{cases} 0 & ; \quad \alpha \leq u \leq \beta \\ 1 & ; \quad \beta < u < \alpha \end{cases} \tag{4.5}$$

Thus using the definition of $N$, $M$, their values will be

$$N = \int_{-\alpha}^{\alpha} \frac{1}{\sqrt{2\pi}\sigma_u} \exp\left(-\frac{1}{\sigma_u^2}(u-\mu_u)^2\right) du$$

Let $z = \frac{1}{\sigma_u^2}(u - \mu_u)^2$, the above integral becomes

$$N = \int_{-\frac{\alpha+\mu_u}{\sqrt{2\pi}\sigma_u}}^{\frac{\alpha+\mu_u}{\sqrt{2\pi}\sigma_u}} \frac{1}{\sqrt{\pi}} \exp\left(-z^2\right) dz$$

This last integral is evaluated to become

$$N = \operatorname{erf}\left(\frac{\alpha + \mu_u}{\sqrt{2\pi}\sigma_u}\right) \tag{4.6}$$

Similarly, the constant $M$ can be defined as

$$\begin{aligned} M = \int_{-\infty}^{-\alpha} \frac{-\alpha}{\sqrt{2\pi}\sigma_u} \exp\left(-\frac{1}{\sigma_u^2}(u - \mu_u)^2\right) du \\ + \int_{-\alpha}^{\alpha} \frac{u}{\sqrt{2\pi}\sigma_u} \exp\left(-\frac{1}{\sigma_u^2}(u - \mu_u)^2\right) du \\ + \int_{\alpha}^{\infty} \frac{\alpha}{\sqrt{2\pi}\sigma_u} \exp\left(-\frac{1}{\sigma_u^2}(u - \mu_u)^2\right) du \end{aligned}$$

The first and the last integral will evaluate to become zero, so

$$M = \int_{-\alpha}^{\alpha} \frac{u}{\sqrt{2\pi}\sigma_u} \exp\left(-\frac{1}{\sigma_u^2}(u - \mu_u)^2\right) du$$

This above integral evaluates to

$$A = 2\alpha \operatorname{erf}\left(\frac{\alpha + \mu_u}{\sqrt{2\pi}\sigma_u}\right)$$

$$B = \frac{\alpha + \mu_u}{\sqrt{2\pi}\sigma_u} \operatorname{erf}\left(\frac{\alpha + \mu_u}{\sqrt{2\pi}\sigma_u}\right)$$

$$C = \frac{\alpha - \mu_u}{\sqrt{2\pi}\sigma_u} \operatorname{erf}\left(\frac{\alpha + \mu_u}{\sqrt{2\pi}\sigma_u}\right)$$

$$D = \frac{1}{\sqrt{\pi}} \exp\left(-\left(\frac{\alpha + \mu_u}{\sqrt{2\pi}\sigma_u}\right)^2\right)$$

$$E = \frac{1}{\sqrt{\pi}} \exp\left(-\left(\frac{-\alpha + \mu_u}{\sqrt{2\pi}\sigma_u}\right)^2\right)$$

So all components of the solution combined together

$$M = A - B - C - D + E \tag{4.7}$$

### 4.1.2 Open-Loop Quasilinear Control

Consider open-loop control system shown in FIGURE 4.4. For simplicity let the controller be $G_C(s) = K$, then

$$y(t) = g_P(t) * Kf\left(u(t)\right) * r(t)$$

Where $g_P(t) =^{-1} G_P(s)$ is the impulse response of the plant. Now using the quasilinearization of FIGURE 4.2

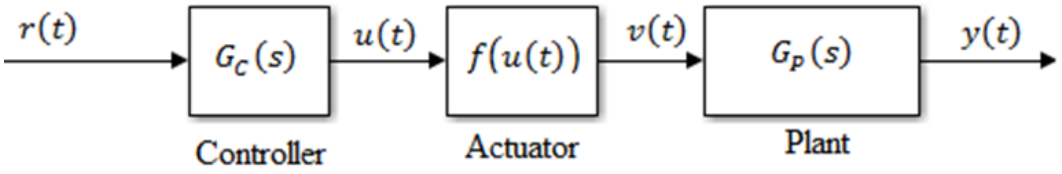


FIGURE 4.4: Open-Loop System

$$y(t) = K\left[g_P(t) * (m + Nu_0(t)) * r(t)\right] \tag{4.8}$$

Using the definitions of quasilinearization, the above relation can be written as

$$Y(s) = K\left(m + NU_0(s)\right) R(s) \tag{4.9}$$

### 4.1.3 Closed-Loop Quasilinear Control and Reference Tracking

FIGURE 4.5 shows a complete model of quasilinear control. The assumptions on which the particular theory will be built are:

- ☐ The filters $F_r(s)$ and $F_d(s)$ are available which help to smooth sudden changes. The randomness is introduced by the parameters of the signal, that is, the standard deviations and means.

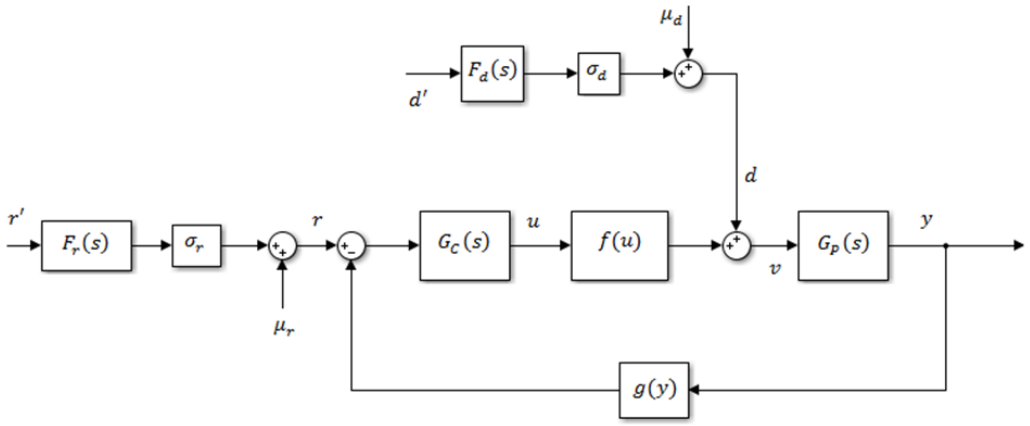


FIGURE 4.5: Closed-Loop Quasilinear Control

- If in the settings above, $u$ is approximated by $u'$ as will be demonstrated shortly, the nature of $u'$ could be of deterministic nature.
- $f(y)$ and $f(u)$ are representative of the saturation non-linearity that might occur in controller and/or sensor.
- Both $f(u)$ and $g(y)$ are representable using the model of FIGURE 4.2 as shown in FIGURE 4.6. Whereas the quasilinear gains have been obtained using definitions (4.2) and (4.3).

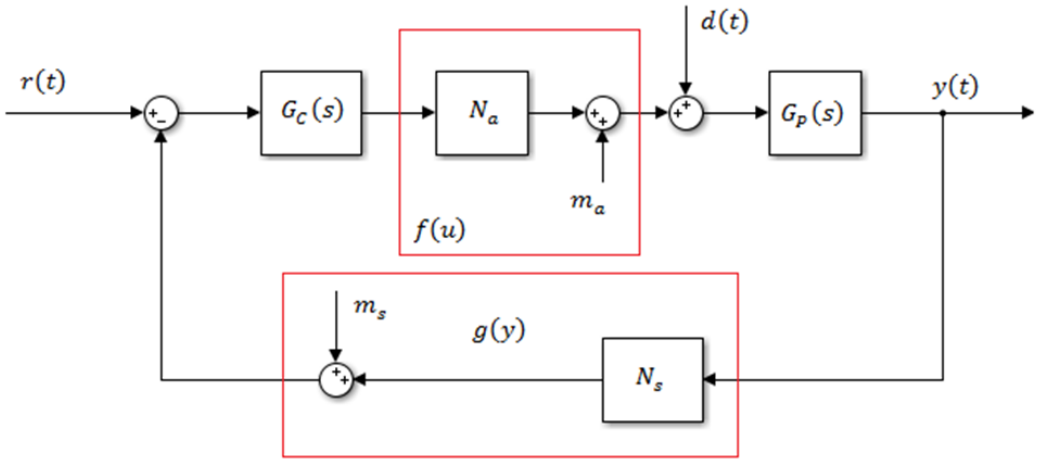


FIGURE 4.6: The Quasilinear Control

Under the settings shown in FIGURE 4.6, the task of closed-loop analysis becomes, determining the relationships between various parameters of the closed loop system. For this purpose, let

- ▷ The disturbance $d(t) = 0$
- ▷ The system is operating in stationary regime
- ▷ $g(y) = y$, which implies that $N_s = 1$, $M_s = \mu_y$ and $m_s = 0$
- ▷ The values of $N_a$, $M_a$ and $m_a$ are available using the definitions of (4.2) and (4.3)

Under the above assumptions

$$\hat{U}(s) = \frac{G_c(s)}{1 + N_a G_C(s) G_P(s)} R(s) - \frac{G_C(s) G_P(s)}{1 + N_a G_C(s) G_P(s)} \frac{m_a}{s} \tag{4.10}$$

Since the second contributor term in (4.10) is a constant, so its variance will be zero. With this a good approximation to variance of $\hat{u}(t)$ can be given by

$$\sigma_{\hat{u}} = \left\| \frac{G_C(s)}{1 + N_a G_C(s) G_P(s)} \right\|_2 \tag{4.11a}$$

$$\sigma_{\hat{u}} = \sqrt{\frac{1}{2\pi} \int \left| \frac{G_C(j\omega)}{1 + N_a G_C(j\omega) G_P(j\omega)} \right|^2 d\omega} \tag{4.11b}$$

It should be noted that since pre-filtering block is absent, it is expected to give good approximation of $N_a$. The value of expectation of $\hat{u}$ can be determined by using the fact that for linear systems H(s)

$$\mu_{OUTPUT} = H(0) \mu_{INPUT}$$

Applying this definition of equation (4.10)

$$\mu_{\hat{u}} = \frac{G_C(0)}{1 + N_a G_C(0) G_P(0)} \mu_r - \frac{G_C(0) G_P(0)}{1 + N_a G_C(0) G_P(0)} m_a$$

Let $C_0 = G_C(0)$, the dc gain of controller and $P_0 = G_P\ (0)$, the dc gain of the plant, the above relationship can be rewritten as

$$\mu_{\hat{u}} = \frac{C_0}{1 + N_a C_0 P_0} \mu_r - \frac{C_0 P_0}{1 + N_a C_0 P_0} m_a \tag{4.12}$$

This can be modified to read as

$$m_a = \frac{\mu_r}{P_0} - \left(\frac{1}{P_0 C_0} + N_a\right) \tag{4.13}$$

Another way to express $mu_{\hat{u}}$ will be

$$mu_{\hat{u}} = C_0(\mu_r - P_0 E[\hat{v}]) = C_0(\mu_r - P_0 E[v]) = C_0(\mu_r - P_0 M_a)$$

Solving this equation for $M_a$

$$M_a = \frac{\mu_r}{P_0} - \frac{1}{C_0 P_0}\mu_{\hat{u}} \tag{4.14}$$

From equations (4.6) and (4.7) it can be seen that the values of quasilinear gains $N$ and $M$ are the functions of $\sigma$ and $\mu$, using this fact and equation (4.14)

$$N_a = F_N\left(\left\|\frac{G_C(s)}{1 + N_a G_C(s) G_P(s)}\right\|_2 \sigma_r,\ \mu_{\hat{u}}\right) \tag{4.15a}$$

$$\frac{\mu_r}{P_0} - \frac{\mu_{\hat{u}}}{C_0 P_0} = F_M\left(\left\|\frac{F_r(s) G_C(s)}{1 + N_a G_C(s) G_P(s)}\right\|_2 \sigma_r,\ \mu_{\hat{u}}\right) \tag{4.15b}$$

These equations (4.15) give a simultaneous but non-linear system of equation of equation in two unknowns $N_a$ and $\mu_{\hat{u}}$, which can easily be solved using MATLAB. Once latter parameters are known, the value of $m_a$ can be determined using (4.13). The parameters $P_0$ and $C_0$ are the DC gains of plant and the controller respectively.

As in this work, the symmetric non-linearity will be considered, the solution of equations (4.15) will always exist, but there are certain limits for the existence of solution, if non-symmetric linearity is assumed [48].

### 4.1.4 Closed-Loop Quasilinear Control and Disturbance Rejection

Similar to reference tracking, the system of the equations involving can be found. To do this, followings are the assumptions.

- ▷ The sensor is linear that is $g(y) = y$ and let $r(t) = 0$
- ▷ The system is operating in stationary regime.

The transfer function from $d(t)$ to $\hat{u}$ will be

$$Y_{d\to\hat{u}}(s) = \frac{G_C(s)G_P(s)}{1 + N_a G_C(s)G_P(s)}$$

From where, the relationship between $\sigma_d$ and $\sigma_{\hat{u}}$ will be

$$\sigma_{\hat{u}} = \left\| \frac{G_C(s)G_P(s)}{1 + N_a G_C(s)G_P(s)} \right\|_2 \sigma_d \tag{4.16}$$

The relationship between $\mu_d$ and $\mu_{\hat{u}}$ will be

$$\mu_{\hat{u}} = -C_0 P_0 (M_a + \mu_d) \tag{4.17}$$

Using the definitions of quasilinear gains

$$N_a = F_N \left( \left\| \frac{F_d(s)G_C(s)G_P(s)}{1 + N_a G_C(s)G_P(s)} \right\|_2 \sigma_d,\ \mu_{\hat{u}} \right) \tag{4.18a}$$

$$-\mu_d - \frac{\mu_{\hat{u}}}{C_0 P_0} = F_M \left( \left\| \frac{F_r(s)G_C(s)G_P(s)}{1 + N_a G_C(s)G_P(s)} \right\|_2 \sigma_d,\ \mu_{\hat{u}} \right) \tag{4.18b}$$

The solution of above equations will also exist for symmetric nonlinearities.

### 4.1.5 Statistical Accuracy

This subsection presents a method to measure the accuracy of quasilinearization. As this this work is concerned about the saturation

non-linearity, so the all discussion will be focused on it. The particular system setting are shown in FIGURE 4.5, where $f(u)$ is the saturation non-linearity.

The accuracy is defined by the probability by which the corners of the non-linearity are reached. That is

$$A = P[\mu \leq \alpha] - P[\mu \geq \alpha] \tag{4.19}$$

The parameter $A$ is representing the accuracy of approximation proposed by FIGURE **??**. The value of $A = 0$ signifies the fact that saturation is activated equally to upper and lower levels. But if $A > 0$, this implies that the non-linearity has been touched to its upper level and $A < 0$ indicates that lower level of saturation is being touched. As $A$ is the difference of two probabilities, it satisfies the inequalities

$$-1 < A < 1 \tag{4.20}$$

The probabilities in (4.21) and hence the value of $A$ can be computed using (4.21)

$$A = \frac{1}{2}\left[\text{erf}\left(\frac{\alpha + \mu_u}{\sqrt{2}\sigma_u}\right) - \text{erf}\left(\frac{\alpha + \mu_u}{\sqrt{2}\sigma_u}\right)\right] \tag{4.21}$$

Following comments are in order for the value of $A$ and its interpretation. The value of $A$ indicates the accuracy of quasilinear gains. Smaller the value of $A$, better the approximation is. From its definition in (4.21), it can be seen that $A$ will be small if:

- $\mu_u$ near to ZERO, which is the midpoint of non-linearity.
- $\sigma_u$ is reasonably large (not too large) and $\mu_u$ lies on the linear region of saturation. This fact signifies that the actuating signal remains within limits and the saturation is never activated.

- $\sigma_u$ is much bigger than the saturation buff. Bigger value of $\sigma_u$ infers that the saturation is equally triggered from above and below.

## 4.2 Quasilinear System Performance

This section is concerned with the development of tools for the performance analysis of QLC systems. In classical control theory these tools are, stability analysis, state-state analysis, transient analysis, root locus and frequency domain methods of bode diagrams, Nichols charts and Nyquist plots. In QLC theory almost all concepts are carried forward but under constrained conditions. As mentioned above, saturation could be symmetric and asymmetric. The performance analysis for symmetric saturation has extensively been developed in [11]. While the performance analysis for asymmetric saturation is developed in [48]. So, in this section, comprehensive treatment to both works is given. Because this theory will be applied for the design QLC controller for the proposed plant in this work.

### 4.2.1 Reference Tracking Performance

In this subsection, stochastic linearization is applied to closed-loop QLS to analyze the tracking performance of closed-loop QLS. The discussion begins with an exciting example to establish that stochastic linearization offers a good tactic for the analysis of tracking performance of systems modeled as linearized plants-non-linear- instrumentation (LPNI). The concept of trackable of domain defined as the maximum step that could be tracked will be established. Finally, quality indicators are introduced being used to give numerical interpretations to tracking performance of quasilinear systems. Almost all the results are based on symmetric non-linearity. Consider

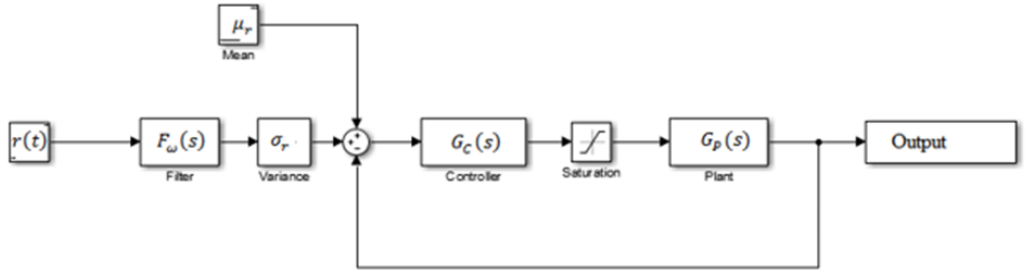


(a) Analysis of Tracking Performance

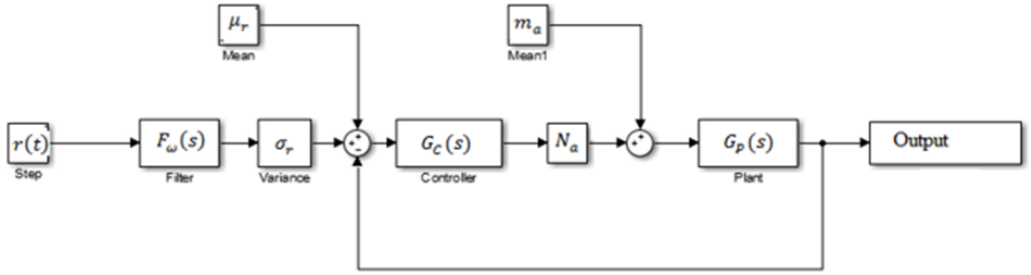


(b) Analysis of Tracking Performance

FIGURE 4.7: Analysis of Tracking Performance

the closed loop system of FIGURE 4.7(a) described by

$$G_P(s) = \frac{10}{s(s+10)} \quad G_C(s) = 5 \tag{4.22}$$

Assume that $\omega_r$ is the standard white noise process defined using Gaussian random process with $\sigma_r = 1$ and $\mu_r = 0$ and the filter $F_{\Omega r}(s)$ is Butterworth low pass filter, with order 3 given by

$$F_{\Omega r}(s) = \frac{\sqrt{3}}{s^3 + 2s^2 + 2s + 1} \tag{4.23}$$

The quasilinearized version of this quasilinear system is shown in FIGURE 4.7(b). From the description of the plant $P_0 = \lim_{s\to 0} G_P(s) = \lim_{s\to\infty} \frac{10}{s(s+10)} = \infty$ and $C_0 = 5$, then the use of equations (4.10) and (4.12) gives

$$\sigma_{\hat{\mu}} = \left\| \frac{5\sqrt{3}s(s+10)}{(s^3 + 2s^2 + 2s + 1)(s^2 + 10s + 50N_a)} \right\|_2 \tag{4.24a}$$

$$M_a = 0 \tag{4.24b}$$

Now from equations (4.15), the system of simultaneous equations will become

$$N_a - F_N\left(\left\|\frac{5\sqrt{3}s(s+10)}{(s^3+2s^2+2s+1)(s^2+10s+50N_a)}\right\|_2,\ \mu_{\hat{u}}\right) \quad (4.25a)$$

$$F_M\left(\left\|\frac{5\sqrt{3}s(s+10)}{(s^3+2s^2+2s+1)(s^2+10s+50N_a)}\right\|_2,\ \mu_{\hat{u}}\right) = 0 \quad (4.25b)$$

Following three cases of saturation non-linearity will be considered in this analysis.

- Symmetric saturation with $\alpha = -1$ and $\beta = +1$
- Asymmetric saturation with $\alpha = -0.5$ and $\beta = +1.5$
- Asymmetric saturation with $\alpha = -0.2$ and $\beta = +1.8$

It should be noted that $\beta + |\alpha| = 2$ that total saturation prone to activation remains equal with asymmetric distribution in two cases. For each case, luckily unique solution to (4.25) is obtained and closed-loop QLS is obtained as shown in FIGURE 4.7(b). The performance is indicated using the accuracy measure A of (E4.20). For the first case, the value of accuracy parameter A is zero, as expected because the saturation is symmetric. Second and third case produce the value of A -0.46 and -0.8 respectively. The non-zero values of A indicate that the non-linearities are asymmetric. From the above analysis it can be seen that tracking performance deteriorates proportionally with the magnitude of asymmetry.

Moreover, stochastic linearization gives closer approximates of all three quantities for the original nonlinear system. Consequently, as far as the estimate of loss of tracking is concerned, the quasilinear system is a good approximation to the LPNI and A-LPNI systems.

This example validates that stochastic linearization may be apposite to envisage the quality of tracking in A-LPNI systems. Obviously,

if $\sigma_{\hat{e}}$ is lesser, dynamic tracking is good and small value of $\mu_{\hat{e}}$ is small, steady state tracking is good. It implies that for good tracking requires both error signal mean and variance be small.

But, if they are large, the reason for poor tracking is not directly clear. For this reason, the notions of step and ramp trackable domains are developed, which determine the set of step sizes and ramp slopes that can be tracked in the presence of saturation. These domains are proper extensions of the ones in the symmetric case.

### 4.2.2 The Notion of Trackable Domains

Consider the system of FIGURE 4.8, where $r(t) = r_0 u_s(t)$ with $r_0 \in R$ and $u_s(t)$ is the unit step function. The trackable domains (TD) are determined using the concept of steady state error which is defined as

$$e_{ss} = \lim_{t\to\infty} = \lim_{s\to 0} sE(s)$$

Under the assumption that $e_{ss}$ exists, for LTI systems it can be given by

$$e_{ss} = \frac{1}{1 + P_0 C_0} r_0$$

For any A-LPNI systems this is not true at all times. This fact is recognized by the following. If the signal $u$, the input to the


FIGURE 4.8: Trackable Domains

saturation non-linearity, never touches either bounds, or , then

$$-\alpha < u_{ss} = \frac{r_0 C_0}{1 + C_0 P_0} < \alpha$$

$$-\alpha < \frac{r_0}{\frac{1}{C_0} + P_0} < \alpha \Longrightarrow \left| \frac{r_0}{\frac{1}{C_0} + P_0} \right| < \alpha \tag{4.26}$$

The relationship in (4.26) defines the step trackable domain. If $r_0^*$ is the maximum step that can be tracked by QLC system, then it is given by

$$r_0^* < \left| \frac{1}{\frac{1}{C_0} + P_0} \right| \tag{4.27}$$

As the design process concerns with avoiding the nonlinearity, this implies that (4.26) is the design equation, because it is usually the case that $C_0$ and $P_0$ are positive. The use of (4.26) will help design the steps that could be tracked smoothly.

Equation (4.26) can be written as

$$-\alpha \left( \frac{1}{C_0} + P_0 \right) < |r_0| < \left( \frac{1}{C_0} + P_0 \right) \alpha \tag{4.28}$$

From (4.28), it can be seen that if $P_0 = \infty$, the trackable values of steps cover the entire real number line. This implies that step of any size can be tracked by the controller. But if $C_0 = \infty$, the trackable steps become $\alpha \left( \frac{1}{C_0} + P_0 \right) < |r_0| < (P_0)\, \beta$. Thus (4.28) forms the design equation for the determination of trackable domains.

Considering again the closed system shown in FIGURE 4.8, and let the input be $r(t) = r_0 u_s(t)$. The steady state error for the closed-loop system in general is given by

$$e_{ss} = \lim_{s \to 0} \frac{r_1}{1 + G_C(s) G_P(s)}$$

This definition might not work in QLC settings. The steady state error for a closed-loop QLC system is given by

$$e_{ss} = \frac{r_1}{C_0 P_1} \iff \alpha P_1 \leq \beta P_1 \tag{4.29}$$

whereas $P_1 = \lim_{s\to 0} sG_P(s)$. From above equation it can be seen that ramp track-ability is completely dependent upon $P_1$.

### 4.2.3 Tracking Quality Indicators

In this section some relations will be developed that will be used to quantify the quality of reference tracking. The tracking is of two types: steady state tracking and dynamic tracking. The last section presented the concepts of steady state tracking. In this section, dynamic tracking will of major focus.

Considering FIGURE 4.7(b) again, representing quasilinearized system, in which $r(t)$ is the colored Gaussian process having standard deviation of $\sigma_r$ and expectation of $\mu_r$. As usual the constant $N_a$, $\mu_{\hat{u}}$ are the solutions of

$$N_a - F_N\left(\sigma_{\hat{u}}, \mu_{\hat{u}}\right) = 0 \tag{4.30a}$$

$$\frac{\mu_r}{P_0} - \frac{\mu_{\hat{u}}}{P_0 C_0} \tag{4.30b}$$

Whereas

$$m_a = \frac{\mu_r}{P_0} - \left(\frac{1}{P_0 C_0} + N_a\right)\mu_{\hat{u}} \tag{4.31}$$

To have good tracking, the value of $\sigma_{\hat{e}}$ and $\mu_{\hat{e}}$ must as small as possible. These values are given by

$$\sigma_{\hat{e}} = \left\| \frac{1}{1 + N_a G_P(s) G_C(s)} \right\|_2 \sigma_r \tag{4.32a}$$

$$\mu_{\hat{e}} = \frac{\mu_{\hat{u}}}{C_0} \tag{4.32b}$$

The quality of dynamic tracking can be quantified using the definition of Saturating Random Sensitivity (SRS) function. Similarly, Amplitude truncation and rate saturation are two other quantifiers of tracking. As it will be explained that the definition of SRS remains the same as suggested for symmetric case. However, some will be

manipulated appropriately to incorporate asymmetry as well. Furthermore, rate saturation and steady state tracking presented here will open new insights regarding tracking indicators.

The Saturating Random Sensitivity (SRS) function is defined as the standard deviation of the error signal in the quasilinear system of FIGURE 4.7(b) normalized by $\sigma_r$

$$\mathrm{SRS}(\Omega_r, \sigma_r, \mu_r) = \left\| \frac{F_r(s)}{1 + N_a G_P(s) G_C(s)} \right\|_2 \tag{4.33}$$

The definition of SRS given in (4.33) serves both symmetric and asymmetric cases. Note, however, that the symmetry property is embedded by the quasilinear gain $N_a$, whereas $N_a$ is smaller in the asymmetric case as compared with the symmetric case. SRS satisfies the following properties:

1. $\forall\ \Omega_r > 0,\ \lim_{\sigma_r \to 0} \mathrm{SRS}(\Omega_r, \sigma_r, \mu_r) =$
$$\begin{cases} \mathrm{SRS}(\Omega_r, \sigma_r, \mu_r) = \left\| \frac{F_r(s)}{G_P(s) G_C(s)} \right\|_2; & \mu_r \in TD_{STEP} \\ 1; & \text{Otherwise} \end{cases}$$
2. $\forall\ \sigma_r > 0,\ \lim_{\Omega_r \to \infty} \mathrm{SRS}(\Omega_r, \sigma_r, \mu_r) = 1$
3. $\forall\ \sigma_r > 0,\ \lim_{\Omega_r \to 0} \mathrm{SRS}(\Omega_r, \sigma_r, \mu_r) = \left| \frac{1}{1 + N_0 C_0 P_0} \right|$

   Where $N_0$ is the solution of

$$N_0 - F_N\left( \left| \frac{F_r(0) C_0}{1 + N_0 P_0 C_0} \right| \sigma_r, \mu_{\hat{u}} \right) = 0$$

$$\frac{\mu_r}{P_0} - \frac{\mu_{\hat{u}}}{C_0 P_0} - F_M\left( \left| \frac{F_r(0) C_0}{1 + N_0 C_0 P_0} \right|_2 \sigma_r,\ \mu_{\hat{u}} \right) = 0$$

4. $\forall\ \sigma_r > 0,\ \Omega_r > 0\ \lim_{\Omega_r \to \pm\infty} \mathrm{SRS}(\Omega_r, \sigma_r, \mu_r) =$

$$\begin{cases} 1\ ; & |P_0 C_0| \neq 0 \\ \left\| \frac{F_r(s)}{1+G_P(s)G_C(s)} \right\|_2\ ; & |P_0| = \infty \\ \text{Undefined}\ ; & \text{Otherwise} \end{cases}$$

Where $N_a$ is the solution of

$$N_a - F_N\left( \left\| \frac{F_r(s)G_C(s)}{1 + N_a G_C(s) G_P(s)} \right\|_2 \sigma_r,\ \mu_{\hat{u}} \right) = 0$$

$$F_M\left( \left\| \frac{F_r(s)G_C(s)}{1 + N_a G_C(s) G_P(s)} \right\|_2 \sigma_r,\ \mu_{\hat{u}} \right) = 0$$

To ensure good tracking $\mu_r \in TD_{STEP}$, then followings can be used to characterize SRS(.)

(a) **Saturated Random DC Gain:** this quantity represents the sensitivity of error signal against constant reference and is defined by

$$\mathrm{SRS}_{DC}(\mu_r) = \lim_{\sigma_r \to 0 \Omega_r \to 0} \mathrm{SRS}(\Omega_r, \sigma_r, \mu_r)$$

(b) **Saturated Random Bandwidth:** this parameters represents the bandwidth of SRS(.) as the function of $\sigma_r$ and $\mu_r$ and is given by

$$\mathrm{SRS}_{BW}(\mu_r,\ \sigma_r) = \min_{\Omega_r > 0} \left\{ \mathrm{SRS}(\Omega_r, \sigma_r, \mu_r) = \frac{1}{\sqrt{2}} \right\}$$

(c) **Saturated Random Resonant Frequency:** the value of frequency $\omega_r$ at which maximum of $SRS(.)$ occurs as a function of $\sigma_r$ and $\mu_r$ is called saturated random resonant frequency. It is defined as

$$\mathrm{SRS}_{\omega_r}(\mu_r,\ \sigma_r) = \arg\ \sup_{\Omega_r > 0} \{\mathrm{SRS}(\Omega_r, \sigma_r, \mu_r)\}$$

(d) **Saturated Random Resonant Peak:** the maximum value of SRS(.) as a function of $\sigma_r$ and $\mu_r$ is called saturated random resonant peak. It is defined as

$$\mathrm{SRS}_M(\mu_r,\ \sigma_r) = \sup_{\Omega_r>0} \{\mathrm{SRS}(\Omega_r, \sigma_r, \mu_r)\}$$

From the above analysis it can be seen that, all these performance parameters are bases on the frequency content of reference signal. With inputs of random references, the frequency content is made band-limited by pre-filtering. The transfer function $F_r(s)$ is serving the purpose of pre-filtering. Base on above definition following indicators are defined.

**Static Un-Responsiveness Indicators** ($I_1$)**:** when the response has reached steady state, the unresponsive-ness of the system to the changes in inputs is quantified by this parameter, which is defined by

$$I_1 = \mathrm{SRS}_{DC}(\mu_r) \tag{4.34}$$

**Dynamics Indicator** ($I_2$)**:** this parameter quantifies the magnitude of dynamics in the system and is defined by

$$I_2 = \frac{\Omega}{\mathrm{SRS}_{BW}(\mu_r,\ \sigma_r)} \tag{4.35}$$

**Differentiator Between Statics and Dynamics** ($I_3$)**:** this parameter distinguishes between $I_1$ and $I_2$ and quantifies the relative intensity of latter two. This is defined as

$$I_3 = \min\left\{\mathrm{SRS}_M(\mu_r,\ \sigma_r) - 1,\ \frac{\Omega}{\mathrm{SRS}_{BW}(\mu_r,\ \sigma_r)}\right\} \tag{4.36}$$

**Amplitude Truncation Indicator** ($I_0$)**:** this parameter measure the degree of possibility of saturation activation. If $\mu \in$ TrackableDomain (TD), the value of this parameter is finite and if $\mu \in$ Trackable Domain (TD),

$I_0 = \infty$. Under the assumption that $\mu_r \in TD$, it is defined as

$$I_0 = \max\left\{ \frac{\sigma_r}{\left|\frac{1}{C_0} + P_0\right| \beta - \mu_r}, \frac{\sigma_r}{\left|\frac{1}{C_0} + P_0\right| \alpha - \mu_r} \right\} \tag{4.37}$$

**Rate Saturation** ($I_{0(rate)}$)**:** if the plant has pole(s) at origin, the trackable domain of steps will be infinite and $I_0 = 0$. But this results in another problem called rate saturation. Rate saturation measures the ability to track the ramps inputs. It is defined as

$$I_{0(rate)} = \max\left\{ \frac{\sigma_r \Omega}{|P_1|\beta}, \frac{\sigma_r \Omega}{|P_1|\alpha} \right\} \tag{4.38}$$

All these parameters give enough information about a system.

### 4.2.4 Disturbance Rejection Performance

The disturbance rejection will be demonstrated using the system configuration of FIGURE 4.7(a) and using the example plant and controller of (4.22). Assuming that $r(t) = 0$ and $d'(t)$ is the Normal white noise with $\sigma_d = 1$ and $\mu_d = 0$. The filter transfer function $F_d(s)$ is a third order Butterworth filter with bandwidth of $_d = 2$. Under these conditions the equation of stochastic linearization become

$$N_a - F_N(\sigma_{\hat{u}}, \mu_{\hat{u}}) = 0 \tag{4.39a}$$

$$F_M(\sigma_{\hat{u}}, \mu_{\hat{u}}) = 0 \tag{4.39b}$$

Using the parameter of system in (4.22)

$$\sigma_{\hat{u}} = \left\| \frac{400\sqrt{1.5}}{(s^3 + 4s^2 + 8s + 8)(s^2 + 10s + 50N_a)} \right\|_2 \tag{4.40}$$

The property of disturbance rejection is investigated under following cases:

- $\alpha = -2,\ \beta = 2$

- $\alpha = -1,\ \beta = 3$
- $\alpha = -0.5,\ \beta = 3.5$

For every case, the system of simultaneous equations (4.39) is solved to obtain the value of unknowns $\sigma_{\hat{u}}$ and $N_a$. These values are used to calculate the measure of ASYMMETRY. Case-1 gives $A = 0$, case-2 gives $A = -0.3$ final case produces a value of $A = -0.73$. Plots of $y(t)$, $y'(t)$ against $d(t)$ are shown in FIGURE 4.9 From these plots it can be seen that as the degree of ASYMMETRY increases, the disturbance rejection performance deteriorates. As this work considers the symmetric saturation only, so good rejection of disturbance will be attained.

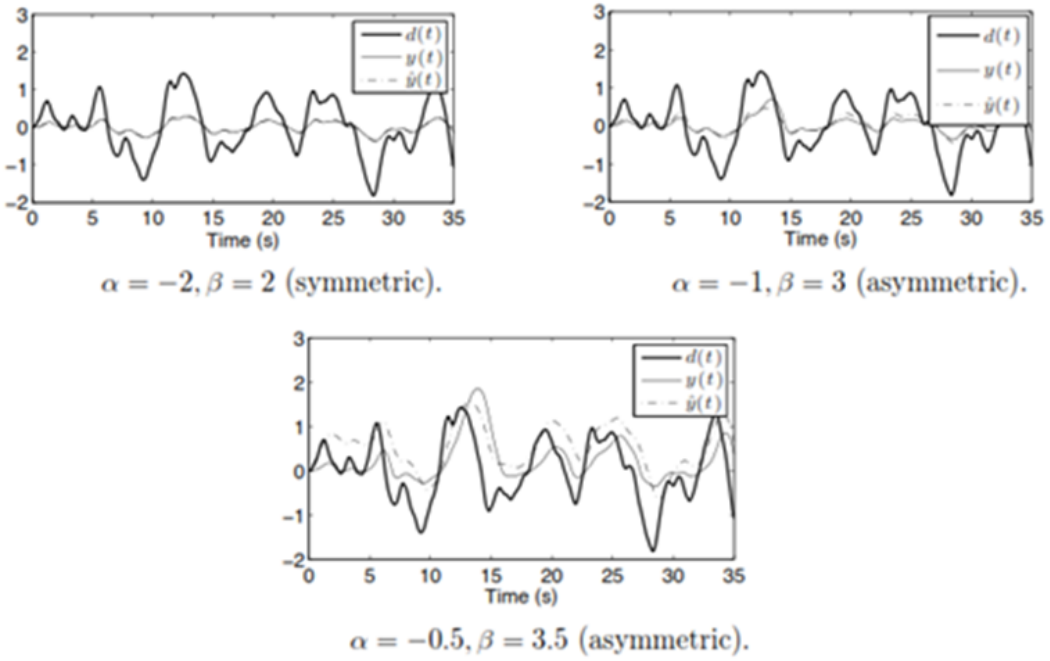


$\alpha = -2, \beta = 2$ (symmetric). $\alpha = -1, \beta = 3$ (asymmetric).

$\alpha = -0.5, \beta = 3.5$ (asymmetric).

FIGURE 4.9: Disturbance Rejection

## 4.3 Saturating Root Loci and Error Loci

In the previous section steady-state and transient performance of the systems were analyzed. This section is devoted to the development of root loci for the analysis of quasilinear system under saturation

actuation. When the system is quasilinearized, the available is truncated by the quasilinear gain to avoid saturation actuation. The root locus indeed begins at poles of the systems but it finishes prematurely before infinity due gain truncation. These points where the loci terminate are called truncation points.

Such a kind of truncation can definitely initiate the generation of error in the steady state performance. So another locus is developed for the sole purpose of completeness to give a graphical view, how the quasilinearization might the error performance of the system. Such a locus is truncation error (TE) locus.

Two significant works can be found in this regard. The pioneers (Shinung Ching Et. El from MIT) of Modern Quasilinear Control Theory have developed the root locus methods for the analysis of systems containing symmetric saturations. This is called S-locus [11]. While Hamid-Reza Ossareh have applied and extended theories for the systems containing asymmetric saturations. In this work, a brief but comprehensive treatment of both works will be presented.

### 4.3.1 Fundamentals of S/AS Root Locus

Considering the system of FIGURE 4.10(a) where $G_P(s)$ is the plant, $KG_C(s)$ is the controller, the filter $F_r(s)$ is third order Butterworth filter with bandwidth of $\|F_r(s)\|_2 = 1$. The reference input $r(t)$ being white noise is the filtered through $F_r(s)$ and afterwards it is scaled with $\sigma_r$ and shifted by $\mu_r$. The stochastic linearization of system in FIGURE 4.10(a) gives the system in FIGURE 4.10(b), where the parameters $N_a$ and $\mu_{\hat{u}}$ are the solutions of

$$N_a - F_N\left(K\left\|\frac{F_r(s)G_C(s)}{1+KN_aG_C(s)G_P(s)}\right\|_2\sigma_r,\ \mu_{\hat{u}}\right) \tag{4.41a}$$

$$-\frac{\mu_r}{P_0} - \frac{\mu_{\hat{u}}}{KC_0P_0} - F_M\left(K\left\|\frac{F_r(s)G_C(s)}{1+KN_aG_C(s)G_P(s)}\right\|_2\sigma_r,\ \mu_{\hat{u}}\right) \tag{4.41b}$$

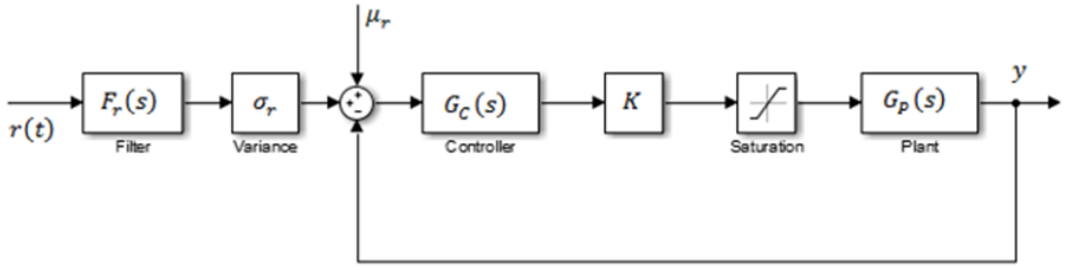


(a) Closed-Loop System with Non-linear Actuator

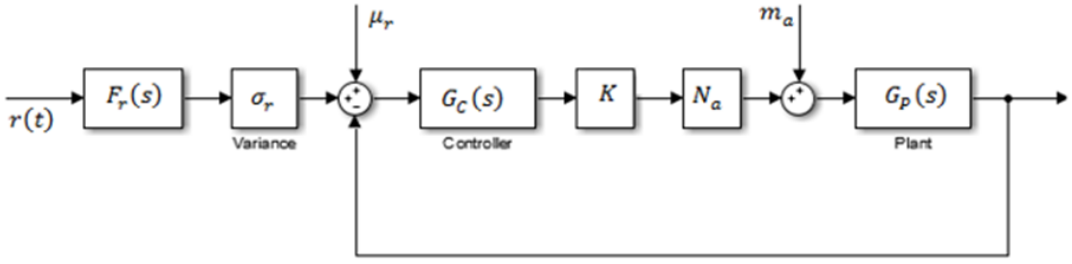


(b) Quasilinearization of System

FIGURE 4.10: The Effect of Quasilinearization

Based on the solution of above system, the parameter $m_a$ is given by

$$m_a = \frac{\mu_r}{P_0} - \left(\frac{1}{KP_0C_0} + N_a\right)\mu_{\hat{u}}$$

The objective is to use the theory of quasilinear system for the design tracking controllers. To do this, note from Figure-4.10(b) that the quasilinear bias $m_a$ and the quasilinear gain $N_a$ enter the system as an additional disturbance input and the gain, respectively. Also, both are the functions of controller gain as can be seen from (4.41). So the effects of controller gain should be studied on the locations of poles and zeros of quasilinear system. This investigation can graphically be represented by two loci: by the classical root locus, and another one called tracking error locus. Together, they are termed as performance loci.

Let the product of controller gain K and quasilinear gain $N_a$ be effective gain and denoting it by $K_e = KN_a$, the system of equations

in (4.41) becomes

$$K_e - KF_N\left(K\left\|\frac{F_r(s)G_C(s)}{1+K_eG_C(s)G_P(s)}\right\|_2\sigma_r,\ \mu_{\hat{u}}\right) \quad (4.42a)$$

$$-\frac{\mu_r}{P_0} - \frac{\mu_{\hat{u}}}{KC_0P_0} - F_M\left(K\left\|\frac{F_r(s)G_C(s)}{1+K_eG_C(s)G_P(s)}\right\|_2\sigma_r,\ \mu_{\hat{u}}\right) \quad (4.42b)$$

The mean of the error signal $\mu_{\hat{e}}$ is dependent upon $\mu_{\hat{u}}$ and $\mu_{\hat{u}}$ is itself the function of K, this implies that

$$\mu_{\hat{e}}(K) = \frac{\mu_{\hat{u}}(K)}{KC_0} \quad (4.43)$$

Before the procedure of sketching the performance loci is outlined, some definitions are introduced.

**AS-Poles:** the closed-loop transfer function of the system in 4.10(a) after quasilinearization shown in 4.10(b) $r \to \hat{y}$ can be written as

$$T(s) = \frac{F_P(s)G_C(s)}{1+K_eG_C(s)G_P(s)} \quad (4.44)$$

As the transfer function in (4.44) is developed under the assumption of asymmetric saturation non-linearity, the poles of $T(s)$ are called AS-Poles.

**AS-Root Loci:** the paths traced by AS-poles as the function of K is called the AS-root loci.

**TE-Locus:** the plot of $\mu_{\hat{e}}(K)$ as $K$ varies from 0 to $\infty$ is the TE (Tracking Error) locus. Both AS-Poles loci and TE locus are the continuous functions of K under the following assumption that $\mu_{\hat{e}}(K)$ and $\mu_{\hat{u}}(K)$ are unique $\forall\ K > 0$.

From (4.44) it can be seen that $0 < K_e < K$ because $0 < N_a < 1$. This implies that AS-root locus is the proper subset of classical root locus. Therefore, the AS-root locus is a proper subset of the usual linear root locus. The sketching of root locus requires certain

information as is the case with usual root locus. For instance, the sketching of root locus (RL) requires, the points of origin, the points of termination etc. In the classical RL, the points of terminations are zeros of the closed-loop system. But in quasilinear system, the RL might terminate prematurely due to presence of saturation. In the following sub-section, a detailed procedure for the AS-RL will be developed.

### 4.3.2 Root Loci Procedure

The procedure for sketching AS-RL is quite similar to the classical RL with the exceptions that the determination of termination points and truncation points is required, since the RL is limited by asymmetric saturation.

**AS-RL Termination Points:** let $K_e^*$ be the terminating gain, that is

$$K_e^* = \lim_{K\to\infty} K_e(K) \tag{4.45}$$

If $K_e^* = \infty$, the termination points meet the open-loop zeros. But as $K_e = KN_a$ and $0 < N_a < 1$, so $K_e^*$ might be finite. As it turns out, to compute $K_e^*$ the following two equations in the unknowns $\phi^*$ and $\eta^*$ must first be solved

$$\phi^* - \left\| \frac{F_r(s)G_C(s)}{1 - \frac{2\alpha}{\sqrt{2\pi}\phi^*}\exp(-\frac{\eta^{*2}}{2})G_C(s)G_P(s)} \right\|_2 \sigma_r = 0 \tag{4.46a}$$

$$\frac{\mu_r}{P_0} - \frac{\eta^*\phi^*}{P_0C_0} = \alpha \exp\left(\frac{\eta^*}{\sqrt{2}}\right) \tag{4.46b}$$

Before the solution of (4.46) to determine $K_e^*$ is presented, some properties are in order. The solution of (E4.46) has the following properties:

1 $\phi^* \geq 0$

2 As $\phi^* \geq 0$, $\eta^* = \sqrt{2}\,\mathrm{erf}^{-1}\left(\frac{\frac{\mu_r}{\alpha} - \alpha}{\alpha}\right)$

3 The point $(\phi^*, \eta^*) = \left(0, \sqrt{2}\,\mathrm{erf}^{-1}\left(\frac{\frac{\mu_r}{\alpha}-\alpha}{\alpha}\right)\right)$ always satisfies the system (4.46)

4 Assuming that $K_e$ and $\mu_{\hat{u}}(K)$ exist and are unique for any value of $K$, then

(a) If $\phi^* = 0$ is the only solution, then $K_e^* = \infty$ and AS-RL meets the open zeros of $T(s)$

(b) If $\phi^* > 0$ then, $K_e^* = \frac{2\alpha}{\sqrt{2\pi}\phi^*}\exp(-\frac{\eta^{*2}}{2})$

5 From (4.46) if $P_0C_0 = \infty$, $\eta^* = \sqrt{2}\,\mathrm{erf}^{-1}\left(\frac{\frac{\mu_r}{\alpha}-\alpha}{\alpha}\right)$. This also implies that $^*$ is independent of $^*$

6 From (4.46) if $P_0C_0 \neq \infty$, then

$$\phi^* = \frac{P_0C_0}{\eta^*}\left[\frac{\mu_r}{P_0} - \alpha\,\mathrm{erf}(\frac{\eta^*}{\sqrt{2}})\right]$$

Based on above discussion the definition of AS-poles can re-narrated as follows. As the solution $K_e^*$ always exists under the assumption that $K_e$ and $_u(K)$ exist and are unique for any value of K, the AS-poles are the poles of

$$T(s) = \frac{K_e^* G_C(s) G_P(s)}{1 + K_e^* G_C(s) G_P(s)} \tag{4.47}$$

The properties of AS-RL might imply that performance never enter the right half s-plane.

**AS-RL Truncation Points:** The AS-truncation points are introduced based on the notion of the trackable domain TD and the quality indicator $I_0$ introduced in section 4-2. In the discussion to follow, for simplicity, it will be assumed that $C_0 > 0$, $P_0 > 0$, and $\mu_r \to TD$for all $K > 0$. The indicator $I_0$ , being the function of $K$

is defined as

$$I_0(K) = \max\left\{\frac{\sigma_r}{\left(\frac{1}{KC_0}+P_0\right)\beta-\mu_r}, -\frac{\sigma_r}{\left(\frac{1}{KC_0}+P_0\right)\beta-\mu_r}\right\} \quad (4.48)$$

Equation (4.48) indicates that $I_0$ is the function of $K$, this is just to the fact that in this analysis $K$ is a variable parameter. As a rule of thumb, amplitude truncation is typically small when $I_0(K) < 0.4$. Based on this idea, the following definition for the AS-RL-truncation points can be defined as the poles of

$$T(s) = \frac{K_e(K_0)G_C(s)G_P(s)}{1+K_e(K_0)G_C(s)G_P(s)} \quad (4.49)$$

Where

$$K_0 = \min K : I_0(K) = 0.4$$

As the AS-locus is the subset of classical root locus, the AS-truncation points must occur before the termination points in classical RL as K tends to infinity. Black squares are used to symbolize the locations of AS-truncation points on the AS-locus.

**Gain Calibration:** Finding unknown $K$ for a given point of AS-RL is called RL calibration. Let $\tilde{s}$ is a point on AS-RL, then there exists a unique $\tilde{K}$, such that $0 < K_e(\tilde{K}) < K_e^*$. Such a value of gain satisfies

$$1 + K_e(\tilde{K})G_C(\tilde{s})G_P(\tilde{s}) = 0 \quad (4.50)$$

Whereas $K_e(\tilde{K})$ is the solution of

$$K_e(\tilde{K}) - KF_N\left(K\left\|\frac{F_r(s)G_C(s)}{1+K_e(\tilde{K})G_C(s)G_P(s)}\right\|_2\sigma_r, \mu_{\hat{u}}\right) \quad (4.51a)$$

$$-\frac{\mu_r}{P_0} - \frac{\mu_{\hat{u}}}{KC_0P_0} - F_M\left(K\left\|\frac{F_r(s)G_C(s)}{1+K_e(\tilde{K})G_C(s)G_P(s)}\right\|_2\sigma_r, \mu_{\hat{u}}\right) \quad (4.51b)$$

Also from (4.50)

$$K_e(\tilde{K}) = -\frac{1}{G_C(\tilde{s})G_P(\tilde{s})} \tag{4.52}$$

In (4.51) $N_a$ and $\mu_{\hat{u}}$ are the unknowns which in turn are used to calculate $\tilde{K}$

### 4.3.3 Tracking Error Locus

Tracking error (TE) can be sketched using equations (4.42) and (4.43). The plot of TE against $K$ may be an increasing function, decreasing or non-monotonic function. The concept of TE will be explained using the system of (4.53) and using the system of FIGURE 4.10.

$$G_P(s) = \frac{1}{s+1}, \quad G_C(s) = 1, \quad \sigma_r = 1 \tag{4.53}$$

Figure-4.11 shows TE loci for three cases:

- Case-1: $\alpha = -1.5$, $\beta = 0.5$, $\mu_r = 0$
- Case-2: $\alpha = -1.5$, $\beta = 0.5$, $\mu_r = 0.5$
- Case-3: $\alpha = -1.5$, $\beta = 1.5$, $\mu_r = 0.5$

From FIGURE 4.11, it can be seen that first case produces increases error response, second case produces non-monotonic error response, while the last case produces decreasing response. Another point can be noted that error does not go to zero in any case. So this locus can be a good check for deciding on the final controller design. Following discussion about the properties of $\mu_{\hat{u}}(K)$ provides some rules of thumb for TE sketching. These properties give us the value of locus at points of origination, termination and at intermediate point. These information proves enough for the sketch of TE locus.

Assuming that $\alpha \leq 0 \leq \beta$ and (4.46) produces unique solution for each value of K, then

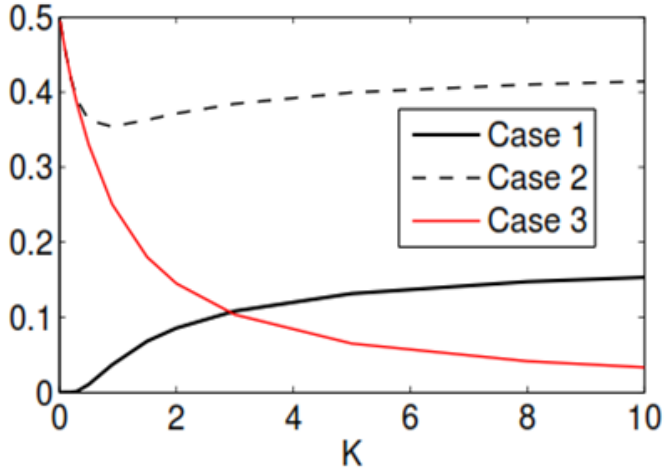


FIGURE 4.11: TE Loci [48]

1 $\lim_{K\to 0^+} \mu_{hate}(K) = \begin{cases} \mu_r & P_0C_0 \neq 0 \\ 0 & P_0C_0 = 0 \end{cases}$

2 $\lim_{K\to 0^+} \mu_{hate}(K) = \frac{\eta^*\phi^*}{C_0}$

3 If $\frac{\mu_r}{P_0} > \frac{\alpha+\beta}{2}$, then $\mu_{\hat{e}}(K) = \frac{1}{1+KC_0P_0}$ whereas $K = \frac{1}{C_0\left(\frac{2\mu_r}{\alpha+\beta} - P_0\right)}$

For instance, applying the above conclusions to system of (4.53) with $\mu_r = 1, \alpha = 0.5, \beta = 1.5$, following values of $\mu_{hate}(K)$ are obtained.

$$\mu_{\hat{e}}(0) = 0 \quad \mu_{\hat{e}}(\infty) = 0.18 \quad \mu_{\hat{e}}(1) = 0.5$$

The following theorem provides structural properties of the TE locus. Assuming that $\alpha \leq 0 \leq \beta$ and (E4.46) produces unique solution for each value of $K$, then

1 If $C_0 = \infty$, then $\mu_{\hat{e}}(K) = 0$ for any $K$

2 If $\lim_{K\to 0^+} \mu_{\hat{e}}(K) = 0$, then one of the following could be the reason

(a) $K_e^* = \infty$

(b) $C_0 = 0$

(c) $\frac{\mu_r}{P_0} = \frac{\alpha+\beta}{2}$

3 If $P_0 \neq \infty$, then $\mu_r - P_0\beta \leq \mu_{\hat{e}}(K) \leq \mu_r - P_0\alpha$

4 $\mu_{\hat{e}}(\infty) < \mu_{\hat{e}}(0)$, then TE is decreasing function of $K$

5 $\mu_{\hat{e}}(0) < \mu_{\hat{e}}(\infty)$, then TE is increasing function of $K$

### 4.3.4 Control Design with S/AS Root Locus

In the theory of linear systems, the sizes of trackable signals are determined using the time domain performance indicators of the system, they are overshoot, rise time, etc., of the step response. For random references, though, the permissible domains are established on the quality indicators $I_2$ and $I_3$ as defined and described in section 4.2. They are repeated here for reference purposes.

$$I_2 = \frac{\Omega}{\mathrm{SRS}_{BW}(\sigma_r, \mu_r)} \tag{4.54a}$$

$$I_3 = \min\left\{\mathrm{SRS}_M(\sigma_r, \mu_r) - 1, \frac{\Omega}{\mathrm{SRS}_{BW}(\sigma_r, \mu_r)}\right\} \tag{4.54b}$$

Here, $\Omega$ is the bandwidth of the input coloring filter, BW is the random bandwidth and M is the resonant peak at resonant frequency.

In classical theory the design process is performed such that the dominant closed-loop poles are placed in some admissible region of left half s-plane. Such admissible regions are defined using the performance indicators $I_2$ and $I_3$. The aim of design is to select gain $K$ so that all AS-poles are within the permissible domain and positioned earlier than to the AS-truncation points. The value of gain K should be chosen in a way static responsiveness is gained along with amplitude truncation is completely avoided by the closed-loop system. The design will be explained with the example of (E4.55)

$$G_P(s) = \frac{(s+20)}{(s+15)(s+0.5)}, \quad G_C(s) = 1, \quad \sigma_r = 1 \tag{4.55}$$

FIGURE 4.12(a) gives the AS-locus for the system in (E4.55) along

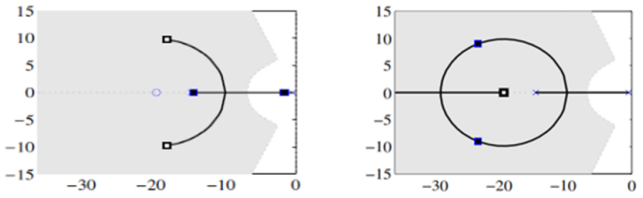


(a) AS-RL Before Design [50] (a) AS-RL After Design [63]

FIGURE 4.12: AS-RL Design

with a sketch of permissible region of poles locations. From here it can be observed, that the truncation, denoted by solid square is outside the permissible region, so this need redesign. One possible solution will be to increase the saturation level. When saturation bound is increased to a value of 1.3, the value of $K_e^*$ becomes 104. When the locus is sketched again with new gain range, the resulting plot is shown in FIGURE 4.12(b). From the new locus, it can clearly be concluded that now the complete is within the permissible region, so no amplitude truncation will occur. The steady state performance requires that $e_{ss} < 0.05$, this implies that $\frac{1}{1+KC_0P_0} < 0.05$ or $K > 7.2$. Therefore, to achieve both good dynamic tracking and steady state approachability, $K$ must satisfy $7.2 < K < 39$.

Suppose that the steady state specifications require for $|\mu_{\hat{e}}(K)| < \bar{\mu}$. According to this requirement, a permissible area for TE can be presented (see the shaded area in FIGURE 4.13. Then the design objective would be to choose a value of K, such that the TE locus stays within the permissible region. Returning to the example, suppose that the specifications require $|\mu_{\hat{e}}(K)| < 0.05$. The TE locus of the system, along with the permissible region, is plotted in FIGURE 4.13. As it follows from this diagram, the TE loci for $\beta = 0.92$ and $\alpha = 1.3$ are in the admissible domain for $K > 17$ and $K > 7.6$, respectively. Combining the above results, we conclude that, for the case of $\beta = 1.3$, for good static and dynamic tracking, $K$ must satisfy $7.6 < K < 39$. Selecting $K = 35$, the quality of tracking for both

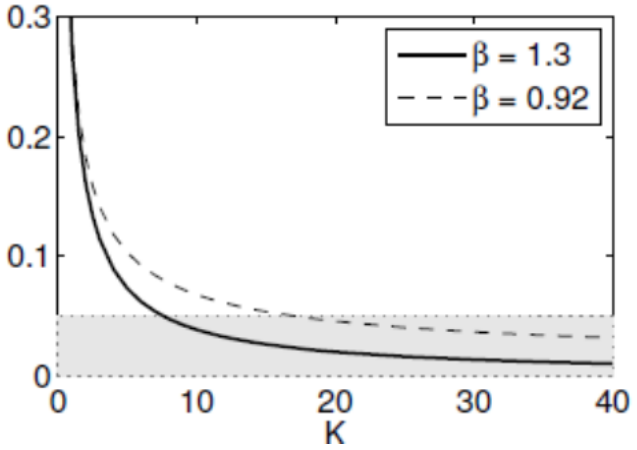


FIGURE 4.13: Tracking Quality in Steady State [47]

$\beta = 0.92$ and $\beta = 1.3$ in FIGURE 4.13. Clearly, the quality of tracking is good for $\beta = 1.3$, but poor for $\beta = 0.92$ because of amplitude truncation. There may be cases where the AS-poles and TE cannot be placed in their respective admissible domains simultaneously.

# Chapter 5

# Quasilinear Controller Design

This is the concluding chapter of this work. This will begin with the design process of step tracking controllers. The design process will be elaborated with some examples. After the process and its requirements are established, this will be applied on the proposed plant of this work, the MLS plant. The chapter will end with a comparative analysis of the all controllers investigated in this work.

Consider the feedback system of FIGURE 5.1(a) where

## 5.1 Tracking Controller Design

$$G_P(s) = \frac{1}{s^2 + 0.4s + 1} \tag{5.1}$$

And $\text{sat}_\alpha(u)$ is the symmetric saturation function shown in FIGURE 5.1(b). The problem is to design a controller, $F_r(s)$, so that the closed loop system tracks unit step reference signal satisfying the following specifications:

$$\text{Steady state error} \leq 1\%; \quad \text{Overshoot} \leq 5\%$$

$$\text{Settling Time} \leq 1\text{sec}$$

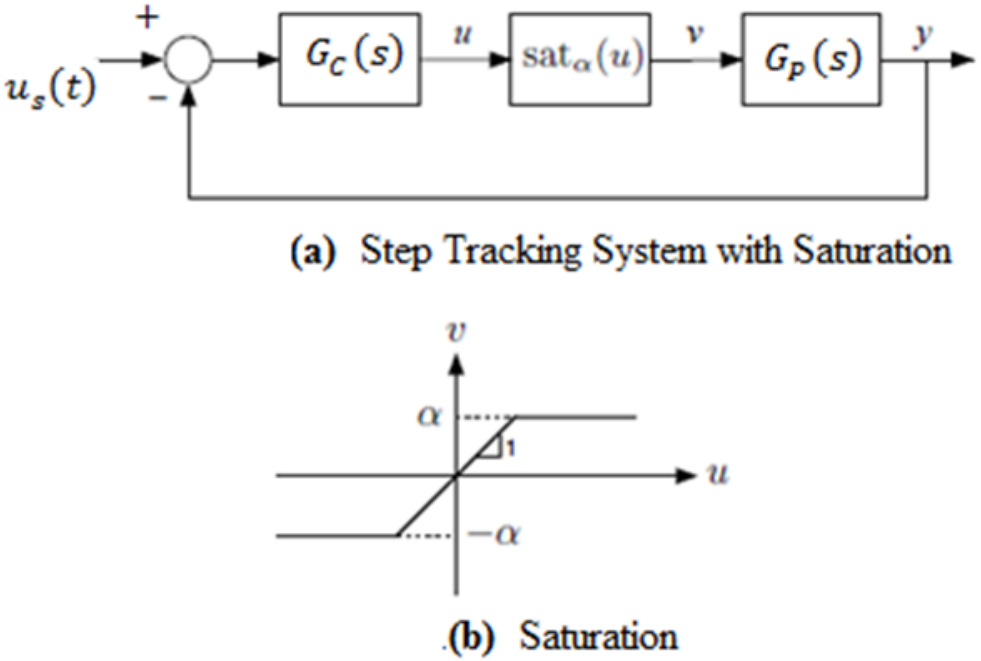


FIGURE 5.1: Step Tracking in Quasilinear System

Since there are no rigorous methods for designing step-tracking controllers for systems with saturating actuators, one usually designs a controller assuming that the actuator is linear and then verifies the performance using simulations. Under such assumptions, for the system in (E5.1) a controller can be given as (satisfying the given specifications above)

$$G_C(s) = \frac{22s + 200}{0.01s + 1} \tag{5.2}$$

The performance of the controller is investigated for four values of $\alpha$ : $\alpha = 25, 10, 5, 0.5$. As the saturation bound is tightened, the performance of the controller degrades. The controller shows the best performance for the highest value of $\alpha$ and its performance deteriorates badly for $\alpha = 0.5$. All these conclusions are explained with the help of figures, from FIGURE-5.2(a) through FIGURE-5.2(d). from these results it can clearly be seen that the selection of saturation level strongly determines the resulting performance. This section is based upon the development of such methods. The

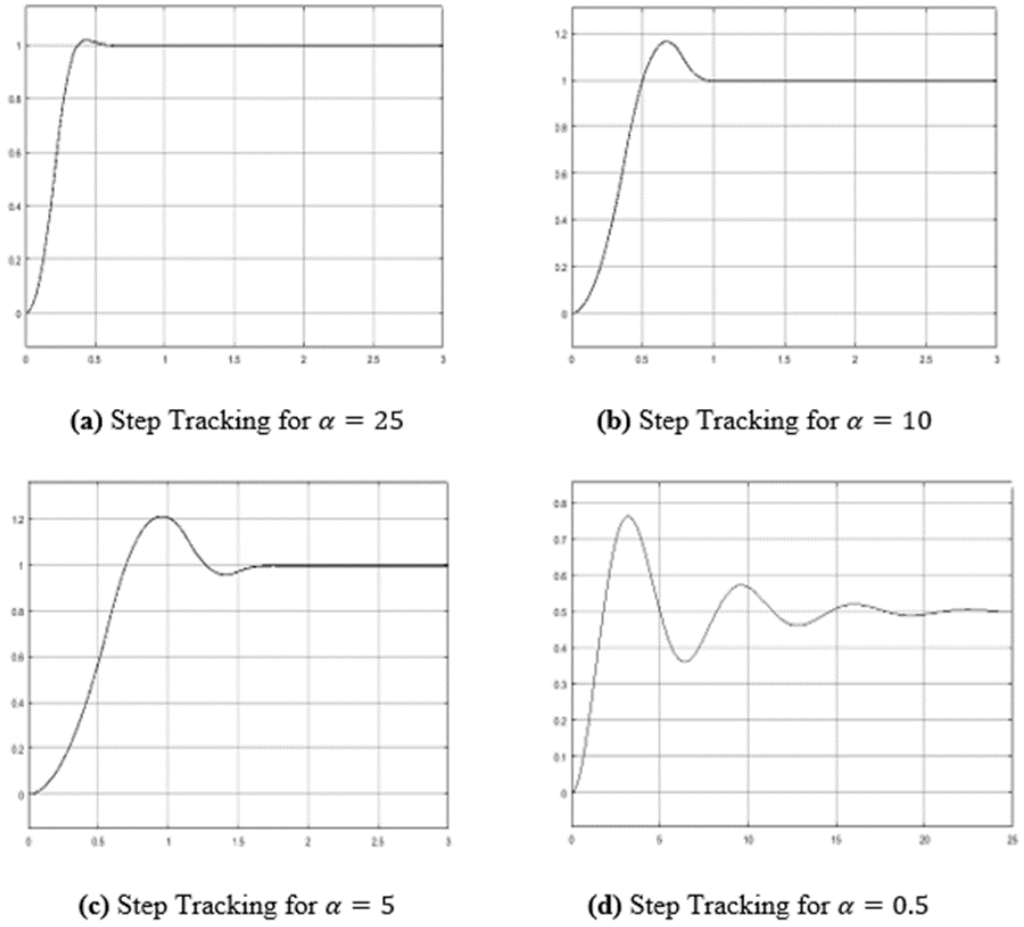

**(a)** Step Tracking for $\alpha = 25$ **(b)** Step Tracking for $\alpha = 10$

**(c)** Step Tracking for $\alpha = 5$ **(d)** Step Tracking for $\alpha = 0.5$

FIGURE 5.2: Step Tracking for Various Value of $\alpha$

development here entails from the time domain design methods of Chapter-4. Chapter-4 is concerned about the design of controllers for the random reference tracking. In this section, the design process of step tracking controllers will be expounded.

$$F_r(s) = \sqrt{\frac{3}{\Omega}} \frac{\Omega^3}{s^3 + 2\Omega s^2 + 2\Omega^2 s + \Omega^3} \tag{5.3}$$

The system block-diagram representing the theme this development is expounded in FIGURE-5.3(a). For the tracking of random references, the reference signal is passed through a Butterworth filter as given by (E5.3), but in this section, the filter could be based on second order prototype system. If the second order filter of type given

by (E5.4) is used, the resulting system configuration is FIGURE-5.3(b).

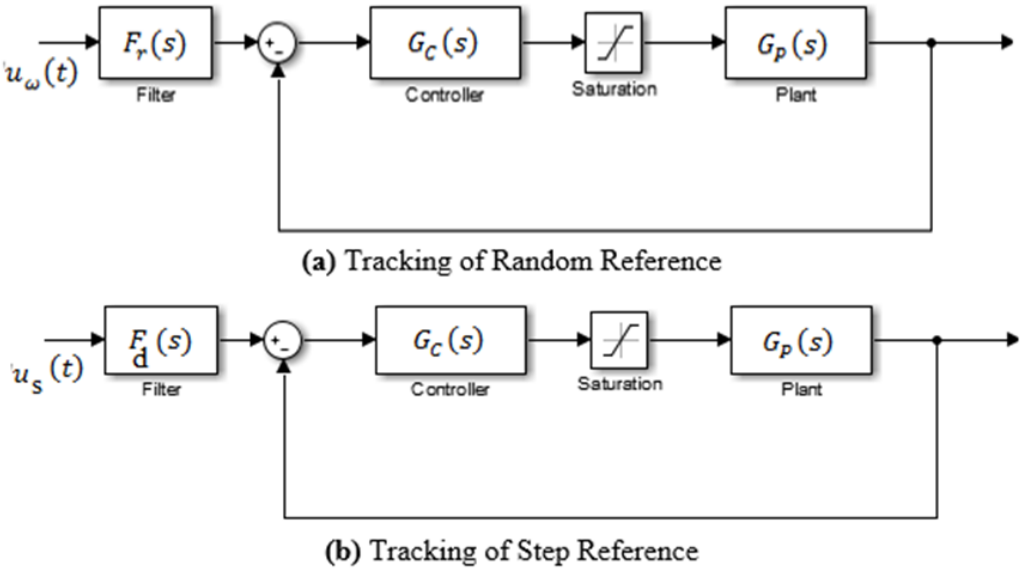


FIGURE 5.3: Tracking the Random and Step References

$$F_d(s) = \frac{\omega_n^2}{s^2 + 2\zeta\omega_n s + \omega_n^2} \tag{5.4}$$

Where $\zeta$ and $\omega_n$ are selected such that the output of $F_d(s)$, $r(t)$ satisfies the given specifications above. The goal is to design a controller $G_C(s)$, if possible, such that the output $y(t)$ tracks well $r(t)$ according to the specifications. This section is concerned with following design steps.

1 **Controller Existence:** before the actual design process begins, it is mandatory that the given system and the specifications be explored to determine the existence of a controller.

2 **The Adjoint Bandwidth:** in this step, the dynamics part of the specifications is transformed in a way that they become the specifications for stochastic signal tracking. This transformation results in adjoint bandwidth denoted as $\Omega_a$.

3 **Controller Design:** design a controller for the system of FIGURE-5.3(a) with $\Omega = \Omega_a$ using the S-root locus tactic which

is a special case of AS-root locus and is only applicable to symmetric systems.

4 **Explore Possibilities:** Finally, use the controller designed in above stage and design the filter called pre-filter as shown in FIGURE-5.3(b). Simulate the system and the design does not satisfy the specifications, explore other design possibilities. This two-fold design process gives extra freedom to the designer, called two-degree of freedom.

This design process signifies two key points:

1 The design process creates the connection between adjoint bandwidth and the step tracking specifications.

2 It sees the filtered signal to be tracked rather than the reference itself. This is the freedom bestowed by this design process.

The above tactic may guide to a conformist design since the adjoint bandwidth may be too large. Nonetheless, as established in this section, the projected technique is usefully systematic and practical. The inventive contribution of this section is in engaging Quasilinear Control Theory to deliver a straight technique for linear step tracking controller design in systems with saturating actuators.

Underneath, a necessary and sufficient condition for existence of a step-tracking controller satisfying steady state specs is presented. It will be followed by a method of calculating the adjoint bandwidth. Lastly, the QLC method with the anti-windup technique will be compared.

### 5.1.1 Conditions for the Existence of Controller

Consider the system of FIGURE-5.3(b) and the following steady state specifications:

$$\begin{cases} r_0 \leq r_0^* \\ e_{ss} = \frac{\lim\limits_{t\to\infty} |e(t)|}{r_0} \leq e_{ss}^* \end{cases} \tag{5.5}$$

Where $r_0^*$ is the target step-size, $e(t)$ is the tracking error, $e(t) = r(t) - y(t)$, and $e_{ss}^* < 1$. As it is case most of the time, it is assumed that only positive steps are essential to be tracked. $P_0$ and $C_0$ are representing the dc-gains of the plant and controller, respectively. The following proposition provides a necessary and sufficient condition for existence of a controller that satisfies the above specifications in (E5.5).

**Controller Existence Condition:** assuming that $P_0 > 0$, $C_0 > 0$, then there exists a controller $G_C(s)$, if

$$r_0^* \leq \frac{r_0 P_0}{1 - e_{ss}^*} \tag{5.6}$$

(E5.6) is a necessary and sufficient condition for existence of a controller satisfying the steady state part of the specifications. It is the necessary condition for existence of a controller satisfying transient response specifications as well.

Returning to the motivating example of (E5.1), we observe that for $\alpha = 5$, the value of $\frac{P_0\alpha}{1-e_{ss}^*}$ is 5.05, and therefore, the condition for existence of a unit step tracking controller is satisfied. On the other hand, for $\alpha = 0.5$, $\frac{P_0\alpha}{1-e_{ss}^*} = 0.505$, and therefore, no controller satisfying the specs exists.

### 5.1.2 Adjoint Bandwidth

Assume that the dynamic part of step-tracking specifications is as follows:

$$\begin{gathered}\text{Overshoot} \leq \text{OS}^*\% \\ \text{Settling Time} \leq t_s^* \text{sec} \\ \text{Rise Time} \leq t_r^* \text{sec}\end{gathered} \tag{5.7}$$

Let $F_d(s)$ be the nominal second order transfer function (E5.4), whose step response satisfies specifications (E5.7). Then, the adjoint bandwidth is given by

$$\Omega_a = \sqrt{2}\,\omega_n \exp\left\{-\frac{\sigma}{\omega_d}\tan^{-1}\left(\frac{\omega_d}{\sigma}\right)\right\} \tag{5.8}$$

Whereas $\sigma = \zeta\omega_n$ and $\omega_d = \omega_n\sqrt{1-\zeta^2}$. The adjoint bandwidth is demarcated by equating the maximum rate of change of $r(t)$ in Figure FIGURE-5.3(b) with the standard deviation of the rate of change of $r(t)$ in FIGURE-5.3(a). It can be shown that the maximum rate of change of $r(t)$ in FIGURE-5.3(b) is given by

$$\max t \geq 0 \dot{t}(t) = \omega_n \exp\left\{-\frac{\sigma}{\omega_d}\tan^{-1}\left(\frac{\omega_d}{\sigma}\right)\right\} r_0 \tag{5.9}$$

and the standard deviation of the rate of change of $r(t)$ in FIGURE-5.3(a) is the $H_2$-Norm of $sF_\Omega(s)$, that is

$$\|sF_\Omega(s)\|_2 = \frac{\Omega_a}{\sqrt{2}} r_0 \tag{5.10}$$

Thus equating (E5.9) and (E5.10) the result in (E5.8) is obtained. For the motivating example of (E5.1), based on the dynamic part of the specifications, the forward-path transfer function will be

$$F_d(s) = \frac{34}{s^2 + 8s + 34} \tag{5.11}$$

This results in adjoint bandwidth of $\Omega_a = 3.8$.

### 5.1.3 Exploring Design Possibilities with Examples

In this section, the method developed so far will be illustrated with several examples. The section will begin with the complete design process for (E5.1) and various time domain specifications will be investigated to determine the usefulness this methodology.

**Example-1:** considering the example of (E5.1), FIGURE-5.4(a) displays the permissible region in grey and the S-root locus with $\alpha = 25$. The adjoint bandwidth for the system is $\Omega_a = 3.8$. Following controller is selected

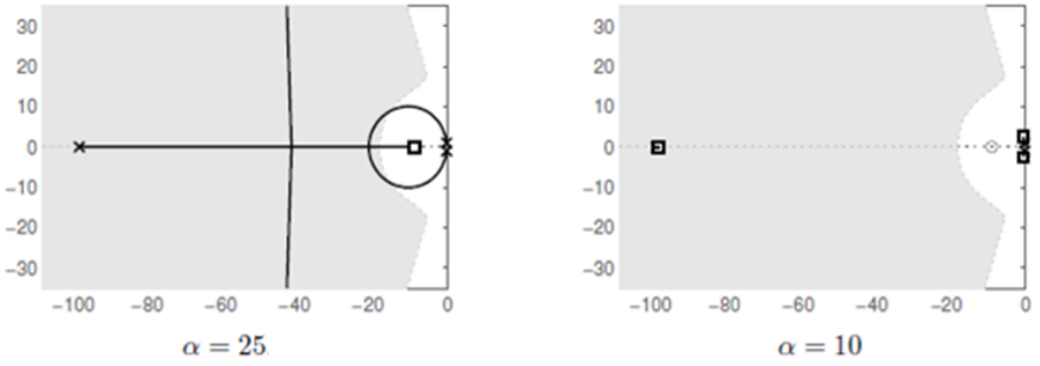


FIGURE 5.4: S-Locus of Illustrative Example-1

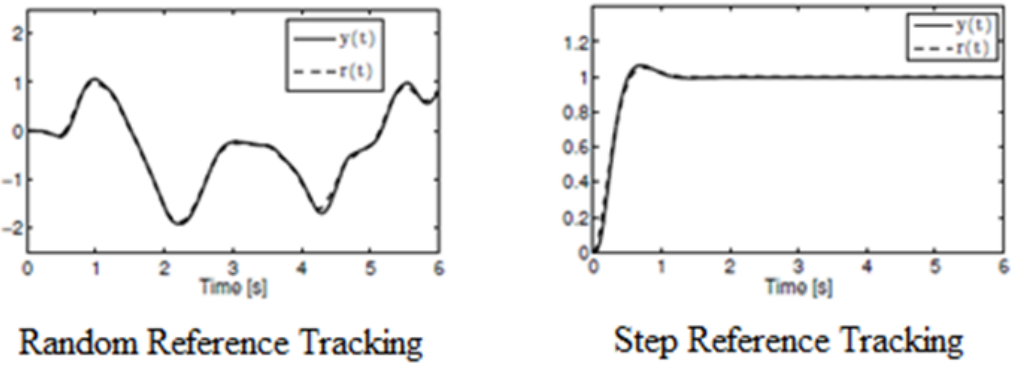


FIGURE 5.5: Tracking Performance of the System in Example-1

$$G_C(s) = K\frac{22s + 200}{0.1s + 1} \tag{5.12}$$

For this example, the termination and truncation points of the S-root locus coincide with the open loop zeros; therefore, the S-poles should be selected within the permissible region. For $K = 1$, the saturating locus of closed loop system is shown in FIGURE-5.3(a) is given in FIGURE-5.5. Clearly, the value of random reference tracking is good.

Since the unit step is in the traceable area when $\alpha = 25$, the controller given by (E5.12) is used in FIGURE-5.3(b). The resulting response is shown in FIGURE-5.5. It shows that the specifications have been satisfied and the quality of tracking is satisfied.

With $\alpha = 10$, using the same controller (E5.12), the S-root locus of the motivating example is shown in FIGURE-5.5(on right). Clearly, the S-root locus ends before arriving the permissible area. So, the quality of tracking is poor for random references as demonstrated in FIGURE-5.6(a). FIGURE-5.6(b) displays the tracking quality for the system of FIGURE-5.3(b). As can be seen, overshoot does not satisfy the specs and the quality of tracking is poor. When  is even reduced, the termination points move closer to the open loop poles, and the quality of tracking degrades further.

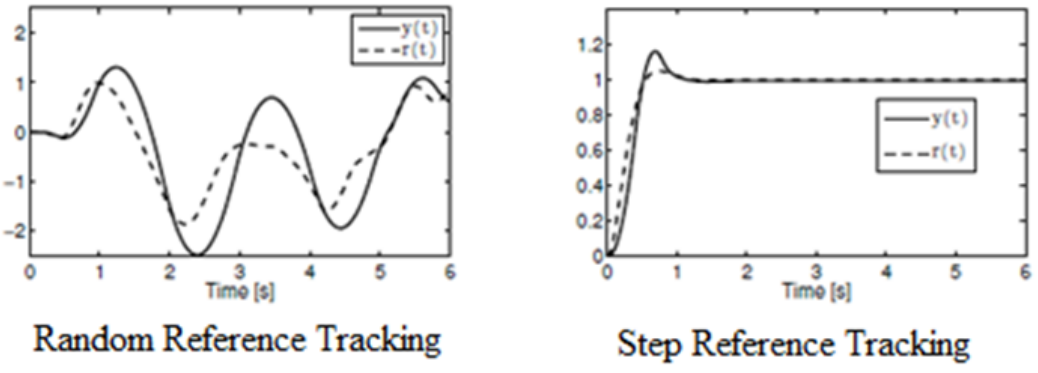


FIGURE 5.6: Tracking Performance for $\alpha = 10$ (Example-1)

**Example-2:** Consider the system of FIGURE-5.3(b) with

$$G_P(s) = \frac{116}{(s^2 + 20s + 116)(0.02s + 1)} \tag{5.13}$$

And $\alpha = 1.5$. The objective is to design a pre-filter $F_d(s)$ and a controller $G_C(s)$ to realize the following step-tracking specifications:

$$\begin{gathered} r_0 \leq 1.5 \\ e_{ss} \leq 2.5\% \\ \text{POS} \leq 5\% \\ t_s \leq 1 \end{gathered} \tag{5.14}$$

First, the condition (E5.6) be satisfied and it come out to be $r_0^* = 1.5 < \frac{P_0\alpha}{1-e_{ss}^*} = 1.54$, so this requirement is met. As far as the dynamic part of the specifications is concerned, since they are same as that in Example-1, $F_d(s)$ is given by (E5.11) and the adjoint bandwidth is $\Omega_a = 3.8$ as before.

The poles of the plant $G_P(s)$ are at $s_{1,2,3} = -104j, -50$. Clearly, the complex conjugate poles are dominant. It can be demonstrated that the concepts dominant poles entails from the classical control theory without significance deterioration. Therefore, a controller be designed such the given dominant poles enter the dominant region. After some design iteration following controller is suggested.

$$G_C(s) = K\frac{s + 30}{0.01s + 1}$$

The S-root locus of the resulting system is shown in FIGURE-5.7. With the controller gain $K = 1.5$, the S-poles are within the admissible domain and prior to the truncation points (black squares on the S-root locus); thus, both steady state and dynamic specifications are satisfied. The resulting performance of systems of FIGURE-5.3 is

illustrated in FIGURE-5.8, respectively. Clearly, step tracking specifications are satisfied.

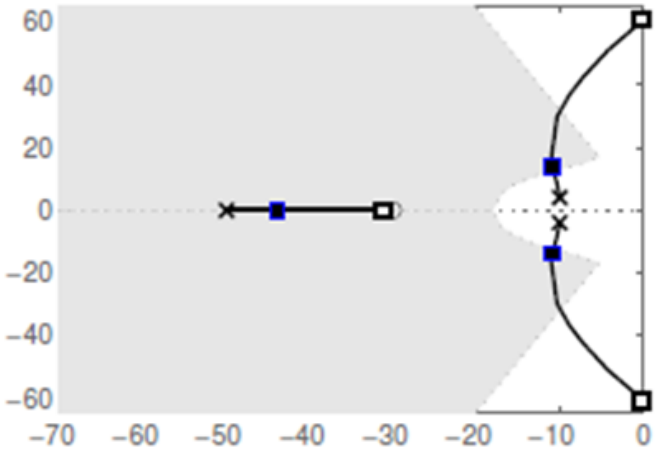


FIGURE 5.7: S-Locus for Example-2

Note that in FIGURE-5.8(a), the quality of random reference tracking deteriorates at two time moments (around $t = 2s$ and $t = 4s$). This is because with the selected $K$, the S-poles are close to the S-truncation points. However, since $r_0 = 1$ is inside the trackable domain, tracking of the unit step in FIGURE-5.8(b) is good.

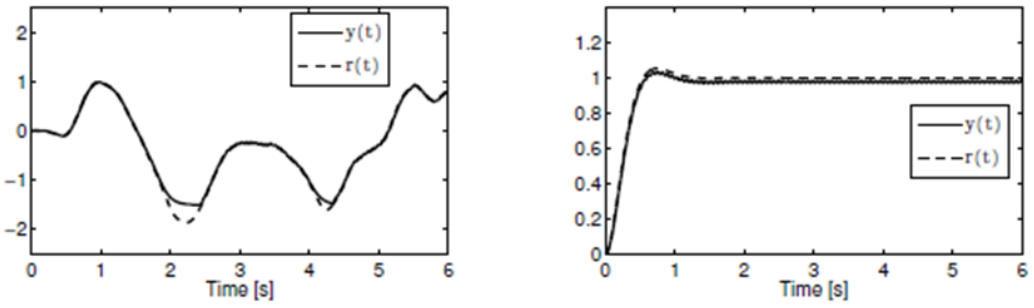


FIGURE 5.8: Random and Step Reference Tracking for Example-2

## 5.2 Controller Design for MLS Plant

From (E2.28)

$$\frac{Y(s)}{V(s)} = -\frac{3473}{s^3 + 213s^2 - 980s - 208363}$$

It state space representation will be

$$\begin{bmatrix}\dot{x}_1\\ \dot{x}_2\\ \dot{x}_3\end{bmatrix} = \begin{bmatrix}0 & 1 & 0\\ 0 & 0 & 1\\ 208363 & 980 & -213\end{bmatrix}\begin{bmatrix}x_1\\ x_2\\ x_3\end{bmatrix} + \begin{bmatrix}0\\ 0\\ -3473\end{bmatrix} v \tag{5.15a}$$

$$y = \begin{bmatrix}1 & 0 & 0\end{bmatrix}\begin{bmatrix}x_1\\ x_2\\ x_3\end{bmatrix} \tag{5.15b}$$

### 5.2.1 Quasilinear Controller Design for MLS Plant

Considering the presence of saturation non-linearity

$$v = \text{sat}_\alpha(u) \tag{5.16}$$

As the plant is a type-0 system, so the following servo type control law is used for the design of feedback controller

$$u = -\mathbf{K}_1\mathbf{x} + k_i\eta = \begin{bmatrix}-\mathbf{K}_1 & k_i\end{bmatrix}\begin{bmatrix}\mathbf{x}\\ \eta\end{bmatrix} \tag{5.17}$$

Where

$$\dot{\eta} = r - y = r - \mathbf{C}\mathbf{x}$$

From (E5.15a) and (E5.17)

$$\begin{bmatrix}\dot{x}_1\\ \dot{x}_2\\ \dot{x}_3\\ \dot{\eta}\end{bmatrix} = \begin{bmatrix}0 & 1 & 0 & 0\\ 0 & 0 & 1 & 0\\ 208363 & 980 & -213 & 0\\ 1 & 0 & 0 & 0\end{bmatrix}\begin{bmatrix}x_1\\ x_2\\ x_3\\ \eta\end{bmatrix} + \begin{bmatrix}0\\ 0\\ -3473\\ 0\end{bmatrix} v + \begin{bmatrix}0\\ 0\\ 0\\ 1\end{bmatrix} r(t) \tag{5.18}$$

The control law proposed in (E5.17) ensures that the state vector $x(t)$, $\eta(t)$ approach their specified steady state values of $x(\infty)$, $\eta(\infty)$ as the step input $r(t)$ approaches its steady state value $r(\infty) = r$.

An error vector can be defined as $\begin{bmatrix}\mathbf{x}(t)-\mathbf{x}(\infty)\\ \eta(t)-\eta(\infty)\end{bmatrix}$ given the error input to $v_e(t)=v(t)-v(\infty)$. Based on this fact the above equation can be rewritten as

$$\begin{bmatrix}\dot{\mathbf{x}}_e(t)\\ \dot{\eta}_e(t)\end{bmatrix}=\begin{bmatrix}0 & 1 & 0 & 0\\ 0 & 0 & 1 & 0\\ 208363 & 980 & -213 & 0\\ 1 & 0 & 0 & 0\end{bmatrix}\begin{bmatrix}\mathbf{x}_e(t)\\ \eta_e(t)\end{bmatrix}+\begin{bmatrix}0\\ 0\\ -3473\\ 0\end{bmatrix}v_e(t)$$

Using the controller law in (E5.17) along with saturation definition (E5.16)

$$\begin{bmatrix}\dot{\mathbf{x}}_e\\ \dot{\eta}_e\end{bmatrix}=\begin{bmatrix}0 & 1 & 0 & 0\\ 0 & 0 & 1 & 0\\ 208363 & 980 & -213 & 0\\ 1 & 0 & 0 & 0\end{bmatrix}\begin{bmatrix}\mathbf{x}_e\\ \eta_e\end{bmatrix}+\begin{bmatrix}0\\ 0\\ -3473\\ 0\end{bmatrix}\text{sat}_\alpha\left(\begin{bmatrix}-\mathbf{K}_1 & k_i\end{bmatrix}\begin{bmatrix}\mathbf{x}_e\\ \eta_e\end{bmatrix}\right)$$

Using the stochastic linearization of saturation non-linearity and letting $\begin{bmatrix}-\mathbf{K}_1 & k_i\end{bmatrix}$

$$\text{sat}_\alpha(v_e(t))=Nv_e(t)$$

Whereas

$$N=\text{erf}\left(\frac{\alpha+\mu_u}{\sqrt{2}\sigma_(v_e)}\right)$$

From the definition of $N$, it can be seen that value of $N$ is dependent upon the variance of $v_e(t)$. Assuming that the reference can be modeled by Gaussian process, the value of $N$ is $N=0.63$, given saturation level of $\pm 18$. With this the error relation can be described

by

$$\begin{bmatrix}\dot{\mathbf{x}}_e\\ \dot{\eta}_e\end{bmatrix} = \begin{bmatrix}0 & 1 & 0 & 0\\ 0 & 0 & 1 & 0\\ 208363 & 980 & -213 & 0\\ 1 & 0 & 0 & 0\end{bmatrix}\begin{bmatrix}\mathbf{x}_e\\ \eta_e\end{bmatrix} + N\begin{bmatrix}0\\ 0\\ -3473\\ 0\end{bmatrix}\left(\begin{bmatrix}-\mathbf{K}_1 & k_i\end{bmatrix}\begin{bmatrix}\mathbf{x}_e\\ \eta_e\end{bmatrix}\right)$$

$$\begin{bmatrix}\dot{\mathbf{x}}_e\\ \dot{\eta}_e\end{bmatrix} = \begin{bmatrix}0 & 1 & 0 & 0\\ 0 & 0 & 1 & 0\\ 208363 - 2188k_1 & 980 - 2188k_2 & -213 - 2188k_3 & 2188k_i\\ 1 & 0 & 0 & 0\end{bmatrix}\begin{bmatrix}\mathbf{x}_e\\ \eta_e\end{bmatrix}$$

The controller parameters in the above equation can be calculated using arbitrary pole placement design. The design has been completed for a settling time of 0.3 seconds and a percentage overshoot of 5%. The parameters come out to be $k_1 = -2952.8$, $k_2 = 19.21$, $k_3 = -3459.8$ and $k_i = -13649$. The controller implementations and the simulation results are shown in FIGURE-5.9 and FIGURE-5.10 respectively.

### 5.2.2 Simulations and Results

From FIGURE-5.10 it can be seen that all goals have been achieved. The input reference is tracked perfectly and the saturation is never activated. Thus it represents the best solution.

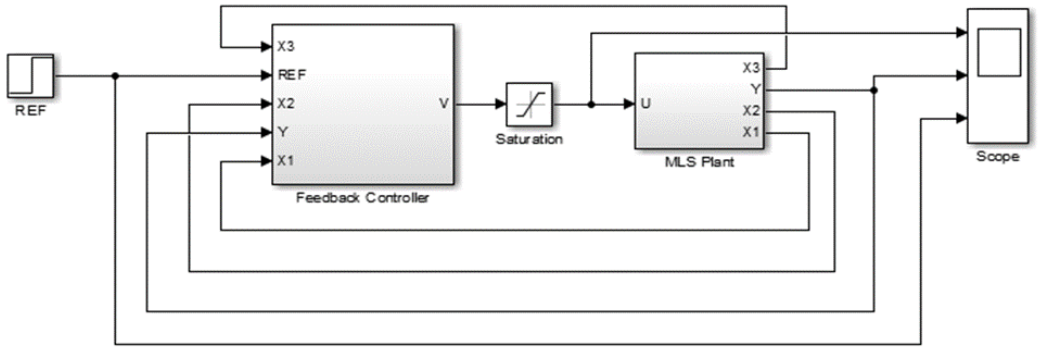


FIGURE 5.9: QLC Implementation

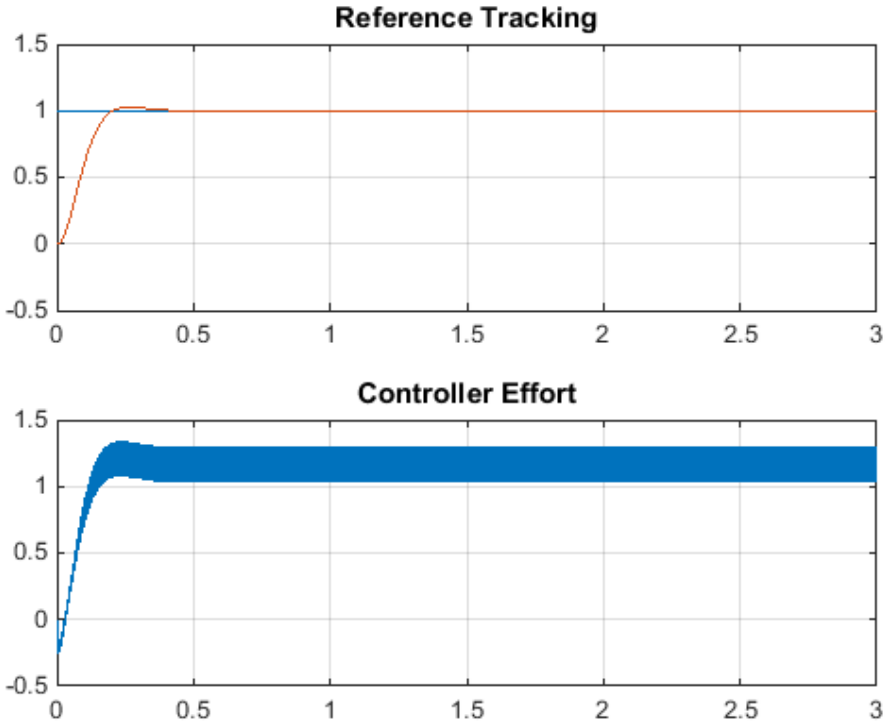


FIGURE 5.10: QLC Performance

# Chapter 6

# Cobclusion and Future Work

In this chapter, a comparison of all controllers will be presented.

## 6.1 Conclusion

In this section performance comparison will be presented with the help of simulations. The results will be presented for step inputs, sinusoidal inputs and random processes with unit variance and zero mean. As it has been demonstrated in sections, QLC controller will show the best performance.

### 6.1.1 Comparison with Loop-Shaping Performance

FIGURE-6.1 shows the performance comparison between Loop-Shaping Control and the QLC control. Purple color (bold) lines are the input curves. Solid line is showing the step input, while dashed line is showing the disturbance input. From here it can be seen that transient response performance of QLC is far better than Loop-Shaping control. Loop-shaping control produces a percentage overshoot of nearly 80%, which could be very dangerous in practical situations and it is completely unacceptable. While QLC control is producing the percentage of about 4%, which is quite reasonable. Rise time performance of loop-shaping is better than QLC. Both controllers offer

excellent steady state performance and disturbance rejection capability. It can be noted even a small trace has not been allowed to appear in the input. FIGURE-6.2 shows the sketches for controller efforts. From here it can be seen that QLC has superseded the performance of loop-shaping. Controller effort is excellently reasonable according to the design specifications. While essentially no practical controller can be implemented for the required effort in loop-shaping control. Table-1 gives quantitative comparison between the two controls.

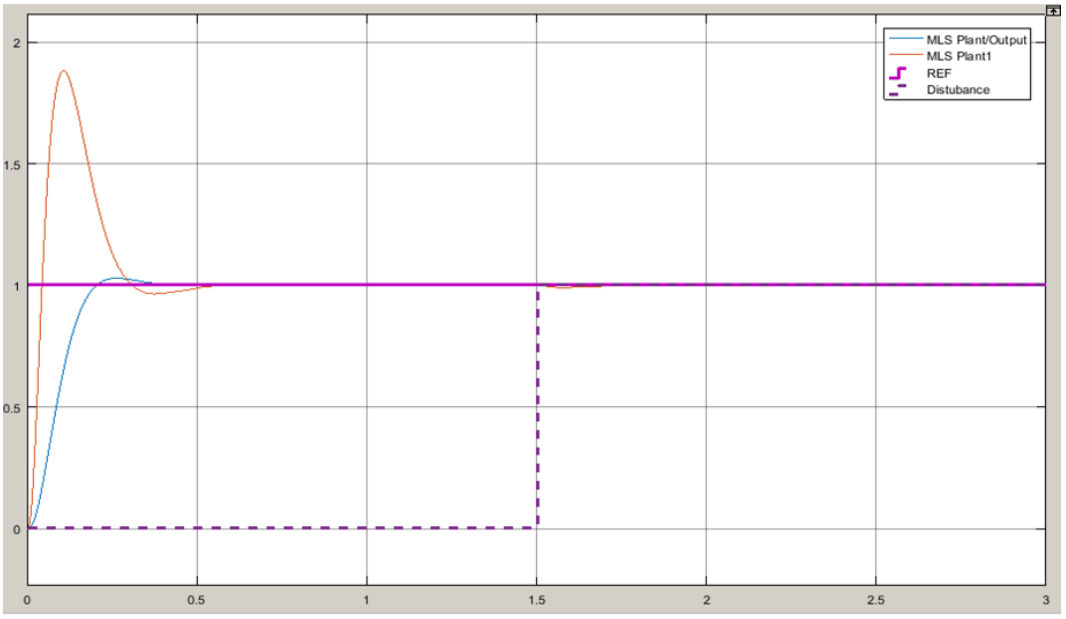


FIGURE 6.1: Response of Loop-Shaping and QLC to Step Input and Disturbance

| | **Loop Shaping** | **QLC** |
|---|---|---|
| **Rise Time** | 0.05 Seconds | 0.1 Seconds |
| **Overshoot** | 80% | 4% |
| **Settling Time** | 0.3 Seconds | 0.3 Seconds |
| **Steady State Error** | 0 | 0 |
| **Controller Effort** | 62 Units | Equal to Reference Input |

TABLE 6.1: Loop-Shaping and QLC Performance Comparison

### 6.1.2 Comparison with ADRC Performance

FIGURE-6.3 shows the ADRC and QLC control system responses to step and disturbance inputs. The inputs are shown in BOLD, while

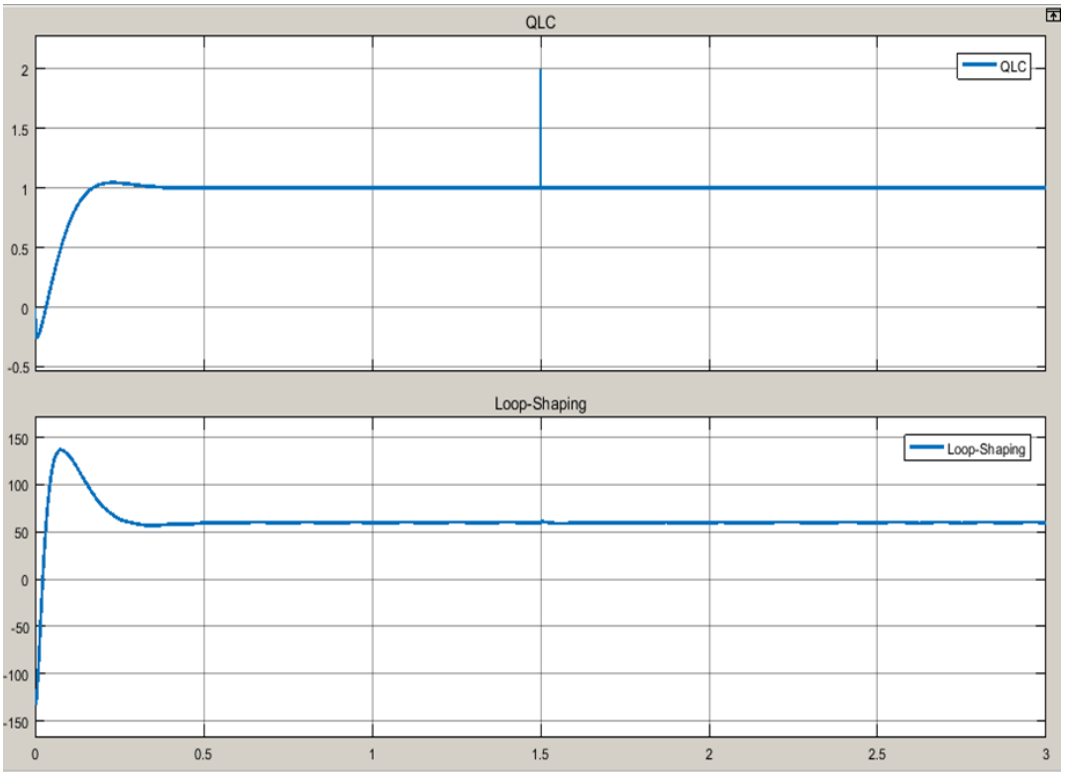


FIGURE 6.2: QLC and Loop Shaping Controller Efforts

the outputs are shown in normal lines. From here it can be seen that both controller give excellent rejection to disturbance, ADRC is far better than QLC. The transient response of ADRC is better than that of QLC. But in steady state, ADRC has some error. FIGURE-6.4 shows the controller efforts. From here it can be seen that the effort from ADRC is almost unbounded, while the effort from QLC remains within limits. Table-2 gives the quantitative comparison between the two controllers.

| | **ADRC** | **QLC** |
|---|---|---|
| **Rise Time** | 0.052 Seconds | 0.1 Seconds |
| **Overshoot** | 0% | 4% |
| **Settling Time** | 0.057 Seconds | 0.3 Seconds |
| **Steady State Error** | 0.01 | 0 |
| **Controller Effort** | $6 \times 10^5$ Units | Equal to Reference Input |

TABLE 6.2: ADRC and QLC Performance Comparison

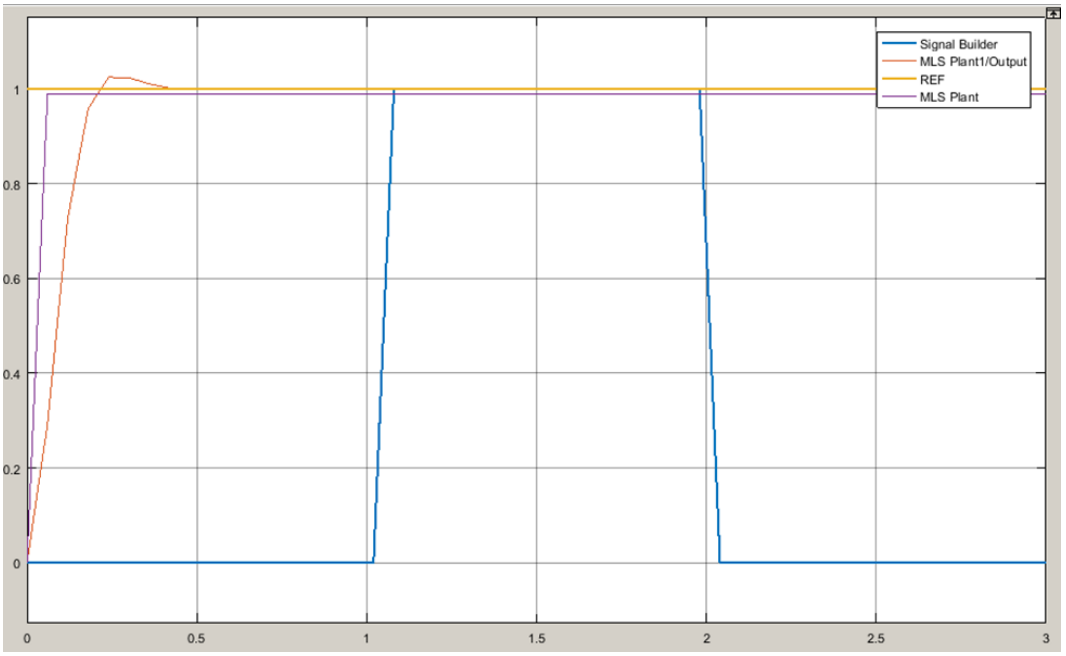


FIGURE 6.3: Response of ADRC and QLC to Step Input and Disturbance

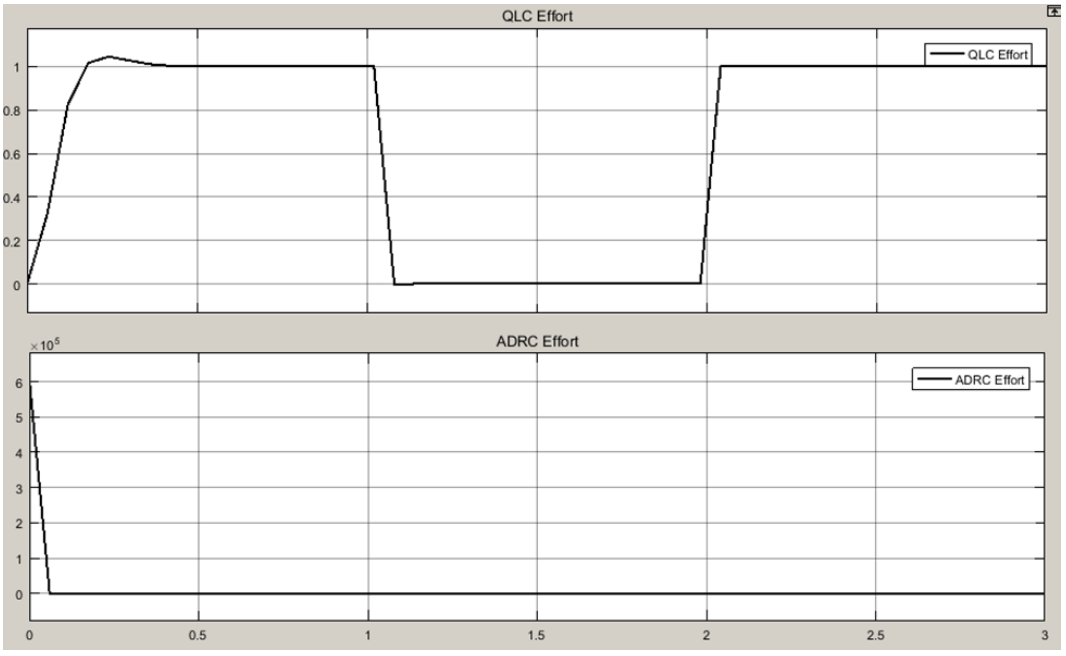


FIGURE 6.4: QLC and ADRC Controller Efforts

### 6.1.3 Remarks

From above discussion it can be seen that ADRC is the best control in the sense that it does not required the model of the plant and its tracking performance is good with a very small and ignorable steady-state error. Although, steady-state performance of loop-shaping control is excellent, but it cannot be accepted because un-acceptable transient response. Additionally, both controller exert unbounded efforts, so they cannot be accepted in practical scenarios. The only option remains that of QLC Control.

## 6.2 Future Work

Quasilinear control has presented a remarkable and practical control method. This is attracting many researchers and will play excellent role product development industry. But yet it has not got complete maturity in terms of acceptability as an alternate to conventional control schemes. Following concepts can be highlighted which need the attention future researchers.

The phenomenon of Gaussianization must analytically be proven, and the ac-curacy of stochastic linearization for Gaussianizing systems thoroughly studied. While such a study has been done for a small class of systems, the general case has not been treated. The method of cumulants may be applicable for the study of Gaussianization.

QLC theory can be extended to other nonlinearities in the sensors and actuators. For example, the performance loci and A-SLQR approaches can be extended to systems with saturating sensor, sensor with deadzone or quantization, actuator with deadzone or relay, etc. It has been observed that if the solution of quasilinear gain and bias equations is not unique, the jumping phenomenon occurs. As a future direction, this phenomenon can be thoroughly studied and

analytically proven.

The results can be extended to the MIMO case. Multi-loop and state feedback control of systems with decoupled saturating actuators is a natural extension of this work.

The relationship between existence of solution to the quasilinear gain and bias equations and existence of an invariant measure in the original LPNI system can be explored.

Other linear control methods such as H-Infinity and LMI approaches can be extended to the quasilinear control of S- and A-LPNI systems. QLC can be applied to standard nonlinear control techniques (e.g., feedback linearization of systems with saturating actuators) for performance analysis and controller design.

The robustness of the quasilinear gain and bias must be analyzed with respect to the system parameters. Moreover, robustness of the resulting QLC controllers must be quantified in terms of stability and performance.

Lastly, a comprehensive experimental validation of the theory in an industrial setting is important. The solutions of these problems will provide a relatively complete theory of Quasilinear Control.

# References


[1] Ishtiaq Ahmad and Muhammad Akram Javaid. Nonlinear model & controller design for magnetic levitation system. *Recent Advances in Signal Processing, Robotics and Automation*, pages 324–328, 2010.

[2] Baris Baykant Alagoz, Nusret Tan, Furkan Nur Deniz, and Cemal Keles. Implicit disturbance rejection performance analysis of closed loop control systems according to communication channel limitations. *IET Control Theory & Applications*, 9(17): 2522–2531, 2015.

[3] Baris Baykant Alagoz, Nusret Tan, Furkan Nur Deniz, and Cemal Keles. Implicit disturbance rejection performance analysis of closed loop control systems according to communication channel limitations. *IET Control Theory & Applications*, 9(17): 2522–2531, 2015.

[4] Karl J Åström and Björn Wittenmark. *Adaptive control*. Courier Corporation, 2013.

[5] Karl Johan Åström and Tore Hägglund. *Advanced PID control*. ISA-The Instrumentation, Systems and Automation Society, 2006.

[6] Karl Johan Aström and Richard M Murray. *Feedback systems: an introduction for scientists and engineers*. Princeton university press, 2010.

[7] Luis Angel Castañeda, Alberto Luviano-Juárez, and Isaac Chairez. Robust trajectory tracking of a delta robot through adaptive active disturbance rejection control. *IEEE Transactions on Control Systems Technology*, 23(4):1387–1398, 2015.

[8] Xiaoyong Chang, Yongli Li, Weiya Zhang, Nan Wang, and Wei Xue. Active disturbance rejection control for a flywheel energy storage system. *IEEE Transactions on Industrial Electronics*, 62(2):991–1001, 2015.

[9] Chieh Chen. Backstepping control design and its applications to vehicle lateral control in automated highway systems. *University of California at Berkeley*, 1996.

[10] Lei Cheng, Lei Cao, Huai-yu Wu, Quan-min Zhu, Wen-xia Xu, and Ling Liu. Trajectory tracking control of nonholonomic mobile robots by backstepping. In *Modelling, Identification and Control (ICMIC), Proceedings of 2011 International Conference on*, pages 134–139. IEEE, 2011.

[11] ShiNung Ching, Yongsoon Eun, Cevat Gokcek, Pierre T Kabamba, and Semyon M Meerkov. *Quasilinear Control: Performance Analysis and Design of Feedback Systems with Nonlinear Sensors and Actuators*. Cambridge University Press, 2010.

[12] ShiNung Ching, Yongsoon Eun, Pierre T Kabamba, and Semyon M Meerkov. Quasilinear control theory: An overview. *IFAC Proceedings Volumes*, 44(1):10958–10963, 2011.

[13] Saptarshi Das and Indranil Pan. On the mixed h2/h-infinity loop-shaping tradeoffs in fractional-order control of the avr system. *IEEE TRANSACTIONS ON INDUSTRIAL INFORMATICS*, 10(4):1982–1991, 2014.

[14] Jaya Deepti Dasika, Behrooz Bahrani, Maryam Saeedifard, Alireza Karimi, and Alfred Rufer. Multivariable control of single-inductor dual-output buck converters. *IEEE Transactions on Power Electronics*, 29(4):2061–2070, 2014.

[15] Jaya Deepti Dasika, Behrooz Bahrani, Maryam Saeedifard, Alireza Karimi, and Alfred Rufer. Multivariable control of single-inductor dual-output buck converters. *IEEE Transactions on Power Electronics*, 29(4):2061–2070, 2014.

[16] Romain Delpoux, Laurentiu Hetel, and Alexandre Kruszewski. Parameter-dependent relay control: Application to pmsm. *IEEE Transactions on Control Systems Technology*, 23(4):1628–1637, 2015.

[17] Markus Dick, Martin Gugat, and Günter Leugering. Feedback stabilization of quasilinear hyperbolic systems with varying delays. In *Methods and Models in Automation and Robotics (MMAR), 2012 17th International Conference on*, pages 125–130. IEEE, 2012.

[18] Guang-Ren Duan. Direct parametric control of fully-actuated high-order quasi-linear systems via dynamical feedback. In *Information and Automation (ICIA), 2014 IEEE International Conference on*, pages 418–424. IEEE, 2014.

[19] Guang-Ren Duan. Parametric control of quasi-linear systems by output feedback. In *Control, Automation and Systems (ICCAS), 2014 14th International Conference on*, pages 928–934. IEEE, 2014.

[20] Guang-Ren Duan. Quasi-linear eigenstructure assignmenta case study. In *Information and Automation (ICIA), 2014 IEEE International Conference on*, pages 182–187. IEEE, 2014.

[21] Adrian-Vasile Duka, Mircea Dulău, and Stelian-Emilian Oltean. Imc based pid control of a magnetic levitation system. *Procedia Technology*, 22:592–599, 2016.

[22] Ahmed El Hajjaji and M Ouladsine. Modeling and nonlinear control of magnetic levitation systems. *IEEE Transactions on industrial Electronics*, 48(4):831–838, 2001.

[23] Philippe Feyel. *Loop-shaping robust control*. John Wiley & Sons, 2013.

[24] Jan Friedmann, Felix Groedl, and Ralph Kennel. A novel universal control scheme for transcutaneous energy transfer (tet) applications. *IEEE Journal of Emerging and Selected Topics in Power Electronics*, 3(1):296–305, 2015.

[25] Peter Gruber and Silvano Balemi. Overview of non-linear control methods. 2010.

[26] Mikkel PS Gryning, Qiuwei Wu, Mogens Blanke, Hans Henrik Niemann, and Karsten PH Andersen. Wind turbine inverter robust loop-shaping control subject to grid interaction effects. *IEEE Transactions on Sustainable Energy*, 7(1):41–50, 2016.

[27] Yi Guo, Pierre T Kabamba, Semyon M Meerkov, Hamid R Ossareh, and Choon Yik Tang. Quasilinear control of wind farm power output. *IEEE Transactions on Control Systems Technology*, 23(4):1555–1562, 2015.

[28] Richard Haberman. *Applied partial differential equations with Fourier series and boundary valve problems*. Pearson Higher Ed, 2012.

[29] Jingqing Han. From pid to active disturbance rejection control. *IEEE transactions on Industrial Electronics*, 56(3):900–906, 2009.

[30] Ola Härkegård and S Torkel Glad. Flight control design using backstepping. *IFAC Proceedings Volumes*, 34(6):283–288, 2001.

[31] Gernot Herbst. A simulative study on active disturbance rejection control (adrc) as a control tool for practitioners. *Electronics*, 2(3):246–279, 2013.

[32] Gernot Herbst. Practical active disturbance rejection control: Bumpless transfer, rate limitation, and incremental algorithm. *IEEE Transactions on Industrial Electronics*, 63(3):1754–1762, 2016.

[33] Qibing Jin, Qie Liu, and Biao Huang. Control design for disturbance rejection in the presence of uncertain delays. *IEEE Transactions on Automation Science and Engineering*, 2015.

[34] Marcos B Ketzer and Cursino B Jacobina. Sensorless control technique for pwm rectifiers with voltage disturbance rejection and adaptive power factor. *IEEE Transactions on Industrial Electronics*, 62(2):1140–1151, 2015.

[35] Torsten Knüppel and Frank Woittennek. Control design for quasi-linear hyperbolic systems with an application to the heavy rope. *IEEE Transactions on Automatic Control*, 60(1):5–18, 2015.

[36] George Kopsakis. Feedback control systems loop shaping design with practical considerations. 2007.

[37] Pawan Kumar and Shashi Minz. Control of magnetic levitation system using pd and pid controller.

[38] Benjamin C Kuo. *Automatic control systems*. John Wiley & Sons, 2010.

[39] Chien-Liang Lai and Pau-Lo Hsu. The butterfly-shaped feedback loop in networked control systems for the unknown delay compensation. *IEEE Transactions on Industrial Informatics*, 10 (3):1746–1754, 2014.

[40] CK Li, WL Lee, and YW Chou. Fuzzy control of power converters based on quasilinear modelling. *Electronics Letters*, 31 (7):594–595, 1995.

[41] Jie Li, Hai-Peng Ren, and Yan-Ru Zhong. Robust speed control of induction motor drives using first-order auto-disturbance rejection controllers. *IEEE Transactions on Industry Applications*, 51(1):712–720, 2015.

[42] Jie Li, Yuanqing Xia, Xiaohui Qi, Zhiqiang Gao, Kai Chang, and Fan Pu. Absolute stability analysis of non-linear active disturbance rejection control for single-input–single-output systems via the circle criterion method. *IET Control Theory & Applications*, 9(15):2320–2329, 2015.

[43] Zuliang Lu and Xiao Huang. Error estimates of variational discretization and mixed finite element methods for quasilinear optimal control problems. In *Control and Decision Conference (CCDC), 2012 24th Chinese*, pages 3519–3523. IEEE, 2012.

[44] Rochelle Mellish. *Backstepping control design for the coordinated motion of vehicles in a flowfield*. University of Maryland, College Park, 2011.

[45] Konstantinos Michail, Kyriakos M Deliparaschos, Spyros G Tzafestas, and Argyrios C Zolotas. Ai-based actuator/sensor fault detection with low computational cost for industrial applications. *IEEE Transactions on Control Systems Technology*, 24 (1):293–301, 2016.

[46] Bharathwaj Muthuswamy and K Peterson. Design of magnetic levitation controllers using jacobi linearization, feedback linearization and sliding mode control, project report. *University of California, Berkeley, CA*, 2008.

[47] Hamid-Reza Ossareh. *Quasilinear control theory for systems with asymmetric actuators and sensors*. PhD thesis, University of Michigan, 2013.

[48] Hamid-Reza Ossareh. *Quasilinear control theory for systems with asymmetric actuators and sensors*. PhD thesis, University of Michigan, 2013.

[49] Sybil P Parker. Mcgraw-hill dictionary of scientific and technical terms. 1984.

[50] Zhiqiang Pu, Ruyi Yuan, Jianqiang Yi, and Xiangmin Tan. A class of adaptive extended state observers for nonlinear disturbed systems. *IEEE Transactions on Industrial Electronics*, 62(9):5858–5869, 2015.

[51] Guofa Sun, Xuemei Ren, and Dongwu Li. Neural active disturbance rejection output control of multimotor servomechanism. *IEEE Transactions on Control Systems Technology*, 23(2):746–753, 2015.

[52] Peter Šuster and Anna Jadlovska. Modeling and control design of magnetic levitation system. In *Applied Machine Intelligence and Informatics (SAMI), 2012 IEEE 10th International Symposium on*, pages 295–299. IEEE, 2012.

[53] Rafael Vazquez, Jean-Michel Coron, Miroslav Krstic, and Georges Bastin. Collocated output-feedback stabilization of a 2× 2 quasilinear hyperbolic system using backstepping. In

*American Control Conference (ACC), 2012*, pages 2202–2207. IEEE, 2012.

[54] Igor G Vladimirov and Ian R Petersen. Characterization and moment stability analysis of quasilinear quantum stochastic systems with quadratic coupling to external fields. In *Decision and Control (CDC), 2012 IEEE 51st Annual Conference on*, pages 1691–1696. IEEE, 2012.

[55] Lu Wang and Jianbo Su. Robust disturbance rejection control for attitude tracking of an aircraft. *IEEE Transactions on Control Systems Technology*, 23(6):2361–2368, 2015.

[56] Lu Wang and Jianbo Su. Trajectory tracking of vertical take-off and landing unmanned aerial vehicles based on disturbance rejection control. *IEEE/CAA Journal of Automatica Sinica*, 2 (1):65–73, 2015.

[57] Dan Wu and Ken Chen. Frequency-domain analysis of nonlinear active disturbance rejection control via the describing function method. *IEEE Transactions on Industrial Electronics*, 60(9): 3906–3914, 2013.

[58] Shaofeng Xiong, Weihong Wang, Xiaodong Liu, Zengqiang Chen, and Sen Wang. A novel extended state observer. *ISA transactions*, 58:309–317, 2015.

[59] Wenchao Xue, Wenyan Bai, Sheng Yang, Kang Song, Yi Huang, and Hui Xie. Adrc with adaptive extended state observer and its application to air–fuel ratio control in gasoline engines. *IEEE Transactions on Industrial Electronics*, 62(9):5847–5857, 2015.

[60] Ling Zhao, Yafei Yang, Yuanqing Xia, and Zhixin Liu. Active disturbance rejection position control for a magnetic rodless

pneumatic cylinder. *IEEE Transactions on Industrial Electronics*, 62(9):5838–5846, 2015.

[61] Jinglin Zhou, Hong Yue, Jinfang Zhang, and Hong Wang. Iterative learning double closed-loop structure for modeling and controller design of output stochastic distribution control systems. *IEEE Transactions on Control Systems Technology*, 22 (6):2261–2276, 2014.

[62] Lan Zhou, Jinhua She, Min Wu, Yong He, and Shaowu Zhou. Estimation and rejection of aperiodic disturbance in a modified repetitive-control system. *IET Control Theory & Applications*, 8(10):882–889, 2014.